Functional Studies on the Candidate ATPase Domains of *Saccharomyces cerevisiae* MutLα

By

Phuoc T. Tran

A Dissertation

Presented to the Department of Molecular and Medical Genetics and the
Oregon Health Sciences University School of Medicine in partial
fulfillment of the requirements for the degree of
Doctor of Philosophy

May 2001

School of Medicine
Oregon Health & Science University

CERTIFICATE OF APPROVAL

This is to certify that the Ph.D. thesis of

Phuoc Tran

has been approved

[redacted]
Professor in charge of thesis

[redacted]
Member

[redacted]
Member

[redacted]
Member

TABLE OF CONTENTS

Acknowledgements

The work contained in this thesis would not have been possible without the support of many key individuals. I am forever indebted to my mentor, R. Michael Liskay, for allowing me to join his lab and for providing an environment of intellectual independence tempered with guidance and support. Thank you. I must also thank all past and present labmates, in particular, Andrew Buermeyer, Sue Deschenes, Sandra Dudley, Megan Nguyen and Guy Tomer, for assisting me in my work and development.

Special thanks goes to Eric Alani for allowing me to visit his lab and for providing invaluable comments and direction during my thesis studies. I would also like to acknowledge Eric's former graduate student, Jayson Bowers, for introducing me to biochemical methodologies.

My thesis committee members, Richard Brennan, Michael Forte and Stefan Lanker, have provided suggestions instrumental to the completion of my thesis. Thank you professors.

Senior MD/PhD students, Jae Cho, Bill Chang, and Denis Glenn, have been great role models. I greatly appreciated their relentless efforts in persuading me to substitute time spent at the bench for time at the beach or on the mountain.

I owe the limitless opportunity put before me to my parents who fled their homeland with little more than the clothes on their backs. I will always draw from their courageous act and never be afraid to dive into the uncertain.

Finally, I would like to thank my future wife, Dianne, for moving out to Portland to be with me. Her kind presence has helped sustain my spirits during these past years.

List of illustrations

List of tables

List of abbreivations

BS - base substitution

CI - confidence intervals

dsDNA - double-stranded deoxyribonucleic acid

FS - frameshift

GHL - gyraseb/Hsp90/MutL

Hsp90 - heat shock protein 90

IDL - insertion/deletion loop

MLH - MutL homologue

MMR - DNA mismatch repair

MSH - MutS homologue

MutLα - Mlh1p and Pms1p

MutLβ - Mlh1p and Mlh3p

MutSα - Msh2p and Msh6p

MutSβ - Msh2p and Msh3p

PCNA - proliferating cell nuclear antigen

PMS - post-mieotic segregration

TCR - transcription coupled repair

UV - ultraviolet

Abstract

Contained within this work, I have investigated the function of predicted ATPase motifs in *S. cerevisiae* MutLα (Mlh1p-Pms1p). My results suggest that yeast MutLα has structural and functional properties consistent with other members of a recently identified family of ATPases. Specifically, my genetic results suggest that both the ATPase motifs of Mlh1p and Pms1p are absolutely required for MMR *in vivo*. In addition, biochemical and *in vivo* findings suggest that ATP-binding induces conformational changes in MutLα that are associated with heterodimerization between the NH_2-termini of Mlh1p and Pms1p. Surprisingly, results of my *in vivo* studies suggest differential requirements for Mlh1p and Pms1p ATPase motifs during MMR. Furthermore, I report results showing both physical and genetic interactions between *EXO1* and the components of MutLα, Mlh1p and Pms1p. The genetic interaction results suggest that one function of the MutLα ATPase domains is to direct Exo1p and other exonucleases during mutation avoidance. Finally, my results are consistent with Exo1p having roles in both MMR-dependent and MMR-independent mutation avoidance pathways.

CHAPTER 1: Background and Significance

Replication of the genome in prokaryotes and eukaryotes is a high fidelity process. Three conserved serial mechanisms act to decrease mismatches arising during replication: (i) Watson-Crick base pairing; (ii) 3'-5' exonuclease proofreading and (iii) DNA mismatch repair (MMR) (Schaaper, 1993). Phenotypes of MMR deficiency are diverse, ranging from increased spontaneous mutation rates to cancer predisposition (Buermeyer, et al., 1999; Harfe and Jinks-Robertson, 2000b). Mutations and epigenetic modifications of the human MMR genes are associated with three types of cancer predisposition syndromes, hereditary non-polyposis colorectal cancer (HNPCC), Muir-Torre syndrome and Turcot syndrome, as well as some sporadic forms of colon cancer (Buermeyer, et al., 1999; Kolodner and Marsischky, 1999). Functions of MMR can be dissected using facile model systems such as *Escherichia coli* and *Saccharomyces cerevisiae* (Jiricny, 1998; Kolodner and Marsischky, 1999). As MMR is highly conserved, studies using yeast and bacteria have accelerated our understanding of MMR in mice and human cells.

E. coli MMR: Mutation Avoidance

Genes involved in MMR were first isolated in screens for spontaneous mutators or "mut" mutants in *E. coli.* (Siegel and Bryson, 1967; Liberfarb and Bryson, 1970; Siegel and Kamel, 1974; Siegel and Ivers, 1975). All known genes involved in *E. coli* MMR have since been identified and used to reconstitute a MMR reaction *in vitro* with purified gene products (Modrich and Lahue, 1996). A primary role of MMR is to correct base-base mismatches and small single-strand loops or insertion/deletion loops (IDLs) resulting from DNA replication, DNA damage, and recombination (Modrich and Lahue, 1996; Jiricny, 1998; Buermeyer, et al., 1999; Kolodner and Marsischky, 1999). There are three central components of this pathway, MutS, MutL and MutH. MutS homodimers are ATPases (Haber and Walker, 1991) which have an approximately 15-fold selectivity for binding double-stranded DNAs (dsDNAs) containing a variety of different mismatches over homoduplex substrates (Jiricny, et al., 1988). Recent crystal structural studies have outlined important domains required for mismatch binding and demonstrate that only one of the MutS protomers makes selective contacts with the mismatch (Lamers, et al., 2000; Obmolova, et al., 2000). MutL homodimers are weak ATPases compared to MutS and function to couple mismatch binding by MutS homodimers to downstream components (Sancar and Hearst, 1993; Ban and Yang, 1998a; Ban and Yang, 1998b; Spampinato and Modrich, 2000; Junop, et al., 2001). Recent studies suggest that the coordination of multiple downstream events, such as nicking and excision of the nascent strand, are facilitated by the intrinsic ATPase activities of the MutL dimer (Ban and Yang, 1998a; Spampinato and Modrich, 2000; Junop, et al., 2001). MutH is a monomeric endonuclease that is activated by the MutS/MutL complex and MutL ATP-hydrolysis to cleave at hemi-methylated GATC sites (Ban and Yang, 1998a; Hall and Matson, 1999; Spampinato and Modrich, 2000; Junop, et al., 2001). *E.coli* MMR is thought to proceed by the following steps (Figure 1-1). MutS homodimer binds the mismatch, followed by the formation of an ATP-binding dependent ternary complex with a homodimer of MutL. Next, MutH is stimulated by the ATP-dependent MutS/MutL ternary complex to nick the un-methylated strand at the nearest hemi-methylated GATC site (Grilley, et al., 1990). In

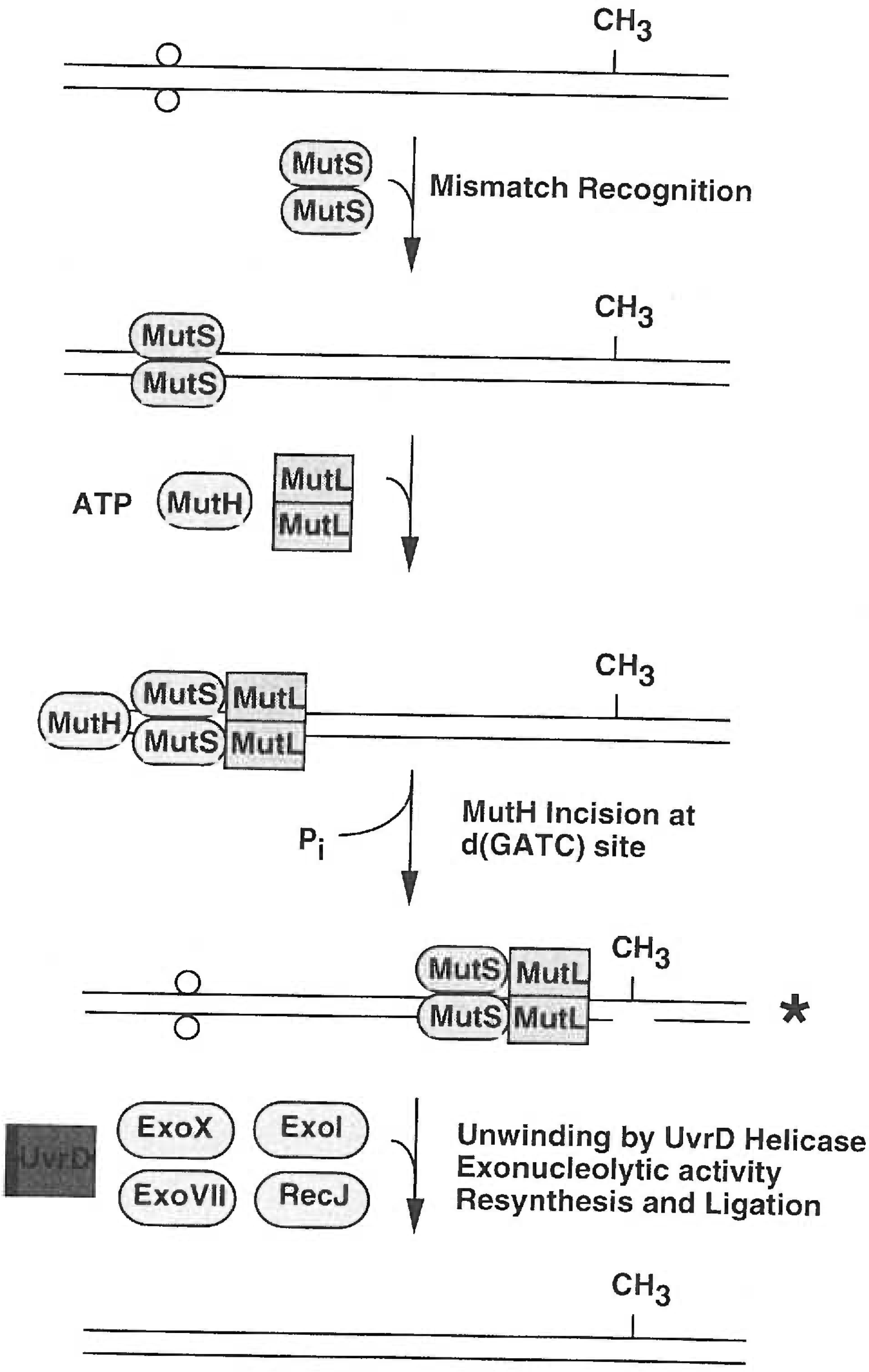

Figure 1-1. ***E. coli*** **MMR.** The details of this model are discussed in the text. The intermediate with an asterisk may proceed via a DNA-loop, with the MutS/ MutL complex fixed at the mismatch or as depicted. Adapted from Shelly, 1999.

E. coli, DNA methylation of the newly synthesized strand lags behind replication on both the leading and lagging strand, with the lagging strand taking twice as long to remethylate (Lyons and Schendel, 1984; Stancheva, et al., 1999). Therefore, the transient un-methylated state of the newly replicated strand provides the "strand discrimination signal" allowing the MMR machinery to differentiate between parental and daughter strands. After incision, UvrD helicase is loaded onto the nick in a MutS/MutL-dependent manner and any one of four exonulceases excise the nascent strand some distance past the mismatch. The *in vitro* system corrects mismatches with strand signals either 5' or 3' to the mismatch, indicating that *in vitro* MMR is bi-directional (Grilley, et al., 1990; Dao and Modrich, 1998; Hall, et al., 1998; Viswanathan and Lovett, 1998; Yamaguchi, et al., 1998; Mechanic, et al., 2000). The resultant single strand gap [up to 1 kilobase (kb)] is filled in by DNA polymerase III and the nick sealed by DNA ligase (Modrich and Lahue, 1996).

E. coli MMR: Suppression of Homeologous Recombination

In *E. coli*, certain MMR proteins prevent recombination between similar, but not identical sequences, so called homeologous recombination. *E. coli* RecBCD dependent recombination occurs 240-fold less between substrates that are 89% identical than between substrates that are 100% identical, but is only 9-fold decreased in a *mutS* strain (Shen and Huang, 1989). Furthermore, MMR *mutS*, *L H* and *U* mutants all result in an increase in conjugation between *E. coli* and *Salmonella typhimurium* which differ by 16% at the sequence level (Rayssiguier, et al., 1989; Zahrt and Maloy, 1997). The mechanism for this MMR-dependent barrier to homeologous recombination is hypothesized to involve disruption of recombination intermediates near sites of heteroduplex formation via two pathways, a MutH-independent early step and a MutH-dependent late step (Zahrt and Maloy, 1997; Stambuk and Radman, 1998).

E. coli **MMR: Transcription-coupled Repair**

Recently, *E. coli* MMR proteins have been shown to be required for transcription-coupled repair (TCR) of cyclobutane pyrimidine dimers arising from ultraviolet (UV) light damage. UV damage to the transcribed DNA strand is repaired in a preferential manner by TCR and appears to be dependent on MutL and MutS. The mechanistic basis for MutL and MutS involvement in TCR is unknown (Mellon and Champe, 1996).

S. cerevisiae **MMR: MutS and MutL Homologues**

In the yeast *S. cerevisiae*, six MutS homologues (MSH) and four MutL homologues (MLH) have been identified (Table 1-1). The diverse functions of each of these homologues in MMR-related processes will be discussed in detail below and are summarized in Figure 1-2.

S. cerevisiae **MMR: Mutation Avoidance**

The mutation avoidance functions of yeast MMR involves multiple MutS and MutL homologues with partially overlapping duties. Nonetheless, eukaryotic MMR appears to operate mechanistically in a similar fashion to their *E. coli* homologues as described above (Jiricny, 1998; Kolodner and Marsischky, 1999). For example, a heterodimer of Msh2p and Msh6p, MutSα, appears to be involved primarily in

Table 1-1. MutS and MutL Homologues.

E. coli	*S. cerevisiae*	**Eukaryotic Functions**
MutS	*MSH1*	Mutation avoidance in mitochondria.
	MSH2	Forms heterodimer with Msh3p or Msh6p to: repair mismatches formed during replication and recombination; remove non-homologous tails during single-strand annealing (only Msh2p-Msh3p); suppression of homeologous recombination; and required for transcription-coupled repair.
	MSH3	Forms MutSβ heterodimer with Msh2p (see above).
	MSH4	Forms heterodimer with Msh5p to promote crossing-over during meiosis.
	MSH5	Forms heterodimer with Msh4p to promote crossing-over during meiosis.
	MSH6	Forms MutSα heterodimer with Msh2p (see above).
MutL	*PMS1*	Forms MutLα heterodimer with Mlh1p to: repair mismatches formed during replication and recombination; suppression of homeologous recombination; and required for transcription-coupled repair.
	MLH1	Forms heterodimer with Pms1p, Mlh2p or Mlh3p and is required for all functions of *PMS1*, *MLH2* and *MLH3* .
	MLH2	Forms heterodimer with Mlh1p to: repair mismatches formed during recombination.
	MLH3	Forms MutLβ heterodimer with Mlh1p to: repair a small fraction of mismatches formed during replication and recombination; and promote crossing-over during meiosis.

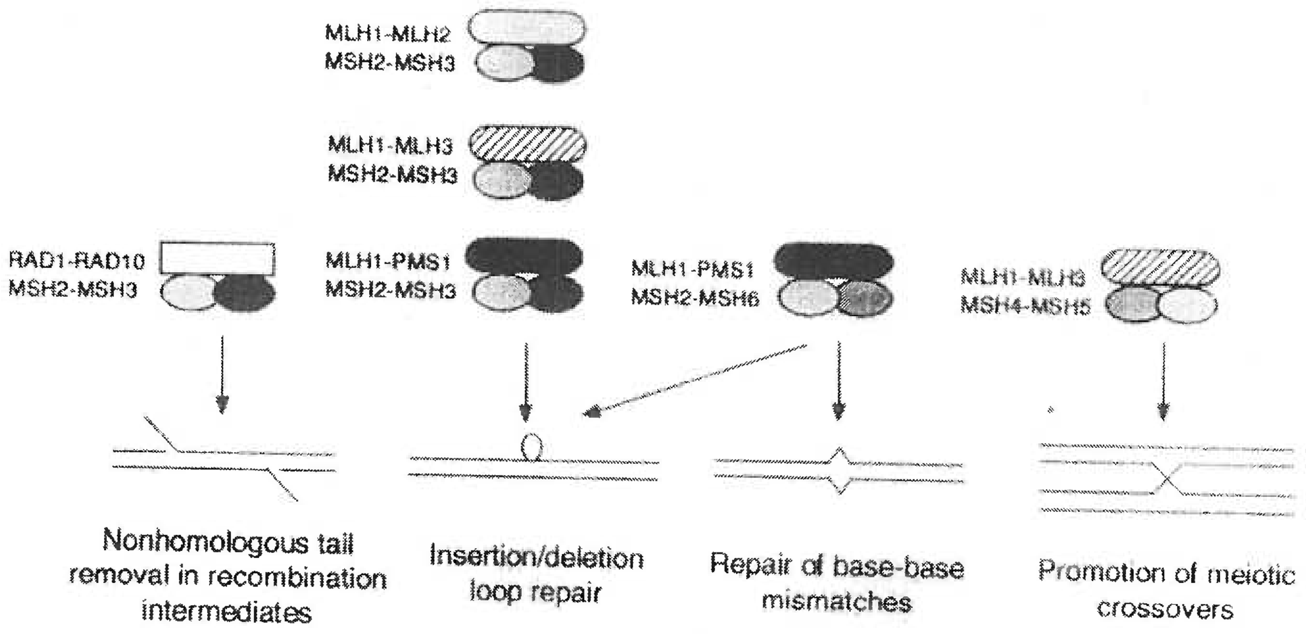

Figure 1-2. Functions of *S. cerevisiae* MSH and MLH heterodimers. Adapted from Harfe and Jinks-Robertson, 2000b.

recognizing base-base mismatches and +1 IDL heterologies (Alani, et al., 1995; Iaccarino, et al., 1996, 1995 #1126; Johnson, et al., 1996b; Marsischky, et al., 1996; Alani, et al., 1997; Studamire, et al., 1998; Bowers, et al., 1999; Marsischky and Kolodner, 1999), whereas, a Msh2p-Msh3p heterodimer, MutSβ, recognizes IDLs of 1-14 bases (Johnson, et al., 1996b; Marsischky, et al., 1996) (Figure 1-2). Similar to *E. coli* MutS both MutSα and MutSβ complexes are also ATPases (Alani, et al., 1997; Studamire, et al., 1998) and only one protomer of each heterodimer is involved in mismatch recognition (Bowers, et al., 1999).

The major MMR MutL activity, MutLα, in yeast is a heterodimer of Mlh1p and Pms1p (Prolla, et al., 1994a; Prolla, et al., 1994b; Habraken, et al., 1997; Pang, et al., 1997). An additional yeast MutL activity, MutLβ, comprised of Mlh1p and Mlh3p, appears to act in conjunction with MutSβ to correct a small fraction of IDLs (Flores-Rozas and Kolodner, 1998) (Figure 1-2). By analogy to *E. coli* MutL, MutLα and MutLβ are most likely necessary to couple the mismatch binding activity of the MutSα/β complexes to downstream effectors in the MMR pathway. Although clearly crucial for MMR, little information has existed on the function of the major MutL activity in yeast, MutLα. Previous studies with yeast have defined COOH-terminal domains as important for Mlh1p and Pms1p interaction (Pang, et al., 1997) and conserved NH_2-terminal residues as necessary for MMR activity (Pang, et al., 1997; Shcherbakova and Kunkel, 1999). However, detailed information on how MutLα couples mismatch binding to downstream steps has not been available. Furthermore, strong sequence similarity between the NH_2-terminus of eukaryotic MLH genes and a novel ATPase fold have recently been reported (Bergerat, et al., 1997), yet no studies have been conducted to directly assess the function that these putative ATPase domains play in MMR.

As with other eukaryotes studied, yeast have no known sequence or structural MutH homologue, partly exemplifying the lack of insight into the mechanism of strand discrimination during eukaryotic MMR. However, one candidate for involvement in strand discrimination is proliferating cell nuclear antigen (PCNA) protein. Physical and genetic studies suggest several possible roles for PCNA protein during the early steps of MMR and during resynthesis of the excision patch (Johnson, et al., 1996a; Umar, et al., 1996; Chen, et al., 1999; Flores-Rozas, et al., 2000; Bowers, et al., 2001). PCNA protein also serves as a processivity factor for polymerase δ and ε and therefore may physically direct MMR towards the nascent strand (Jiricny, 1998; Buermeyer, et al., 1999).

One other likely MMR candidate protein is Exo1p, a 5' -3' dsDNA exonuclease, identified from two independent yeast two-hybrid screens using Msh2p or Mlh1p as baits (Tishkoff, et al., 1997a; Shelley, 1999). In addition, genetic studies suggest that Exo1p performs a catalytic role in MutSα-dependent mutation avoidance (Sokolsky and Alani, 2000). As *E. coli* MMR apparently can utilize any one of four exonucleases (Viswanathan and Lovett, 1998), multiple eukaryotic "MMR" exonucleases are likely to exist. Other potential MMR exonucleases are Rad27p and the proofreading functions of polymerase δ and ε, although more studies are necessary to clarify the roles of these proteins during the excision step of yeast MMR (Johnson, et al., 1995; Tran, et al., 1999). Figure 1-3 incorporates all known and putative eukaryotic protein MMR components in a framework based in part on bacterial MMR (Figure 1-1).

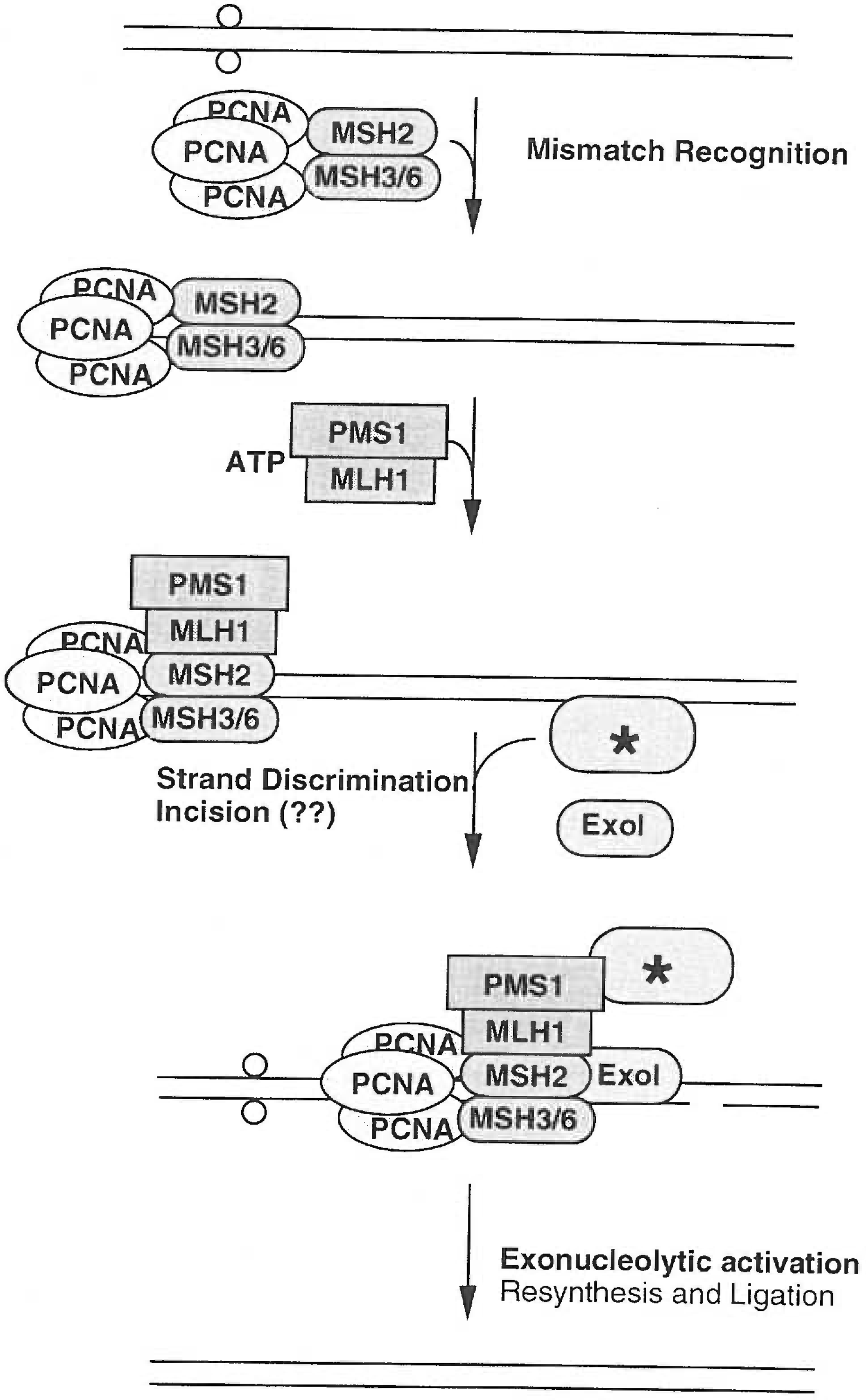

Figure 1-3. Yeast MMR. Details are in the text. Asterisk component represents putative downstream MMR components, i.e. exonucleases and helicases, required for excision of the nascent strand.

S. cerevisiae MMR: Meiosis

MMR was first proposed by Robin Holliday to explain unexpected observations from fungal meiotic recombination (Holliday, 1964). Some fungi, *Ascobulus immersus* and *Neurospora crassa*, produce an ascus that contains all meiotic products in eight (versus four for *S. cerevisiae*) separate spores allowing for simple tracking of recombination events following ascus dissection. Given a heterozygous strain for marker A, the expected Mendelian segregation is 4A:4a. However, in a fraction of dissected asci there will be segregations that result in 6A:2a or 2A:6a patterns, also known as non-reciprocal gene transfers or gene conversions. Occurring even less frequently than gene conversions are 5A:3a or 3A:5a patterns, called post-meiotic segregations (PMS). The frequency of "non-Mendelian" segregations, e.g. 6:2 or 5:3, varies depending on the organism and genetic background. *S. cerevisiae* tetrads are described using the eight-spore nomenclature, for example, a tetrad with the pattern of 1A spore colony, 2a spore colonies and 1 sectored A/a spore colony would be designated as a 3A:5a pattern or PMS. Holliday suggested that gene conversion events (6A:2a or 2A:6a) were the result of heteroduplexes formed during recombination and corrected by a MMR system. Conversely, PMS events could be explained by lack of heteroduplex repair (Figure 1-4) (Holliday, 1964; Paques and Haber, 1999). As predicted, loss of MMR, specifically loss of *MLH1*, *PMS1*, or *MSH2*, results in increases in PMS events and a decrease in gene conversion events (Williamson, et al., 1985; Reenan and Kolodner, 1992; Alani, et al., 1994; Prolla, et al., 1994a). A more subtle role for *MLH2* during correction of meiotic heteroduplexes involving parity or ratios of 5A:3a/6A:2a and 3A:5a/2A:6a has been suggested (Wang, et al., 1999).

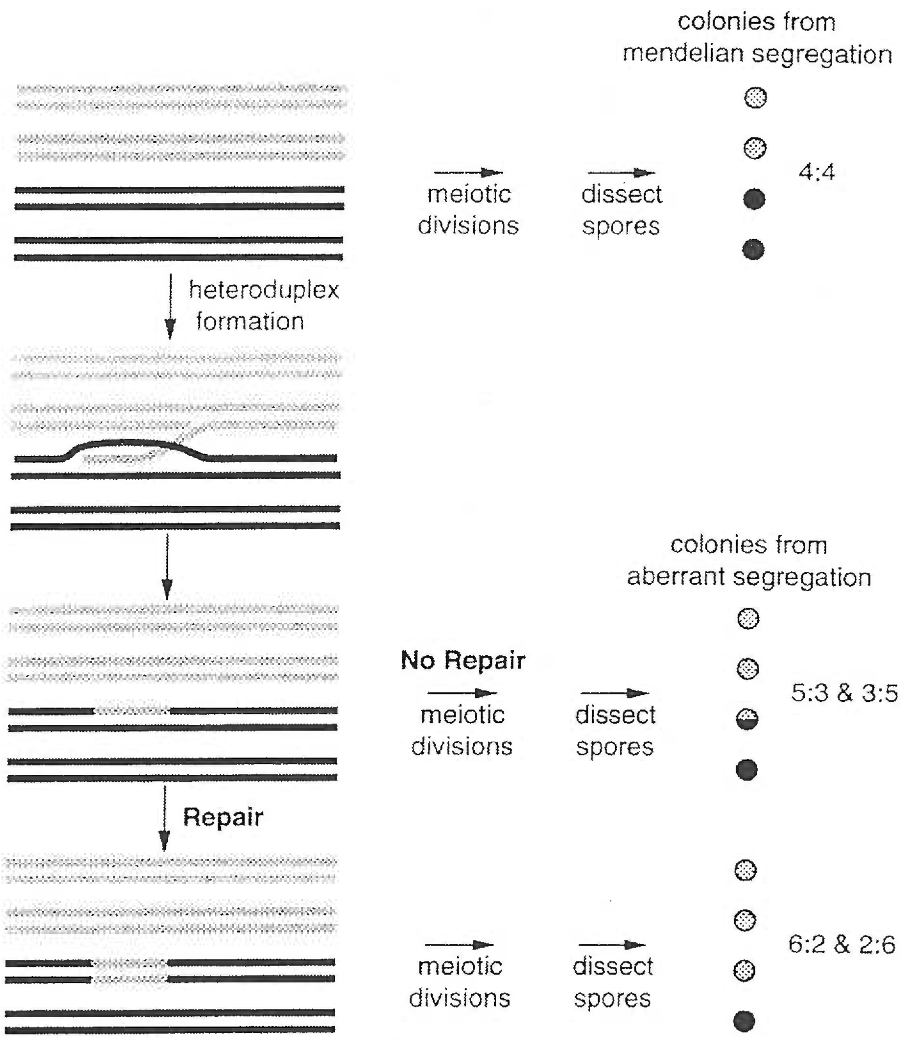

Figure 1-4. Meiotic segregation patterns in *S. cerevisiae.* Details are described in the text. Adapted from Prolla, 1994.

A unique role for MutLβ (Mlh1p/Mlh3p) and the Msh4p-Msh5p complex in crossing-over events during meiosis has been established by several studies in yeast. Epistasis analysis indicates that *MLH1* and *MSH4* operate within the same pathway for crossovers (Ross-Macdonald and Roeder, 1994; Hollingsworth, et al., 1995; Pochart, et al., 1997; Wang, et al., 1999). Three recent studies have also implicated *EXO1* in this *MLH1/MLH3/MSH4/MSH5* pathway for crossing-over (Khazanehdari and Borts, 2000; Kirkpatrick, et al., 2000; Tsubouchi and Ogawa, 2000). The role of MMR proteins in crossing-over during meiosis are unkown.

Spore viability of dissected yeast tetrads is negatively affected by MMR deficiency. Two processes appear to be at work: (i) increased mutation rates result in the accumulation of recessive lethal mutations in diploid yeast (Prolla, et al., 1994a); and (ii) increased non-disjunction at meiosis I as a result of a decrease in crossover events (Ross-Macdonald and Roeder, 1994; Hollingsworth, et al., 1995; Pochart, et al., 1997; Wang, et al., 1999). From Figure 1-2, it is apparent that *MLH1* and *MLH3* mutation can affect both these processes, while mutations in the other MLH and MSH genes should affect spore viability to a lesser degree. In addition, recent reports suggest that *EXO1* also has non-overlapping roles with *MSH4* as the double mutant has a more severe meiotic phenotype than either single mutant (Khazanehdari and Borts, 2000; Tsubouchi and Ogawa, 2000).

S. cerevisiae MMR: Suppression of Homeologous Recombination

Similar to *E. coli*, yeast MMR proteins play a role in suppressing homeologous recombination (Paques and Haber, 1999; Harfe and Jinks-Robertson, 2000c). Studies of either a meiotic interspecific hybrid of *S. cerevisiae* and *S. paradoxus* or a normal *S.*

cerevisiae diploid containing homologous chromosomes with slight sequence divergence have demonstrated that MMR exerts a negative effect on homeologous recombination (Borts and Haber, 1987; Borts, et al., 1990; Chambers, et al., 1996; Hunter, et al., 1996). Studies using an intrachromosomal inverted-repeat assay to analyze the anti-recombinogenic effect of MMR suggest that *MSH2*, *MSH3*, *MSH6*, *MLH1*, *PMS1* and *EXO1* all play roles in suppressing homeologous recombination (Datta, et al., 1996; Datta, et al., 1997; Chen and Jinks-Robertson, 1998; Nicholson, et al., 2000). Furthermore, using this defined system *MSH3*, *MLH1* and *PMS1* exhibited unexpected phenotypes with respect to their roles during mutation avoidance (Datta, et al., 1996; Nicholson, et al., 2000).

S. cerevisiae MMR: Involvement in Single-strand Annealing Recombination

An interesting role for MutSβ (Msh2p-Msh3p) has been demonstrated in a pathway for mitotic recombination termed single-strand annealing (SSA) (Paques and Haber, 1997; Sugawara, et al., 1997; Paques and Haber, 1999). SSA is one means by which to repair a double strand break (DSB) and can result in intrachromosomal deletion products as large as 15 kb (kilobases) between regions of homology as small as 29 bp (Sugawara and Haber, 1992; Sugawara, et al., 2000). MutSβ in conjunction with the Rad1p-Rad10p endonuclease are necessary to cleave non-homologous tails that are encountered during SSA so that DNA synthesis can be primed for completion of the repair event. In contrast to most functions of MMR, *MSH6*, *PMS1* and *MLH1* are not necessary for SSA (Sugawara, et al., 1997).

S. cerevisiae MMR: Transcription-coupled Repair

Yeast MMR proteins appear to have conserved their ability to participate in TCR, as yeast deficient for *msh2* or both *mlh1* and *pms1* are incapable of TCR of thymine glycols, a product of oxidative damage. Remarkably, TCR of UV damage was not affected by defects in MMR and *PMS1* appears to be acting independently of *MLH1* (Leadon and Avrutskaya, 1998). Similar to *E. coli* MMR-dependent TCR, little is known concerning the actions of yeast MMR proteins during TCR.

Mammalian MMR

Phenotypes of MMR deficiency studied thus far in mammalian systems have been a testament to the conservation of MMR between simple and more complex eukaryotes. The majority of overlapping studies conducted in yeast and mammalian systems have produced a wealth of evidence confirming general functions of MMR in the two model systems (Buermeyer, et al., 1999; Harfe and Jinks-Robertson, 2000b). One important advantage of the mammalian system is the ability to examine the effect of MMR deficiency on tumorigenesis. Despite this limitation, MMR studies in yeast continues to stimulate and complement parallel studies performed in mammals.

Thesis Prospectus

Contained within this work, I have investigated the function of predicted ATPase motifs in *S. cerevisiae* MutLα (Mlh1p-Pms1p). My results suggest that yeast MutLα has structural and functional properties consistent with other members of a recently identified family of ATPases. Specifically, my genetic results suggest that both the ATPase motifs of Mlh1p and Pms1p are absolutely required for MMR *in vivo*. In addition, biochemical and *in vivo* findings suggest that ATP-binding induces conformational changes in MutLα that are associated with heterodimerization between the NH_2-termini of Mlh1p and Pms1p. Surprisingly, results of my *in vivo* studies suggest differential requirements for Mlh1p and Pms1p ATPase motifs during MMR. Furthermore, I report results showing both physical and genetic interactions between *EXO1* and the components of MutLα, Mlh1p and Pms1p. The genetic interaction results suggest that one function of the MutLα ATPase domains is to direct Exo1p and other exonucleases during mutation avoidance. Finally, my results are consistent with Exo1p having roles in both MMR-dependent and MMR-independent mutation avoidance pathways.

CHAPTER 2:Materials and Methods

Strains and media.

E. coli strains DH5α and DH-10B were used for plasmid construction and amplification. *E. coli* MAX Efficiency® DH-10Bac™ (F- *mcr*A D(*mrr-hsd*RMS-*mcr*BC) ϕ80d*lac*ZDM15 *ΔlacX74 deo*R *rec*A1 *end*A1 *ara*D139 *Δ*(*ara, leu*)7697 *gal*U *gal*K *λ*- *rps*L *nup*G /bMON14272 /pMON7124) was used to produce recombinant baculoviruses as described below in subsection "Expression and purification of yeast MutLα". *S. cerevisiae* strains used in this thesis are described in APPENDIX A. Bacterial and yeast strains were grown under conditions described previously (Pang, et al., 1997). Yeast transformations were performed by the polyethylene glycol-lithium acetate method (Gietz and Schiestl, 1991).

Deletions of *mlh1Δ* and *pms1Δ* in the GCY35 (New, et al., 1993) background were created as described (Petes, et al., 1991; Pang, et al., 1997).

Genomic *mlh1* point mutant strains used in this thesis (see APPENDIX A) were created with a two-step recombination procedure. Targeting constructs pYI-mlh1-31, and –98 were digested with *Pst*I and transformed into appropriate strains. Purified Ura+ transformants were replica plated onto yeast extract-peptone-dextrose (YPD) plates and grown overnight. YPD replica plates were replica plated to 5-fluoroorotic acid (5-FOA) containing plates. Purified 5-FOA^R isolates were screened for retention of the *mlh1* point mutant allele by mutator replica patch test for *hom3-10* reversion and point mutation confirmed by sequencing a PCR amplicon of the *MLH1* gene. Both alleles were screened using the same PCR oligos: yMLH1.S (5'-

CGGGATCCCTCGAGACACCATGTCTCTCAGAATAAAAGC-3') and yMLH1-F96A anchor.R (5'-GGAGTAAACGCTGTTCAAAGCTCT-3'). Alleles *mlh1-E31A and mlh1-G98A* were sequenced using oligos: ymlh1-98.AS (5'-GGCTAAAGCTTCAGCTCGGAATCCATACGTTTGAATCTG-3') and ymlh1-31.S (5'-CCCGTAAATGCTCTCAAAGCTATGATGGAGAATTCC-3'), respectively. All double point mutant strains, PTY400, 500, 501 and 600, were generated by mutation of the *MLH1* gene last.

Genomic *pms1* point mutant strains were created in a similarly using targeting constructs pYI-pms1-61 and –128 TV II digested with *Mlu*I or *Xba*I. PCR oligos yPMS1-86.S (5'- GTATGTCCAGCAGTTTCCATCAG-3') and yPMS1-1281.AS (5'-GCAAGCTTATCGGTGTATTTCCCAAGCATTC-3') were used to amplify a portion of the *PMS1* gene and the resulting PCR product was sequenced with oligos ypms1-128.AS (5'-GAAGATAGGGCCTCAGCTCTAAACCCTAACGTCTGTACTTTAGC-3') and ypms1-61.S (5'-ACAACTGCAGTGAAAGCTCTCGTTGATAATAGTATAGATGCG-3') for *pms1-E61A* and *pms1-G128A* alleles, respectively.

Disruptions of *mlh3Δ* were generated by transforming with *Xho*I and *Sac*I digested pΔmlh3::hisG-URA3-hisG (Alani, et al., 1987) and selecting on –Ura dropout media. Targeting of *mlh3* was confirmed by southern analysis of *Eco*RV digested genomic DNA with a PCR generated probe using oligos: 5'-TGGTTCGCCGATCTTATC-3' and 5'-AAATACACTCCCTCTCCATCAC-3'.

Disruptions of *EXO1* were generated as described previously (Tishkoff, et al., 1997a). An *exo1::HIS3* disruption cassette was generated by PCR using strain EAY618 (Dr. E. Alani, Cornell University) as a template, transformed into yeast and targeting was confirmed by three-oligo PCR. Oligos exo1-135.S3, 5'-AAGCTATGTTGGGTGGAACTGAGG-3', and exo1-443.AS2, 5'-TCATTATGTGATAATGCCAATCG-3', were used to detect the targeted allele. Oligos exo1-135.S3 and exo1-588.AS3, 5'-AGTGATACT GGATTCTGTATGGGCT-3', were used to detect the wildtype allele.

Disruptions of *REV3* were created by transforming the pYPG101 construct (Dr. D. Hinkle, Rochester University) after *Kpn*I digestion and selecting for Ura+ prototrophs. The *rev3Δ* genotype was confirmed by *SnaB*I Southern analysis and the phenotype by sensitivity to a 1.5-hour exposure to 0.5 mM cisplatin. The *REV3* Southern probe was generated by PCR using oligos, REV3.F, 5'-ATTGAAGTAAAGAGAACC-3', and REV3.R, 5'-TGGAGCAGTATTGTATCG-3'. The generation of the other strains used in this thesis were described previously as referenced in APPENDIX A.

Plasmid construction.

All DNA manipulations were performed using standard molecular biology procedures (Maniatis, et al., 1982). Automated DNA sequencing was done at the Vollum Institute core sequencing facilities with an ABI automated sequencer.

(i) Targeting vectors. pYI-mlh1-31 was created as follows. The *MLH1* ORF and approximately 800 bp of upstream sequence were cloned into pYI-*lac*Z. The E31A mutation was generated in the resultant construct using Quikchange^{TM} Site-Directed Mutagenesis Kit (Stratagene) and the following oligos: ymlh1-31.S and ymlh1-31.AS (5'-GGAATTCTCCATCATAGCTTTGAGAGCATTTACGGG-3'). Desired mutations were detected by sequencing with oligo ymlh1-98.AS. An approximately 400 bp *Kpn*I fragment containing the E31A mutation was cloned back into the parental construct to erase the potential for second site mutations elsewhere in the construct. pYI-mlh1-98 was created in a similar fashion except the following oligos were used instead: ymlh1-98.S (5'-CAGATTCAAACGTATGGATTCCGAGCTGAAGCTTTAGCC-3') and ymlh1-98.AS for mutagenesis; and ymlh1-31.s for identification of the point mutation.

pYI-pms1-61 TV II was constructed as follows. pYI-ypms1 TV II was generated by PCR to contain 686 bp upstream of the ATG codon to position 2426 of the *yPMS1* ORF in pYI-*lac*Z. A *Pst*I-*Bsp*MI fragment from pFB-ypms1-61 (see below) that contained the E61A codon mutation was used to replace the wildtype *Pst*I-*Bsp*MI fragment of pYI-ypms1 TV II to create pYI-pms1-61 TV II. pYI-pms1-128 TV II was created similarly with a *Pst*I-*Bsp*MI fragment from pFB-ypms1-128 (see below) that contained the G128A codon mutation. pYI-ypms1-61 and –128 TV II were both shown to be free of second site mutations in germane regions by sequencing.

pΔmlh3::hisG-URA3-hisG was a kind gift from David Jacobson (Oregon Health Sciences University, Department of Molecular and Medical Genetics).

(ii) Two-hybrid vectors. All the following constructs were sequenced to confirm point mutations were present in the desired plasmids. pNBTM116 was a generous gift of Dr. Stanley Hollenberg (Oregon Health Sciences University, Department of Cell and Developmental Biology) and allows construction of two-hybrid "bait" fusions with the lexA DNA binding domain fused at the carboxy terminus of the "bait" protein. pNBTM-mlh1 N-354 was engineered using oligos ymlh1 N-anchor.S (5'-CGGGATCCATGTCTCTCAGAATAAAAGCAC-3') and ymlh1 N-354.AS (5'-AGCCTCGAGCTCTGGCTTGTTTGTTGAAATTG-3') to generate a PCR amplicon that was cloned into pNBTM116 at *Bam*HI and *Xho*I sites. Plasmid pNBTM-mlh1-31 N-354 was generated in an identical fashion but the PCR was performed on template DNA that contained the E31A codon mutation.

pNBTM-pms1 N-401 and pNBTM-pms1-61 N-401 were generated using a similar procedure to pNBTM-mlh1 N-354 but used oligos ypms1 N-anchor.S (5'-CGGGATCCAAAATGTTTCACCACATCGAAAAC-3') and ypms1 N-401.AS (5'-AGCCTCGAGTTGTGAGCACATTCTTTTGGG-3'). The pNBTM-pms1-61, -128 N-401 double point mutant was made by using Quikchange™ Site-Directed Mutagenesis Kit (Stratagene) with plasmid pNBTM-pms1-61 N-401 and the ypms1-128.S and .AS oligos.

pCAD3 analogous to pNBTM116 allows fusion of the GAL4 activation domain to the carboxy terminus of the "prey" protein (Printen and Sprague, 1994). pCAD-mlh1 N-354 and alanine point mutation version (E31A) were constructed by cloning a PCR product generated from oligos ymlh1 N-anchor.S and ymlh1 N-354(BamHI).AS (5'-AGCGGATCCCTCTGGCTTGTTTGTTGAAATTG-3') into pCAD3 at a *Bam*HI site. Plasmids with correct insert orientation were isolated for further study. The pCAD-mlh1-31, -98 N-354 double point mutant was made by using Quikchange™ Site-Directed Mutagenesis Kit (Stratagene) with construct pCAD-mlh1-31 N-354 and the ymlh1-98.S and .AS oligos.

pCAD-pms1-61 N-401 was created in a likewise fashion except oligos ypms1 N-anchor.S and ypms1 N-401(BamHI).AS (5'-AGCGGATCCTTGTGAGCACATTCTTTTGGG-3') were used.

pBTM-MSH2 and pBTM-MSH6 were constructed by cloning the coding sequences for yeast Msh2p and Msh6p into the two-hybrid "bait" vector pBTM116 (Vojtek, et al., 1993). The other constructs used in this thesis were described previously (Pang, et al., 1997)

(iii) Baculoviral plasmids. The 6xHis-MLH1 recombinant baculovirus was constructed as follows: a PCR product was generated that engineered a 6xHis affinity tag inframe with the *MLH1* ORF after the initiator methionine. This 6xHis encoding PCR product was cloned into the *Bam*HI and *Nde*I restriction sites of pBTM-MLH1, replacing approximately 360 bp of the native gene. Automated sequencing of the construct confirmed that the 6xHis tag was inframe with the *MLH1* ORF and that no PCR generated mutations arose. The 6xHis-*MLH1* ORF was then cloned into pFastBac DUAL (pFBD) (Life Technologies) using polylinker sites *Bam*HI and *Sal*I. Based upon mutator assays, the 6xHis epitope tagged Mlh1p functionally complemented a *mlh1Δ* strain (data not shown).

The PMS1 recombinant baculovirus was produced as follows: the *PMS1* ORF was removed from genomic clone pJH480-PMS1 using *Ase*I and *Sal*I restriction enzymes and ligated to a synthetic linker containing *Ase*I and *Nco*I compatible overhangs. This *PMS1* ORF ligation product was then cloned into pEAE51 at sites *Nco*I and *Sal*I replacing the *MSH6* ORF (Alani, et al., 1997). The *PMS1* ORF was then excised using *Xho*I and *Sal*I restriction enzymes and ligated into the pFastBac1 (pFB) (Life Technologies) polylinker at a *Xho*I site. A pFB-PMS1 construct in the desired orientation was identified and sequenced to examine the site of the synthetic linker.

Two-hybrid screening and mating and β-galactosidase assays.

The two-hybrid screening was performed as described previously (Umar, et al., 1996) with a yeast cDNA expression library (Dr. S. Elledge, Baylor College of Medicine).

Direct "one-on-one" protein-protein interactions were assessed using the two-hybrid technique and experiments repeated at least two times. "Bait" and "prey" plasmids were transformed into L40 and AMR70 yeast, respectively. Transformants were streak purified once on selective media. L40-"bait" strains were mated with AMR70-"prey" strains on YPD plates at 30°C for 5-12 hours, replica plated onto –Trp-His-Ura-Leu-Lys (-THULL) and –Ura-Trp-Leu (-UTL) plates and incubated at 30°C for 2-3 days. Growth on –UTL plates indicated efficiency of mating, while growth on –THULL plates indicated "bait"-"prey" interaction. Expression of a subset of constructs were confirmed by western blotting of L40 strains with the indicated "bait" or "prey". Extracts were made from 10-ml saturated cultures by glass bead lysis for 30 minutes at 4 °C in 25 mM Tris, pH 7.5, 1 mM EDTA, 10 mM mM β -mercaptoethanol (β -ME),1 mM phenylmethylsulfonyl fluoride (PMSF) and Complete proteolysis inhibitor (Roche Molecular Biochemicals); centrifuged at 14,000 xg for 5 minutes; and concentration of soluble fractions determined by Bradford (BioRad). 10-15 µg of each extract was separated by SDS-PAGE on 10% gels, transferred to nylon membranes (Ambion), probed with the either anti-GAL4-TA (1:200 dilution) or anti-lexA-DB (1:200 diltuion) (Santa Cruz Bio. Inc.), followed by the appropriate secondary antibody and detected using chemiluminescence.

Diploid L40/AMR70 is homozygous for a second chromosomal lexA-GAL4A reporter system , *URA3::(lexAop)* $_8$*-lacZ*. β-galactosidase assays were performed on –THULL plates as described (Umar, et al., 1996) or β-galactosidase liquid assays were performed as described previously (Pang, et al., 1997). β-galactosidase units = $[(OD_{420}/OD_{600})60]$/minutes, where OD_{420} and OD_{600} are the optical densities at 420 and 600 nm, respectively.

Strains were streak purified, individual colonies grown to saturation in YPD, then various dilutions plated onto complete synthetic media (CSM), -Thr and +canavanine (+CAN) [@ 60 µg/ml] plates and colonies counted after 2-3 days growth at 30°C. Rates were determined as previously described (Pang, et al., 1997). Statistical analyses were performed for pairwise compairsons of rates using a two-tailed Mann-Whitney test with Prism 2.0a software (GraphPad Software Inc.); P values < 0.05 were considered statistically significant. We used the 95% confidence intervals of relative mutation rates to determine if epistasis conclusions were statistically significant.

Canavanine resistant (Can^R) mutations were identified from genomic preparations using the glass bead lysis method, followed by PCR of the *CAN1* gene as described previously (Tran and Liskay, 2000), and direct sequencing of the QIAquick™ (Qiagen®) purified PCR amplicon with an ABI automated sequencer. χ^2-analysis was used to determine if changes in mutational spectrum were statistically significant ($P < 0.05$). Rates of frameshifts (FS) and base substitutions (BS) at *CAN1* were calculated using absolute mutation rates determined at *CAN1* multiplied by the frequency with which FS or BS mutations occurred in the particular strain. As the calculated rates of FS and BS at

CAN1 possess the product of two different forms of error, statistical analysis was not performed on these values.

Expression and purification of yeast MutLα.

The Bac-to-Bac Baculovirus® (Life Technologies) expression system was used to express MutLα in *Spodoptera frugiperda* (*Sf*9) cells infected with recombinant baculovirus. Recombinant baculoviruses that express 6xHis-Mlh1p and Pms1p were created as described by the manufacturer's instructions (Bac-to-Bac Baculovirus expression system, Life Technologies). A 200-ml culture of *Sf*9 cells, typically 1-2 x10^6 cells/ml, were co-infected with recombinant baculoviruses at multiplicities of infection of 2-2.5 and 11-15 for 6xHis-Mlh1p- and Pms1p-expressing baculoviruses, respectively. Cells were harvested at 44-48 hours of co-infection, frozen as cell pellets using liquid nitrogen and stored at -80 °C.

All subsequent steps were performed at 0-4 °C and purification monitored by sodium dodecyl sulfate-polyacrylamide gel electrophoresis (SDS-PAGE) and western blot analysis. Western blots were probed with a (1:1000) dilution of anti-4xHis monoclonal antibody (Qiagen) or a cross-reacting (1:100) dilution of anti-hPms2p polyclonal antibody and then visualized using (1:2000) of anti-mIgG-HRP (Pierce) or (1:1250) dilution of anti-rIgG-HRP (BioRad), respectively, and Enhanced Luminol Reagent (NEN). All buffers included 0.5-1 mM PMSF (Sigma Chemicals), 4-10 μg/ml leupeptin (Sigma Chemicals), and 4-10 μg/ml aprotinin (Sigma Chemicals). Cell pellets were resuspended in 5-ml of *Sf*9 lysis buffer per gram of wet cell pellet (*Sf*9 lysis buffer: 50 mM Tris-HCl (pH 7.6), 5 mM β-ME, 100 mM KCl, Complete-Mini EDTA

Free® pills (1pill/ 5- or 10-ml) (Roche Molecular Biochemicals), and 1% Nonidet® P-40 (NP-40) (Sigma Chemicals)). The cell lysate was then spun at 10,000xg for 10 minutes. The cleared lysate was incubated in batch with 1.0-ml of a 50% slurry of Ni-NTA® agarose resin (Qiagen) in buffer H (400 mM NaCl, 25 mM Tris-HCl (pH 7.8), 20% glycerol, and 5 mM β -ME) + 0.6 M $(NH_4)_2SO_4$ and 10-15 mM imidazole (pH 8) for 1-hr.. The resin was washed in batch three times: once with 40-ml of buffer H + 0.6 M $(NH_4)_2SO_4$, and 25 mM imidazole; and twice with 40-ml of buffer H + 0.6 M $(NH_4)_2SO_4$, and 50 mM imidazole. The resin was loaded onto an Econo-column® (BioRad) and eluted with buffer H + 0.5 M imidazole. Peak fractions were pooled, desalted into buffer T (50 mM Tris-HCl (pH 7.8) 10% glyercol, and 1 mM DTT) + 100mM NaCl and 0.01% NP-40 using PD-10 desalting columns (Amersham Pharmacia Biotechnologies), and further purified on a 1-ml HiTrap Heparin column using a 4.5% NaCl/ml gradient. Peak fractions were concentrated using Vivaspin 500® (50,000 MWCO) (Vivascience Limited, Brinbrook Hill, UK) as described by the manufacturers. Concentrated fractions were frozen in liquid nitrogen and stored at -80°C. Protein concentration was determined by scanning densitometry with NIH image 1.61 software using bovine serum albumin (BSA) standards (Pierce).

Limited Proteolysis Assays.

Limited proteolysis reactions (20 μl) consisted of 150 ng of MutLα, 30 mM Tris (pH 7.6), 150 mM NaCl, 5 mM $MgCl_2$, 0.5 mM DTE and +/- 5 mM ATP, AMP-PNP, ATPγS or ADP. Reactions were incubated for 15 minutes at 30°C, followed by the addition of 50 ng of modified trypsin (Promega Corp.), incubation at 30°C for a specified interval, addition of SDS-sample buffer and boiling for 7 minutes. Processed reactions were separated on a 10% SDS-PAGE gel, transferred onto PVDF membranes (Ambion) and western blotting performed with specified antibodies. Anti-4xHis westerns were performed as described above. The anti-Mlh1p polyclonal antibody was a kind gift of Dr. T. Kunkel (NIEHS) and was generated against a COOH-terminal peptide of yeast Mlh1p. The anti-Mlh1p polyclonal antibody was used to probe limited proteolysis blots at a (1:10000) dilution and detected as described above.

CHAPTER 3: Functional Studies on the Candidate ATPase Domains of *Saccharomyces cerevisiae* MutLα

Introduction

An important clue to a possible biochemical activity of the MutL homologues was the appreciation of sequence similarity between the highly conserved NH_2-termini of the MutLs and a new family of ATPases (Bergerat, et al., 1997; Mushegian, et al., 1997). The so-called GHL ATPase family is comprised of *E. coli* gyrase b subunit, the Hsp90 homologues and the MutL homologues (Ban and Yang, 1998a; Dutta and Inouye, 2000). The supercoiling activity of *E. coli* DNA gyrase is dependent on the ATPase activity of the homodimeric gyrase b subunits (Sugino and Cozzarelli, 1980). Recently, the homodimer Hsp90 has been demonstrated to have a weak intrinsic ATPase activity required for Hsp90 function (Obermann, et al., 1998; Panaretou, et al., 1998). The crystal structures of the NH_2-termini of Hsp90 and gyrase b revealed strong structural similarity within their ATPase motifs (Wigley, et al., 1991; Prodromou, et al., 1997a; Prodromou, et al., 1997b). In addition, Hsp90 and gyrase b appear to have similar ATPase cycles which include functionally important NH_2-terminal conformational changes (Wigley, et al., 1991; Ali, et al., 1993; Grenert, et al., 1997; Prodromou, et al., 1997a; Prodromou, et al., 1997b; Grenert, et al., 1999). The NH_2-terminal conformational changes for the other GHL ATPases have been associated with dimerization of the NH_2-terminal domains in the ATP-bound form (Wigley, et al., 1991; Ali, et al., 1993; Prodromou, et al., 1997a; Prodromou, et al., 1997b; Ban, et al., 1999; Grenert, et al., 1999; Prodromou, et al., 1999; Chadli, et al., 2000; Prodromou, et al., 2000; Spampinato and Modrich, 2000; Young and

Hartl, 2000). Recently, the crystal structure of an NH_2-terminal fragment of MutL was solved and demonstrated that MutL possesses an ATP-binding pocket homologous to the gyrase b and Hsp90 proteins (Ban and Yang, 1998a; Spampinato and Modrich, 2000). In addition, MutL appears to have the ATPase-dependent NH_2-terminal dimerization cycle found in the other GHL family members. Interestingly, Ban *et. al.* reported that the NH_2-terminal dimerized, ATP-bound form of MutL could activate the MutH endonuclease in a MutS-independent manner (Ban and Yang, 1998a; Ban, et al., 1999).

Previous work from this lab has shown the importance of the NH_2-terminus of yeast Mlh1p and Pms1p in MMR (Pang, et al., 1997). The above mentioned findings for the GHL family of proteins presented a working paradigm for detailed studies of the ATPase motifs found in the eukaryotic MutL homologues. In this chapter, I investigate the function of predicted ATPase motifs in *S. cerevisiae* MutLα (Mlh1p-Pms1p). My results suggest that yeast MutLα has structural and functional properties consistent with other members of the GHL family of ATPases. Specifically, my genetic results suggest that both the ATPase motifs of Mlh1p and Pms1p are required for MMR *in vivo*. In addition, biochemical and *in vivo* findings suggest that ATP-binding induces conformational changes in MutLα that are important for MMR and are associated with heterodimerization between the NH_2-termini of Mlh1p and Pms1p. Surprisingly, my genetic results suggest differential requirements for Mlh1p and Pms1p ATPase motifs during MMR.

Experimental rationale.

To examine the importance of putative ATPase domains of *S. cerevisiae* Mlh1p and Pms1p, I examined the effects of mutations introduced at two of the ATPase motifs, I and III, conserved in the GHL family (Figure 3-1). I chose to examine residues E31and E61 of Mlh1p and Pms1p, respectively, because mutations made at the homologous glutamate of MutL, gyrase B and Hsp90 have been shown to eliminate ATP-hydrolysis with little or no effect on ATP-binding (Jackson and Maxwell, 1993; Ban and Yang, 1998a; Obermann, et al., 1998; Panaretou, et al., 1998; Ban, et al., 1999). In motif III, I focused on residues G98 and G128 of Mlh1p and Pms1p, respectively, which are modeled to affect ATP-binding and/or an associated conformational change induced upon ATP-binding (Grenert, et al., 1997; Ban and Yang, 1998a; Obermann, et al., 1998; Panaretou, et al., 1998; Ban, et al., 1999). For the sake of clarity I will refer to alanine substitution mutations at E31and E61 as "ATP-hydrolysis" mutations and the mutations G98A and G128A as "ATP-binding" mutations.

The genetic analysis of these "ATPase" mutants included mutation rate measurements at *hom3-10* and *CAN1*, and mutational spectrum analysis using the *CAN1* reporter. The *hom3-10* allele is a reversion assay that reports a ΔT-A bp in a run of 7 T-A bp and is considered diagnostic for defects in MMR (Chen, et al., 1999). In contrast, forward mutation at *CAN1* reports a wide variety of inactivating mutations, allowing mutational spectrum determinations (Chen, et al., 1999).

gyrase b	38	mvf**E**vvdnaidea	20	qddgrgi	34	gglh**G**vgvsv	41	gt	640
h_Hsp90	43	flr**E**lisnssdal	35	vdtgigm	32	igqf**G**vgfys	42	gt	549
MutL	25	vvk**E**lvensldag	18	rdngcgi	28	lgfr**G**ealas	40	gt	473
yMlh1p	27	alk**E**mmensidan	18	tdngsgi	28	ygfr**G**ealas	40	gt	624
yPms1p	57	avk**E**lvdnsidan	18	sdngdgi	28	lgfr**G**ealss	39	gt	730

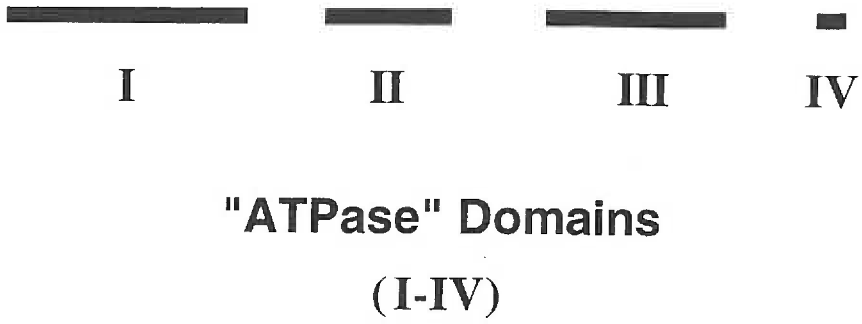

Figure 3-1. **NH2-terminal ATPase domains of GHL ATPases**. ATPase motifs I-IV are designated with black boxes and sequences are shown above motif boxes. Numbers correspond to the number of amino acids preceding or following sequence alignments. Bold letters are the absolutely conserved residues that were substituted with alanine in Mlh1p and Pms1p.

Predicted ATPase residues of MutLα are necessary for MMR *in vivo*.

To address whether the ATP-hydrolysis and –binding motifs of MutLα are necessary for mutation avoidance by MMR, double missense mutants, e.g. *mlh1-E31A pms1-E61A*, were generated and examined for spontaneous mutation rate (see CHAPTER 2: Materials and Methods). Relative to the wildtype strain, both the double ATP-hydrolysis mutant (strain PTY400) and the double ATP-binding mutant (strain PTY600) exhibited spontaneous mutation rates similar to that observed in *mlh1Δ* and *pms1Δ* strains (Table 3-1, compare strains PTY400 and PTY600 vs. PTY100 and PTY101). The mutator phenotype of a complex double mutant, *mlh1* hydrolysis mutant plus *pms1* binding mutant, or vice versa, was also similar to a MMR deficient (e.g. *mlh1Δ*) strain (Table 3-1, compare strains PTY500 and PTY501 vs. PTY100 and PTY101). These data indicate that any combination of double ATP-hydrolysis and/or –binding mutations affecting MutLα result in defects in the mutation avoidance functions of MMR comparable to the defects seen in the single *mlh1Δ* and *pms1Δ* strains.

Mutator effects of single alterations in the putative ATPase domains of *S. cerevisiae* MutLα.

To examine the individual contributions of Mlh1p and Pms1p ATPase motifs to MutLα function, I examined the effect of single missense mutations on mutation avoidance. As shown in Table 3-1, the single missense mutations affecting the ATPase motifs had effects on mutation avoidance that were significantly less than the corresponding *mlh1Δ* and *pms1Δ* strains, with the exception of the *mlh1-G98A* binding mutant (PTY300) which was only slightly less than the *mlh1Δ* strain (PTY100).

Table 3-1. Mutation rate effects of genomic mutations altering the NH_2-termini of MutLα (& MutLβ).

STRAIN[1]	RELEVANT GENOTYPE	BIOCHEMICAL DEFICIENCY[2]	FOLD MUTATOR (RATE ±SD)[3]			
			hom3-10^6		Can^{R,7}	
GCY35	*Wildtype*	--	1		1	
PTY100	*mlh1Δ*	--	1253	±301	29	±6
PTY101	*pms1Δ*	--	1212	±79	28	±5
PTY102	*mlh3Δ*	--	4	±1	2	±1
PTY103	*mlh1Δ mlh3Δ*	--	919	±13	20	±2
PTY104	*pms1Δ mlh3Δ*	--	1051	±199	27	±2
PTY400	*mlh1-E31A pms1-E61A*	ATP hydrolysis[4]	715	±291	26	±8
PTY600	*mlh1-G98A pms1-G128A*	ATP binding/heterodimerization[4]	831	±41	22	±2
PTY200	*mlh1-E31A*	ATP hydrolysis[5]	311	±135	7	±2
PTY201	*pms1-E61A*	ATP hydrolysis[5]	19	±8	1	±0.5
PTY202	*pms1-E61A mlh3Δ*	ATP hydrolysis[5]	60	±31	2	±0.8
PTY300	*mlh1-G98A*	ATP binding/heterodimerization[5]	725	±126	22	±8
PTY301	*pms1-G128A*	ATP binding/heterodimerization[5]	78	±28	4	±1
PTY302	*pms1-G128A mlh3Δ*	ATP binding/heterodimerization[5]	159	±63	5	±0.6
PTY500	*mlh1-E31A pms1-G128A*	Complex effect (?)[4]	681	±80	25	±14
PTY501	*mlh1-G98A pms1-E61A*	Complex effect (?)[4]	651	±104	25	±6

---

[1] – Similar results for strains W303 (*mlh1*) and MW3317-21A (*pms1*) (Unpublished data, P.T.T & R.M.L.).

[2] – Predicted from studies of MutL (Ban and Yang, 1998; and Ban and Yang, 1999), DNA gyrase (Jackson and Maxwell, 1993) and Hsp90 proteins (Obermann *et. al.*, 1998; and Panaretou *et. al.*, 1998).

[3] – Experiments repeated 2-5 times with 5-11 cultures per experiment (CHAPTER 2: Materials and Methods).

[4] – The entire MutLα heterodimer is affected.

[5] – Only one protomer of the heterodimer(s) is affected.

[6] – Wildtype GCY35 rate of $9.90\text{x}10^{-09}$.

[7] – Wildtype GCY35 rate of $3.01\text{x}10^{-07}$.

Interestingly, the homologous ATPase mutations made in *MLH1* and *PMS1* produced different effects on mutation avoidance. The *mlh1-E31A* hydrolysis mutant (PTY200) displayed a 16-fold and 7-fold higher rate of mutation at *hom3-10* and *CAN1*, respectively, than the corresponding *pms1-E61A* hydrolysis mutant strain PTY201 ($P < 0.0286$ for both loci). Likewise, the *mlh1-G98A* binding mutant (PTY300) showed a 9-fold and 5.5-fold higher rate of mutation at *hom3-10* and *CAN1*, respectively, than the corresponding *pms1-G128A* binding mutant strain PTY301 ($P < 0.0286$ for both loci). One trivial explanation for the differential effects of homologous *mlh1* and *pms1* mutations on mutation avoidance was that *MLH3*, which is involved in a minor mutation avoidance pathway (Flores-Rozas and Kolodner, 1998), compensates for the *pms1* mutations. However, as shown in Table 3-1, *pms1* missense mutant strains deleted for *MLH3*, PTY202 (*pms1-E61A mlh3Δ*) and PTY302 (*pms1-G128A mlh3Δ*), still demonstrated mutation rates that were significantly less than that observed for the respective homologous *mlh1* ATPase point mutant strains PTY200 (*mlh1-E31A*) and PTY300 (*mlh1-G98A*) ($P < 0.0159$ for PTY200 vs. PTY202 and $P < 0.0286$ for PTY300 vs. PTY302). These results suggested that the differences seen between homologous *mlh1* and *pms1* ATPase mutations with respect to mutation rate were not due to the redundant functions of *MLH3*, but rather inferred an intrinsic functional asymmetry within the MutLα complex.

In addition to the differential effects of homolgous *mlh1* vs. *pms1* missense mutants noted above, I also observed that ATP-binding mutations produced more severe effects on mutation avoidance than did ATP-hydrolysis mutations. Both ATP-binding mutant strains, PTY300 (*mlh1-G98A*) and PTY301 (*pms1-G128A*), exhibited a 2-4 fold higher rate of spontaneous mutation at *hom3-10* and *CAN1* relative to the hydrolysis mutants, PTY200 (*mlh1-E31A*) and PTY201 (*pms1-E61A*), respectively (all comparisons had a P value < 0.0286).

To define further the effects of Mlh1p and Pms1p ATPase mutations on MMR, I examined the mutational spectra at the *CAN1* reporter (for a comprehensive list of *CAN1* mutations see APPENDIX B). *CAN1* reports forward mutations including base substitutions, frameshifts, deletions, insertions and large chromosomal rearrangements (Chen, et al., 1999). As seen in Table 3-2, the spectra of deletion strains PTY100 (*mlh1Δ*), PTY101 (*pms1Δ*) and PTY104 (*pms1Δ mlh3Δ*), and missense mutant strains PTY200 (*mlh1-E31A*) and PTY300 (*mlh1-G98A*) showed a preponderance of frameshift mutations (FS) relative to base substitutions (BS), similar to previously published reports for an *msh2Δ* strain (Tishkoff, et al., 1997b). In contrast, strain PTY301 (*pms1-G128A*) showed a different spectrum, namely, a majority of base substitutions, represented in Table 3-2 by a FS:BS ratio of 0.8. Because the mutation rate of PTY301 (*pms1-G128A*) for CAN^R is only 4-fold greater than wildtype (Table 3-1), one-quarter of the mutations seen with PTY301 represent the wildtype spectrum. Correcting for wildtype contribution, I still observed a majority of base substitutions [10/18 (56%) vs. 7.5/13.5 (56%)]. Next, because *MLH3* is partially redundant with *PMS1* in correcting frameshift mutations, I examined the *CAN1* spectrum in a *pms1-G128A mlh3Δ* strain (PTY302). As shown in Table 3-2, the *pms1-G128A mlh3Δ* strain (PTY302) showed a spectrum at *CAN1* that was indistinguishable from a MMR null strain (FS:BS ratio of 3.3). In contrast to the asymmetry observed with the mutation rates, the spectra results indicate that the *mlh1* and *pms1* "ATPase" mutations result in the same mutational spectra.

Table 3-2. **Summary of mutation spectra at *CAN1*.**

STRAIN	RELEVANT GENOTYPE	CLASS OF MUTATION				
		Frameshift (FS)		Base substitution (BS)	Complex	FS/BS[c]
		Frequency	Type[a]	Frequency		
GCY35	*Wildtype*	7/20 (35%)	(86%):(14%)	11/20 (55%)	2/20 (10%)[b]	0.6
PTY100	*mlh1Δ*	8/10 (80%)	(100%):(0%)	2/10 (20%)	NA	4.0
PTY200	*mlh1-E31A*	12/20 (60%)	(75%):(25%)	8/20 (40%)	NA	1.9[d]
PTY300	*mlh1-G98A*	17/20 (85%)	(99%):(12%)	3/20 (15%)	NA	5.7
PTY101	*pms1Δ*	8/10 (80%)	(62%):(38%)	2/10 (20%)	NA	4.0
PTY104	*pms1Δ mlh3Δ*	8/10 (80%)	(62%):(38%)	2/10 (20%)	NA	4.0
PTY301	*pms1-G128A*	8/18 (44%)	(87%):(13%)	10/18 (56%)	NA	0.8[d]
PTY302	*pms1-G128A mlh3Δ*	18/25 (72%)	(94%):(6%)	7/25 (28%)	NA	3.3[d]

[a] – Ratio of contractions:expansions.

[b] – Duplication events that are flanked by direct repeats.

[c] – Frameshift (FS): Base substitution (BS) ratio, where a signature MMR defective spectrum is ≥2.

[d] – This value is the FS/BS ratio with the wildtype spectrum contribution subtracted.

The spectrum of an *mlh3Δ* strain is similar to wildtype (R.D. Kolodner, personal communication).

NA - not applicable.

MutLα undergoes an ATP-dependent conformational change.

To investigate further the role of candidate ATP-binding/hydrolysis motifs in MutLα function, I used limited proteolysis to examine the effects of adenine nucleotides on the conformation of recombinant wildtype and mutant forms of MutLα purified from insect cells (data not shown). I used an antibody directed against the 6xHis tag at the NH_2-terminus of Mlh1p to detect NH_2-terminal fragments following limited proteolysis. As depicted in Figure 3-2a, the presence of ATP led to the protection of distinct NH_2-terminal fragments of Mlh1p from trypsin proteolysis. The protected NH_2-terminal fragments of approximately 42 and 38 kDa coincide with the *E. coli* MutL LN40 thrombin proteolytic fragment that possessed the core ATPase domain (Ban and Yang, 1998a; Ban, et al., 1999). I did not observe any differences between MutLα in the presence or absence of ATP using a polyclonal antibody directed against the COOH-terminus of Mlh1p (data not shown), suggesting that the COOH-terminal epitope of Mlh1p detected by this polyclonal antibody is not a region of Mlh1p that undergoes an ATP-dependent conformational change. However, I did detect an approximately 30 kDa band that was resistant to proteolysis in the presence or absence of ATP even after a 30 minute incubation with 750 ng of trypsin (data not shown). This highly trypsin resistant Mlh1p COOH-terminal fragment may represent the COOH-terminal heterodimerization domain of Mlh1p. As shown in Figure 3-2b, lanes 3-5 demonstrate that non-hydrolyzable ATP analogs, AMP-PNP and ATPγS, and ADP also protect the NH_2-terminus of Mlh1p from trypsin proteolysis. Qualitatively, the relative levels of protection from proteolysis in the presence of nucleotide is as follows: ATP ≈ AMP-PMP > ATPγS > ADP. As demonstrated for ATP, I saw no differential protection

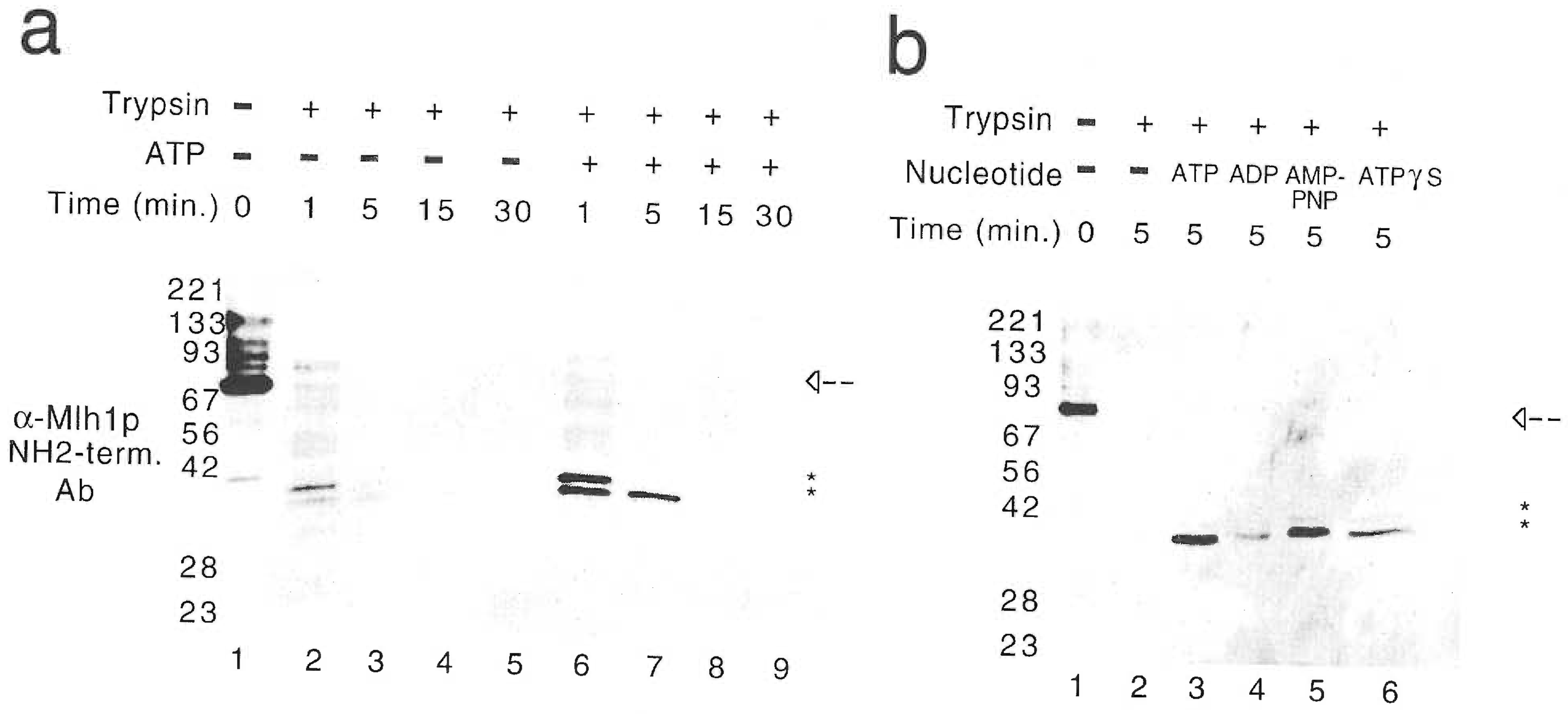

Figure 3-2. **Adenine nucleotides alter trypsin sensitivity of MutLα**. (a) 150 ng of MutLα was subjected to proteolysis with modified trypsin as described in CHAPTER 2: Materials and Methods in the presence or absence of 5 mM ATP for the indicated time at 30°C. Products were treated with SDS-sample buffer, boiled, separated on a 10% SDS-PAGE gel and detected by immunoblotting with α-4xHis antibody. Arrow denotes full-length 6xHis-Mlh1p and asterisks designate NH2-terminal fragments of 6xHis-Mlh1p that are protected from proteolysis in the presence of ATP. Equal loading of samples and even transfer of the blot was demonstrated using a polyclonal antibody raised against the COOH-terminus of Mlh1p (data not shown). (b) The same analysis was performed as described in panel (a), but the effect of 5mM adenine nucleotides ADP, AMP-PNP and ATPγS were examined.

of the COOH-terminus of Mlh1p in the presence of ADP, AMP-PNP or ATPγS by reprobing with the antibody directed against the COOH-terminus of Mlh1p (data not shown).

I next examined the ATP-dependent effects of limited proteolysis on the double ATP-binding (mlh1-G98Ap/ pms1-G128Ap) and ATP-hydrolysis (mlh1-E31Ap/ pms1-E61Ap) mutant forms of MutLα. In constrast to wildtype MutLα, the double ATP-binding mutant (mlh1-G98Ap/ pms1-G128Ap) MutLα did not demonstrate ATP-dependent protection of NH_2-terminal fragments of Mlh1p from trypsin proteolysis (compare Figure 3-2a versus Figure 3-3). The lack of ATP-dependent protection observed in the double ATP-binding mutant (mlh1-G98Ap/ pms1-G128Ap) MutLα is consistent with this mutation affecting ATP-binding by Mlh1p. The effect of limited proteolysis on the double ATP-hydrolysis mutant (mlh1-E31Ap/ pms1-E61Ap) MutLα was interesting. As shown in Figure 3-4, the double ATP-hydrolysis (mlh1-E31Ap/ pms1-E61Ap) mutant form of MutLα showed protection of NH_2-terminal fragments of Mlh1p from trypsin proteolysis even in the absence of ATP. Furthermore, this ATP-independent protection of the double ATP-hydrolysis (mlh1-E31Ap/ pms1-E61Ap) mutant was resistant to increasing amounts of trypsin. This unique trypsin-resistant conformation of MutLα observed in the double ATP-hydrolysis (mlh1-E31Ap/ pms1-E61Ap) mutant is consistent with a model for a MutLα ATPase cycle discussed below.

These limited proteolysis results with wildtype and mutant forms of MutLα indicate that at least the Mlh1p NH_2-terminus of MutLα undergoes an ATP-binding dependent conformational change. Moreover, the *mlh1-G98A* mutation appears

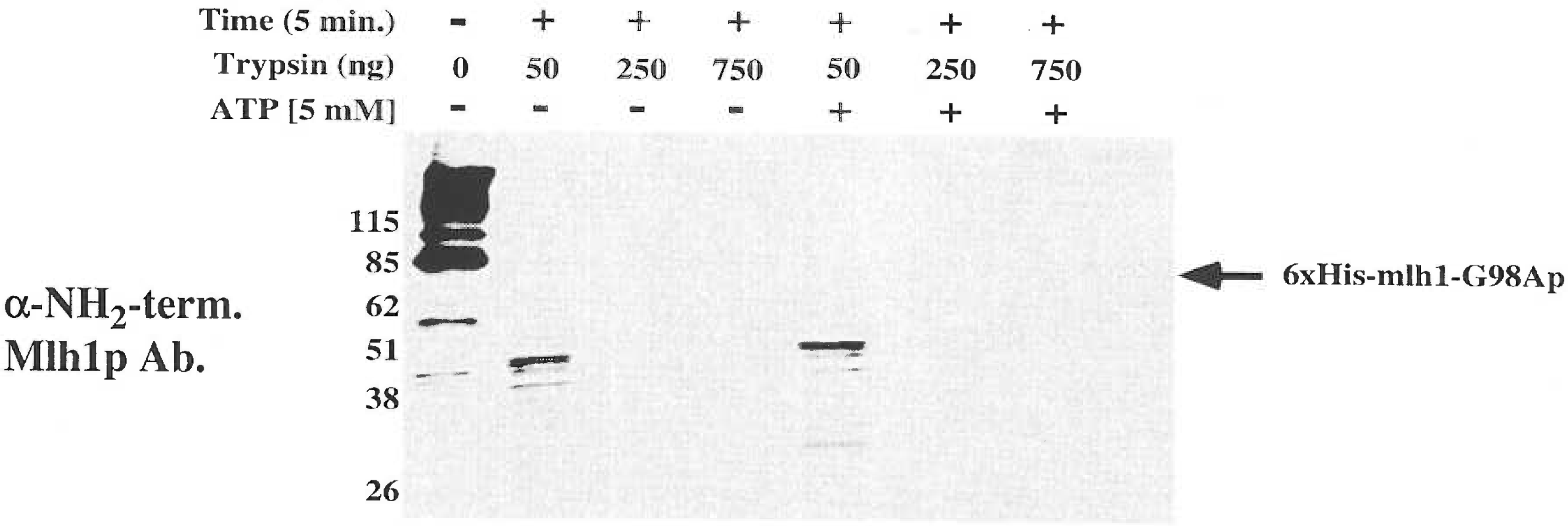

Figure 3-3. **Adenine nucleotides do not alter trypsin sensitivity of double-binding (mlh1-G98Ap/ pms1-G128Ap) mutant MutLα.** Approximately 150 ng of mutant MutLα was subjected to proteolysis with the indicated amount of modified trypsin as described in CHAPTER 2: Materials and Methods in the presence or absence of 5 mM ATP for 5 mintues at 30°C. Products were treated with SDS-sample buffer, boiled, separated on a 10% SDS-PAGE gel and detected by immunoblotting with α-4xHis antibody. Arrow denotes full-length 6xHis-mlh1-G98Ap. Equal loading of samples and even transfer of the blot was demonstrated using a polyclonal antibody raised against the COOH-terminus of Mlh1p (data not shown).

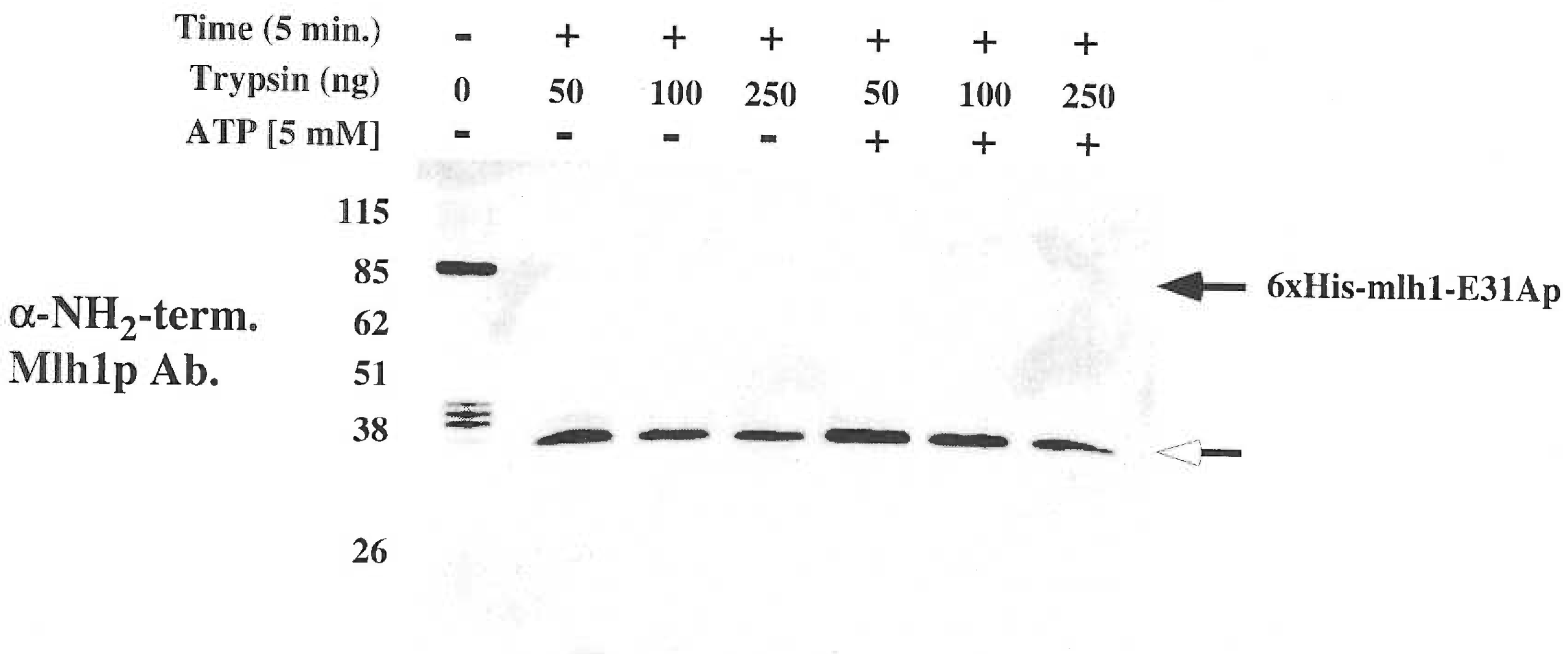

Figure 3-4. The double-hydrolysis (mlh1-E31Ap/ pms1-E61Ap) mutant MutLα is resistant to trypsin proteolysis. Approximately 150 ng of mutant MutLα was subjected to proteolysis with the indicated amount of modified trypsin as described in CHAPTER 2: Materials and Methods in the presence or absence of 5 mM ATP for 5 mintues at 30°C. Products were treated with SDS-sample buffer, boiled, separated on a 10% SDS-PAGE gel and detected by immunoblotting with α-4xHis antibody. Closed arrow denotes full-length 6xHis-mlh1-E31Ap and open arrow designates NH2-terminal fragments of 6xHis-mlh1-E31Ap resistant to trypsin. Equal loading of samples and even transfer of the blot was demonstrated using a polyclonal antibody raised against the COOH-terminus of Mlh1p (data not shown).

to affect Mlh1p ATP-binding dependent conformationl changes. I was unable to address whether the NH_2-terminus of Pms1p undergoes a similar ATP-binding dependent conformational change because an antibody specific for the NH_2-terminus of Pms1p antibody was not available. However, as described below, yeast two-hybrid results suggest that Pms1p also undergoes an ATP-dependent conformational change.

ATP-binding promotes heterodimerization of the NH_2-termini of MutLα *in vivo*.

ATP-binding dependent conformational changes in other GHL family members are associated with dimerization of their NH_2-terminal ATP-binding domains (Wigley, et al., 1991; Ban, et al., 1999). To inquire into the functional significance of the ATP-dependent conformational change data described above, I used the yeast two-hybrid system to assay interactions between wildtype and mutant NH_2-terminal fragments of Mlh1p and Pms1p. Based upon sequence alignments with GHL family members, the fragments 1-354 and 1-401 of Mlh1p and Pms1p, respectively, should each contain the structural elements necessary for ATP-binding and hydrolysis (Ban, et al., 1999). These NH_2-terminal fragments of Mlh1p and Pms1p were fused at their COOH-termini to either the lexA DNA binding domain or the GAL4 activation domain (Figure 3-5). Consistent with previous studies (Pang, et al., 1997), no interaction was seen between wildtype Mlh1p and Pms1p NH_2-terminal fragments (Figure 3-5, group I). As stated before, homologous ATP-hydrolysis mutations in other GHL ATPases have been shown to abolish ATP-hydrolysis activity with little or no effect on ATP binding (Jackson and Maxwell, 1993; Ban and Yang, 1998a; Obermann, et al., 1998; Panaretou, et al., 1998; Ban, et al., 1999). Interestingly, for an NH_2-terminal fragment of gyrase b, ATP-binding

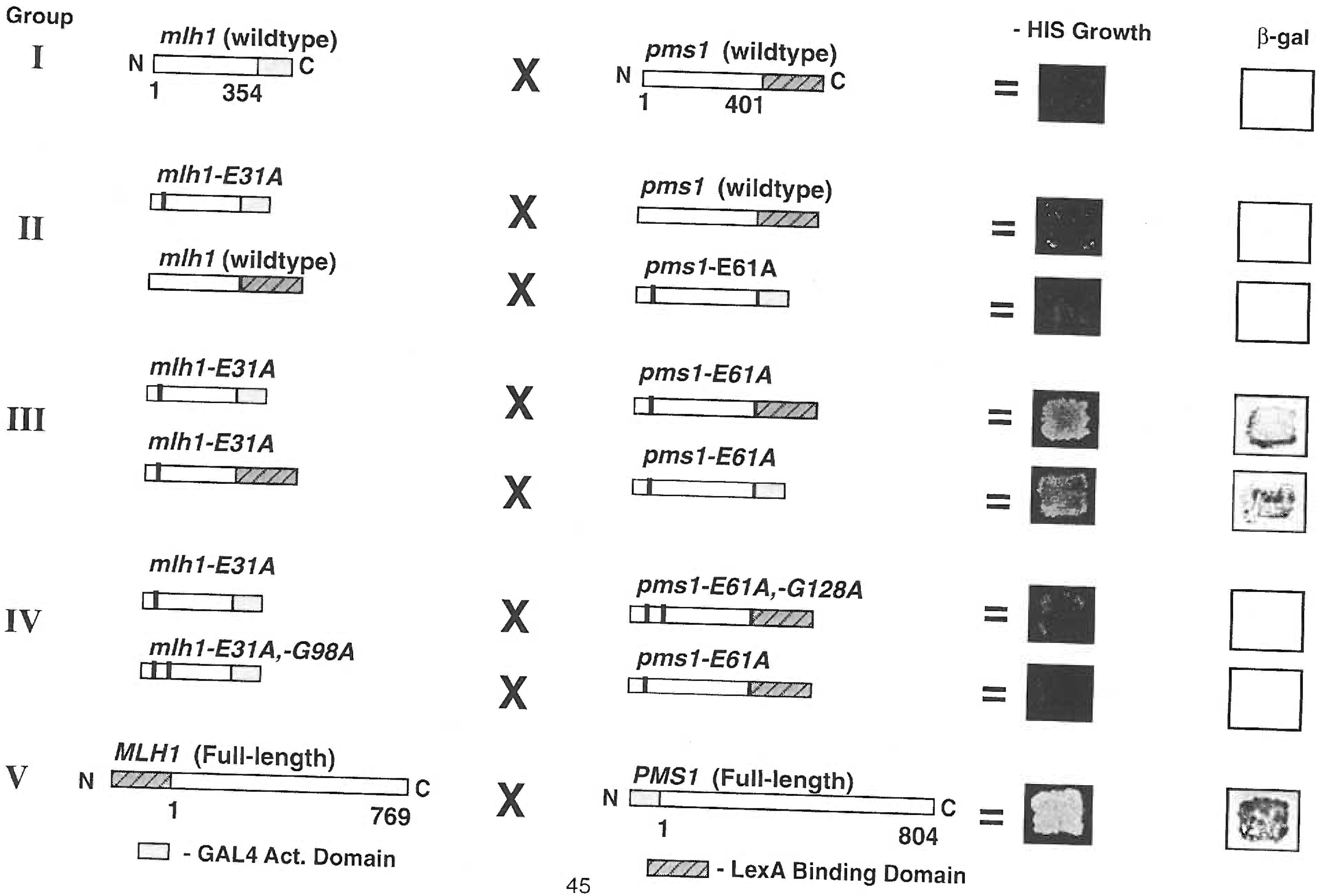Group
I
mlh1 (wildtype)
N
C
1
354
X
pms1 (wildtype)
N
C
1
401
=
- HIS Growth
β-gal
II
mlh1-E31A
X
pms1 (wildtype)
=
mlh1 (wildtype)
X
pms1-E61A
=
III
mlh1-E31A
X
pms1-E61A
=
mlh1-E31A
X
pms1-E61A
=
IV
mlh1-E31A
X
pms1-E61A,-G128A
=
mlh1-E31A,-G98A
X
pms1-E61A
=
V
MLH1 (Full-length)
N
C
1
769
X
PMS1 (Full-length)
N
C
1
804
=
- GAL4 Act. Domain
- LexA Binding Domain

Figure 3-5. **Two-hybrid analysis detects NH_2-terminal Mlh1p and Pms1p interaction**. Boxes correspond to “bait” and “prey” constructs tested for interaction. The residues included in the fusions are indicated below the Group I and V constructs, respectively. Amino acid substitutions designated above each construct are indicated by black bars within the construct boxes. Interaction is scored as growth on –HIS media and blue color development with the substrate X-gal as described in CHAPTER 2: Materials and Methods. Group I, wildtype NH_2-terminal fusion fragments; group II, one NH_2-terminal fusion fragment contains a “hydrolysis” point mutation; group III, both NH_2-terminal fusion fragments contain “hydrolysis” point mutations; group IV, one NH_2-terminal fusion fragment has the indicated compound mutations; and group V, positive control reaction with full-length Pms1p and Mlh1p.

was only observed *in vitro* for a hydrolysis deficient form (Jackson and Maxwell, 1993). Furthermore, my limited proteolysis result with the double ATP-hydrolysis (mlh1-E31Ap/ pms1-E61Ap) mutant form of MutLα (see above and Figure 3-4) led me to reason that ATP-hydrolysis mutations in the NH_2-termini of both Mlh1p and Pms1p might prolong a "double" ATP-bound state *in vivo* and allow interaction to be detected by the yeast two-hybrid. Indeed, as shown in Figure 3-5 (group III) a robust interaction was seen when both Mlh1p and Pms1p NH_2-terminal fragments possessed ATP-hydrolysis mutations. However, interaction was not observed when only Mlh1p or Pms1p fragment possessed the ATP-hydrolysis mutation E31A or E61A, respectively (Figure 3-5, group II). To demonstrate that this novel interaction was dependent on the putative ATP-binding activities of Mlh1p and Pms1p, I superimposed either the *mlh1-G98A* or *pms1-G128A* ATP-binding mutation onto the hydrolysis defective NH_2-terminal fragments of mlh1p-E31A or pms1p-E61A, respectively. Supporting my hypothesis, I observed that superimposing a mutation designed to prevent the putative ATP-binding/conformational change in one fragment ablated the two-hybrid interaction (Figure 3-5, compare group III and IV).

Interestingly, the two-hybrid interaction seen in Figure 3-5, group III, was specific only for the mlh1p-E31A and pms1p-E61A NH_2-terminal fusion pairs, as the NH_2-terminus of mlh1p-E31A did not interact with itself (data not shown). The same observation was seen with the NH_2-terminus of pms1p-E61A (data not shown), suggesting that, similar to their respective COOH-terminal domains (Pang, et al., 1997), the NH_2-termini of Mlh1p and Pms1p do not homodimerize. The two-hybrid results of Figure 3-5 are not due to ATP-hydrolysis or –binding mutations grossly affecting expression or stability of the fusion proteins, as western analysis demonstrates that all fusion proteins are expressed at similar levels (Figure 3-6). Taken together, the two-hybrid results suggest that ATP-binding, but not hydrolysis, by both Mlh1p and Pms1p are necessary for MutLα NH_2-terminal heterodimerization.

Discussion

Although clearly crucial for MMR, little information exists on the function of the major MutL activity in yeast, MutLα, composed of Mlh1p and Pms1p. Previous studies with yeast have defined COOH-terminal domains as important for Mlh1p and Pms1p interaction (Pang, et al., 1997) and conserved NH_2-terminal residues as necessary for MMR activity (Pang, et al., 1997; Shcherbakova and Kunkel, 1999). Recent investigations on MutL and other members of the GHL family of ATPases have suggested guidelines for more detailed studies of MutLα function. Here, I present evidence suggesting that yeast MutLα is a functional member of the GHL ATPase superfamily. First, residues critical for the ATPase function of GHL family members, when substituted for alanine in both Mlh1p and Pms1p, disrupt MMR. Second, the presence of adenine nucleotide protects the NH_2-terminus of wildtype Mlh1p from trypsin proteolysis, but fails to protect the mlh1-G98Ap ATP-binding mutant, suggesting that MutLα undergoes ATP-binding dependent conformational changes. Third, results from the two-hybrid system suggest that one consequence of the ATP-induced conformational changes is an interaction between the NH_2-termini of Mlh1p and Pms1p. Finally, analysis of single *mlh1* and *pms1* ATPase motif mutants indicate a functional asymmetry within yeast MutLα.

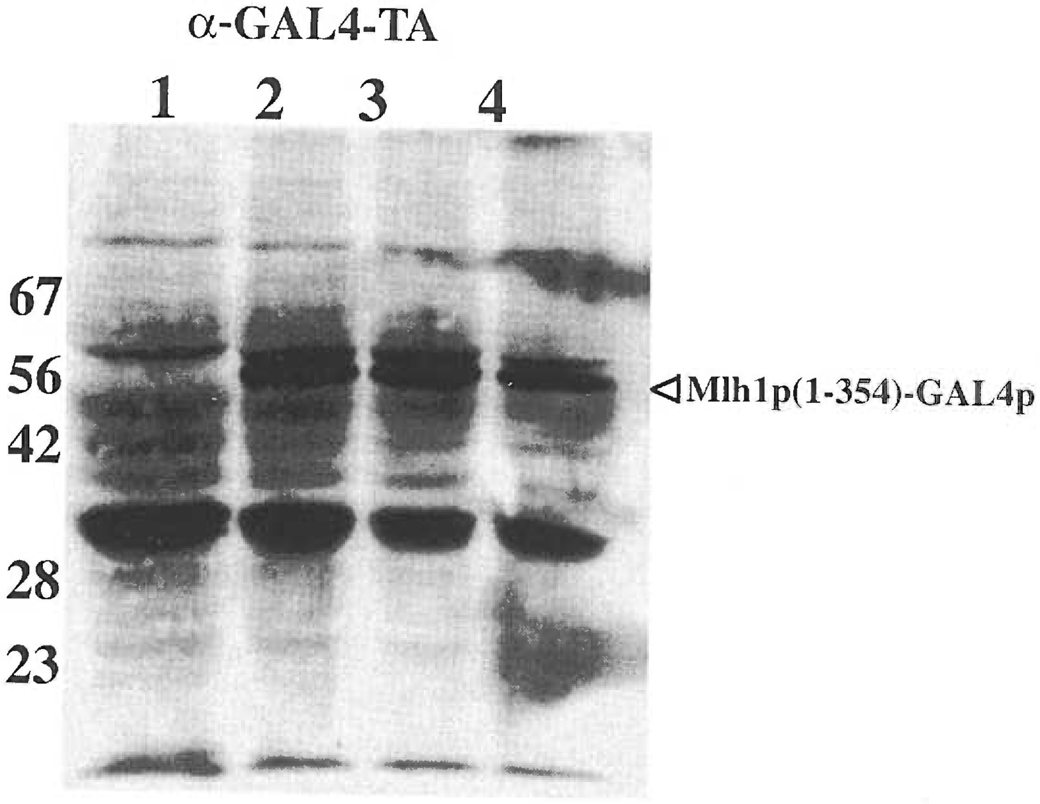
α-GAL4-TA
1
2
3
4
67
56
42
28
23
◁Mlh1p(1-354)-GAL4p

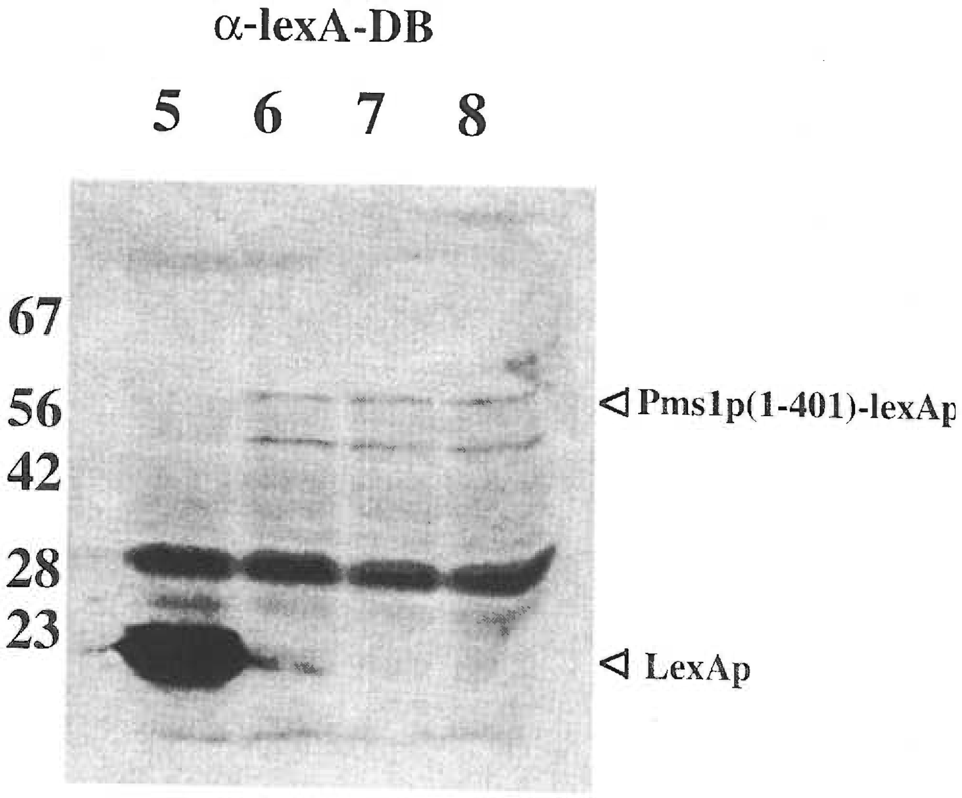
α-lexA-DB
5
6
7
8
67
56
42
28
23
◁ Pms1p(1-401)-lexAp
◁ LexAp

Figure 3-6. **Mlh1p and Pms1p ATPase motif missense mutations do not affect the stability of two-hybrid fusion proteins.** Western analysis of L40 strains with two-hybrid constructs from Figure 3-5 using monoclonal antibodies anti-GAL4-TA or anti-lexA-DB as described in CHAPTER 2: Materials and Methods. 1, pCAD3 (empty vector); 2, pCAD-mlh1 N-354; 3, pCAD-mlh1-E31A N-354; 4, pCAD-mlh1-E31A, -G98A N-354; 5, pNBTM (lexA); 6, pNBTM-pms1 N-401; 7, pNBTM-pms1-E61A N-401; 8, pNBTM-pms1-E61A, -G128A N-401. Fusion products and lexAp are indicated by arrowheads. The approximately 90 kDa band in lanes 1-4 may be endogenous Gal4p. The other bands present in control lanes 1 and 5, and in lanes 2-4 and 6-8, respectively, represent non-specificity by the primary and secondary antibodies. In lanes 6-8, the faster migrating specific anti-lexA-DB reacting species is unknown, but may be a pms1p(1-401)-lexAp degradation product.

GHL family members appear to share an ATPase cycle that is highlighted by an NH_2-terminal dimerized intermediate in the ATP-bound form (Wigley, et al., 1991; Ali, et al., 1993; Prodromou, et al., 1997a; Prodromou, et al., 1997b; Ban, et al., 1999; Grenert, et al., 1999; Prodromou, et al., 1999; Chadli, et al., 2000; Prodromou, et al., 2000; Spampinato and Modrich, 2000; Young and Hartl, 2000). In the case of MutL, this ATP-binding induced NH_2-terminal dimerization activated MutH endonuclease *in vitro* (Ban and Yang, 1998a). The limited proteolysis and two-hybrid analyses presented here support an ATPase cycle for MutLα, composed of at least four intermediates, that is similar to other GHL family members (Figure 3-7). Limited proteolysis suggests that wildtype MutLα undergoes a conformational change *in vitro* that is dependent on ATP-binding, because AMP-PNP (and to a lesser extent ATPγS) produced the same effect as ATP and because this same effect was not observed for the the double ATP-binding (mlh1-G98Ap/ pms1-G128Ap) mutant MutLα (Figure 3-7, intermediate 2). Furthermore, I observed a specific two-hybrid interaction between Mlh1p and Pms1p NH_2-terminal fragments each containing ATP-hydrolysis mutations (Figure 3-7, intermediate 3). Interaction was not detected by yeast two-hybrid with wildtype NH_2-terminal fragments of Mlh1p and Pms1p presumably because ATP-hydrolysis renders the interaction transient. In further support of the existence of intermediate 3, the double ATP-hydrolysis (mlh1-E31Ap/ pms1-E61Ap) mutant form of MutLα is highly resistant to trypsin limited proteolysis even without added ATP suggesting that this intermediate may be stable even after multiple chromatographic steps. Also, that ADP provided some protection from limited proteolysis suggests the existence of an ADP-bound intermediate (Figure 3-7, intermediate 4). Double mutant *mlh1 pms1* strains with alanine substitutions

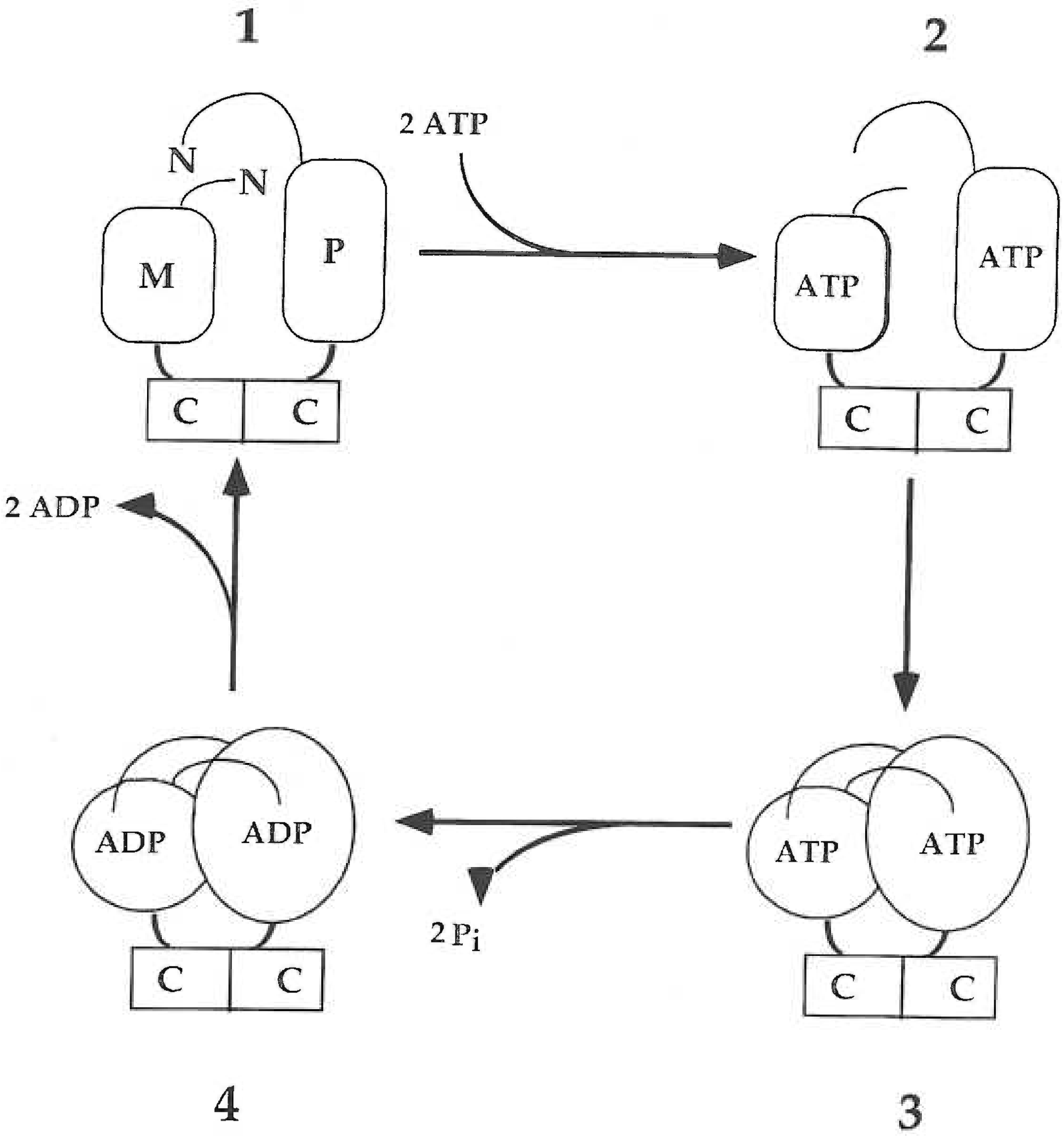

Figure 3-7. A model for the yeast MutLα ATPase cycle. Briefly, intermediate 1 is the nucleotide free state. ATP-binding induces conformational changes in the NH2-terminus of Mlh1p and Pms1p represented by a change in shape from rectangular to oval that occurs in the step(s) between intermediates 2 and 3. Intermediate 3 is heterodimerization of the NH2-termini of Mlh1p and Pms1p in the ATP-bound state. Intermediate 4 is the ADP-bound form following ATP-hydrolysis. The *mlh1-G98A* and *pms1-G128A* ATP-"binding" mutations were constructed to affect the transition(s) from intermediate 1 to 2 and/or intermediate 2 to 3. In contrast the ATP-"hydrolysis" mutations, *mlh1-E31A* and *pms1-E61A*, were modeled to prevent the transition from intermediate 3 to intermediate 4. M, represents the NH2-terminus of Mlh1p; P, the NH2-terminus of Pms1p; and C, COOH-termini of Mlh1p and Pms1p. Each arrow may represent multiple distinct steps. This model, which is consistent with the studies reported here, was adapted from a model for MutL proposed by Ban and Yang, 1999.

at ATP-hydrolysis or ATP-binding residues showed increased spontaneous mutation rates indistinguishable from completely MMR-defective cells. This double mutant analysis suggests that the candidate ATPase domains of both Mlh1p and Pm1p and the ATPase cycle described above are required for MutLα function in yeast MMR for mutation avoidance. It is intriguing to speculate on the function of the NH_2-terminal ATP-bound MutLα intermediate, because similar findings from other GHL ATPases (Prodromou, et al., 1997a; Prodromou, et al., 1997b; Grenert, et al., 1999; Prodromou, et al., 1999; Chadli, et al., 2000; Young and Hartl, 2000), namely MutL (Ban and Yang, 1998a), suggest that this MutLα intermediate may play a significant role in coordinating downstream steps with known and perhaps unidentified MMR proteins. Although my data are consistent with the ATPase cycle represented in Figure 3-7, further biochemical work with MutLα is required to confirm and characterize the contribution of Mlh1p and Pms1p ATP-binding and hydrolysis activities to MutLα function. Similar to earlier work from the Hsp90 field (Jakob, et al., 1996; Scheibel, et al., 1997), I have not been able to specifically assign an intrinsic ATPase activity to MutLα with my current protein preparations (P. T. Tran and R. M. Liskay, unpublished observations). However, similar to what is currently known for GHL ATPases (Jackson and Maxwell, 1993; Ban and Yang, 1998a; Obermann, et al., 1998; Panaretou, et al., 1998; Ban, et al., 1999), my double *mlh1 pms1* hydrolysis mutant phenotype, limited proteolysis results with the double ATP-hydrolysis (mlh1-E31Ap/ pms1-E61Ap) mutant MutLα and two-hybrid results suggest a crucial role for ATP-hydrolysis during mutation avoidance in yeast MMR (refer to Table 3-1, and Figures 3-4 and 3-5).

Interestingly, genetic analysis revealed a functional asymmetry with respect to the two ATPase domains of the MutLα heterodimer. Specifically, alanine substitution mutations affecting the predicted ATPase motifs of Mlh1p had a greater impact on mutation avoidance than the corresponding mutations in Pms1p. Formally, my genetic results argue that Mlh1p can compensate better for ATPase mutations in Pms1p for mutation avoidance, than can Pms1p for the corresponding ATPase mutations in Mlh1p. The apparent genetic asymmetry detected for MutLα may reflect at the mechanistic level a kinetic asymmetry similar to that observed in the homodimeric ATPases, topoisomerase II from *S. cerevisiae* and the γ complex from *E. coli* (Harkins, et al., 1998; Baird, et al., 1999; Hingorani, et al., 1999). Biologically, the genetic asymmetry observed with MutLα may represent distinct but overlapping roles of Mlh1p and Pms1p during mutation avoidance, e.g. excision tracts originating 5' vs. 3' from the mismatch/IDL (Drummond, et al., 1996; Nicolaides, et al., 1998) or differential roles during strand discrimination.

MutL has been referred to as a "molecular matchmaker", coupling the mismatch binding activity of MutS to the latent endonuclease MutH (Sancar and Hearst, 1993). One criterion of a molecular matchmaker that MutL has always appeared to lack was an intrinsic ATPase activity. Recent work has now identified this "missing" activity, and as suggested previously (Sancar and Hearst, 1993) it appears to be critical for MutL activity in MMR (Aronshtam and Marinus, 1996; Ban and Yang, 1998a; Ban, et al., 1999). Moreover, the MutL ATPase activity was responsible for coordinated interaction and activation of MutH *in vitro* (Ban and Yang, 1998a). In this chapter I have shown that the conserved ATPase motifs of MutLα are necessary for mutation avoidance by MMR in yeast. Finally, as for MutL (Ban and Yang, 1998a; Ban, et al., 1999), the ATP-dependent conformational changes in yeast MutLα are likely to facilitate interaction with downstream proteins in MMR.

CHAPTER 4: Interactions of *EXO1* with components of MutLα in *Saccharomyces cerevisiae*

Introduction

In the previous chapter I reported studies suggesting that *S. cerevisiae* MutLα is a member of the gyrase b/Hsp90/MutL (GHL) dimeric ATPase superfamily characterized by highly conserved ATPase motifs (Tran and Liskay, 2000). Although direct demonstration of ATP-binding and hydrolysis was not forthcoming, my genetic and biochemical results suggest that, similar to other GHL ATPases, yeast MutLα appears to undergo ATPase-dependent conformational changes highlighted by NH_2-terminal dimerization of the ATPase domains. These ATP-dependent conformational changes in MutLα and resultant NH_2-terminal dimerization between Mlh1p and Pms1p protomers appear to be crucial for MMR because mutations affecting these activities compromise yeast MMR in vivo. Analogous to other GHL ATPases (Prodromou, et al., 1997a; Prodromou, et al., 1997b; Ban, et al., 1999; Grenert, et al., 1999; Prodromou, et al., 1999; Chadli, et al., 2000; Prodromou, et al., 2000; Spampinato and Modrich, 2000; Young and Hartl, 2000), these MutLα ATP-dependent conformational changes and the NH_2-terminal dimerization may recruit and/or activate downstream effectors. One downstream candidate that may be directed by the MutLα ATPase domains is the 5′-3′ exonuclease, Exo1p, identified as a yeast two-hybrid interactor with Mlh1p (Shelley, 1999) and Msh2p (Tishkoff, et al., 1997a). In addition, recent genetic studies suggest that Exo1p performs a catalytic role during MutSα-dependent MMR (Sokolsky and Alani, 2000).

In this chapter I report results showing both physical and genetic interactions between *EXO1* and the components of MutLα, Mlh1p and Pms1p. Specifically, I characterized further this initial two-hybrid interaction between Mlh1p and Exo1p. More importantly, my genetic interaction results suggest that one function of the MutLα ATPase domains may be to direct Exo1p and other exonucleases during mutation avoidance. Finally, my results suggest that Exo1p is also involved in one or more MMR-independent mutation avoidance pathways.

Exo1p interacts with Mlh1p by yeast two-hybrid.

Using full-length Mlh1p as a bait I recovered a COOH-terminal fragment of Exo1p (residues 400-702) from a two-hybrid screen. This Exo1p fragment was re-tested directly and shown to interact with LexAp-Mlh1p as depicted in Figure 4-1a. Using deletion constructs I mapped the minimal region of Mlh1p required to interact with this COOH-terminal fragment of Exo1p to residues 501-761 (Figure 4-1a). To test whether ATP-binding or ATP-binding dependent conformational changes by Mlh1p were necessary for interaction with Exo1p, I examined LexAp-mlh1-G98A for interaction. As shown in Figure 4-1a, this Mlh1p mutant was still capable of interacting with Gal4p-Exo1p (400-702).

I also tested the Exo1p clone against a panel of other MMR proteins. This COOH-terminal fragment of Exo1p interacted with full-length LexAp-Msh2p (data not shown) similar to a previous report (Tishkoff, et al., 1997a), but not with full-length LexAp-Msh6p (data not shown) or LexAp-Pms1p fusions (Figure 4-1b). However, this

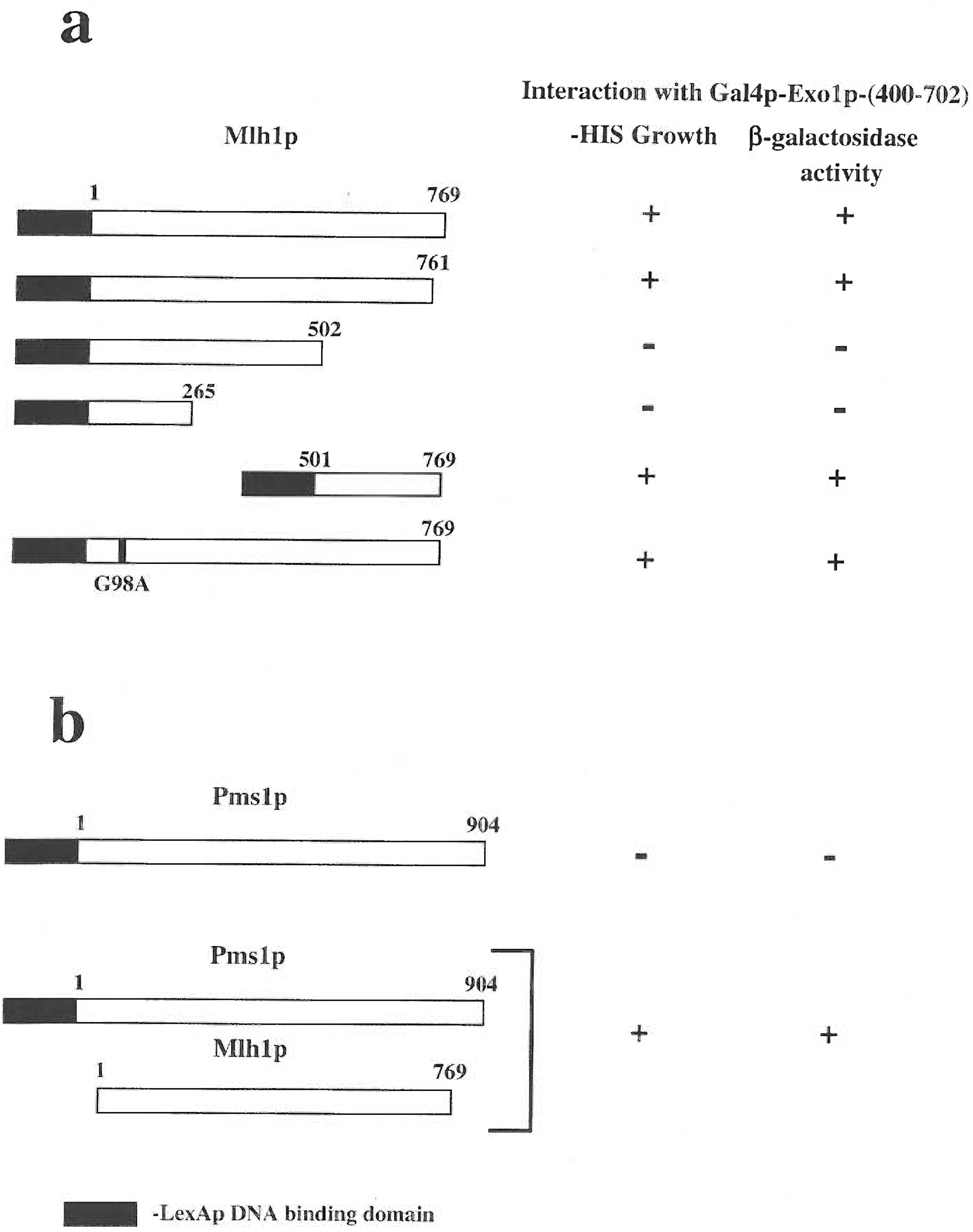
a
Interaction with Gal4p-Exo1p-(400-702)
Mlh1p
-HIS Growth
β-galactosidase activity
1
769
+
+
761
+
+
502
-
-
265
-
-
501
769
+
+
769
G98A
+
+
b
Pms1p
1
904
-
-
Pms1p
1
904
Mlh1p
1
769
+
+
-LexAp DNA binding domain

Figure 4-1. Exo1p and mismatch repair proteins interact by yeast two-hybrid. (a) Boxes correspond to Mlh1p "bait" constructs tested for interaction. The residues of Mlh1p included in the fusions are indicated above each respective construct. The amino acid substitution G98A made in Mlh1p is designated above the construct by a black bar within the construct box. Interaction is scored as growth on –HIS media and > 0.5 β-galactosidase units with the substrate *o*-nitro-phenyl-β-D-galactosidase (ONPG) as described in CHAPTER 2: Materials and Methods. (b) Full-length lexAp-Pms1p fusion alone or with native Mlh1p co-expressed was tested for interaction with the Gal4p-Exo1p-(400-702) fusion using similar analysis to panel a.

COOH-terminal fragment of Exo1p did interact with LexAp-Pms1p in a three-hybrid assay when native Mlh1p was co-expressed (Figure 4-1b).

Epistasis analysis for *mlh1* and *pms1* mutations and *exo1Δ*.

To detect genetic interactions between components of MutLα and *EXO1*, I examined mutation rates in various single and double mutants (Table 4-1). The most striking result was that both *pms1-E61A* and *pms1-G128A* mutations seemed to synergize with *exo1Δ* for mutation rates using *hom3-10* (Table 4-1, PTY204 > PTY105 + PTY201; and PTY304 > PTY105 + PTY301). Likewise *mlh1-E31A* mutation also appeared to synergize with *exo1Δ* using *hom3-10* (Table 4-1, PTY207 > PTY105 + PTY200). In contrast, the small effect of *exo1Δ* at *hom3-10* relative to the large effect produced by the *mlh1Δ*, *pms1Δ*, and *mlh1-G98A* mutations prevented epistasis conclusions from being made with the corresponding double mutants. Using 95% CI I did not see any consistent differences in the mutation rates for the single and double mutant combinations using *CAN1* , however, examination of the *CAN1* spectra below suggested that *exo1Δ* mutation also synergized with *mlh1-E31A*, *pms1-E61A* and *pms1-G128A* mutations for *hom3-10*-like events at *CAN1* (see below).

Analysis of *CAN1* mutation spectra.

To better understand the genetic interactions between *MLH1*, *PMS1* and *EXO1* I examined the *CAN1* mutational spectra of a subset of single and double mutant strains. As shown in Table 4-2, all single *mlh1* and *pms1* mutant strains examined showed a *CAN1* spectrum characterized by a frameshift (FS) to base substitution (BS) mutation

Table 4-1. Mutation rates of *exo1Δ* strains in yeast MutL mutant backgrounds.

STRAIN	RELEVANT GENOTYPE	FOLD MUTATOR RATE (95% CI)[a]			
		hom3-10[b]		*Can*^{R}[c]	
GCY35[d]	*Wildtype*	1	(0-2.3)	1	(0.1-2)
PTY100[d]	*mlh1Δ*	1253	(0-3953)	29	(0-86)
PTY101[d]	*pms1Δ*	1212	(1017-1408)	28	(15-41)
PTY105	*exo1Δ*	8	(0-24)	9	(5-14)
PTY106	*mlh1Δ exo1Δ*	1227	(134-2320)	37	(30-43)
PTY107	*pms1Δ exo1Δ*	1097	(253-1940)	35	(11-60)
PTY200	*mlh1-E31A*	315	(170-461)	9	(3-14)
PTY207	*mlh1-E31A exo1Δ*	1387	(813-1961)	54	(0-108)
PTY201[d, e]	*pms1-E61A*	19	(6-32)	1	(0.5-2)
PTY204[e]	*pms1-E61A exo1Δ*	517	(163-872)	15	(9-20)
PTY300[d]	*mlh1-G98A*	725	(524-926)	22	(10-34)
PTY307	*mlh1-G98A exo1Δ*	1207	(0-2884)	43	(22-63)
PTY301[d, e]	*pms1-G128A*	78	(33-122)	4	(3-5)
PTY304[e]	*pms1-G128A exo1Δ*	611	(361-862)	24	(20-27)

[a] – Experiments repeated two to four times with 5-11 cultures per experiment.

[b] – Relative to wildtype GCY35 rate of 9.90×10^{-09}.

[c] – Relative to wildtype GCY35 rate of 3.01×10^{-07}.

[d] – These rates are taken from Tran and Liskay, 2000.

[e] – Codeletion of *MLH3* did not change the rates significantly (two-tailed Mann-Whitney test, $P > 0.05$).

Table 4-2. Summary of mutation spectra at *CAN1*.

STRAIN	RELEVANT GENOTYPE	CLASS OF MUTATION					
		Frameshift (FS)		Base substitution (BS)		Complex	FS/BS[f]
		Frequency (%)	Type[a]	Frequency (%)	Type[b]	Frequency (%)	
GCY35[h]	*Wildtype*	7/20 (35)	(86):(14)	11/20 (55)	(55):(45)	2/20 (10)[d]	0.6
PTY100[h]	*mlh1Δ*	8/10 (80)	(100):(0)	2/10 (20)	NA[c]	NA[e]	4.0
PTY200[h]	*mlh1-E31A*	12/20 (60)	(75):(25)	8/20 (40)	(63):(37)	NA	1.9[g]
PTY300[h]	*mlh1-G98A*	17/20 (85)	(99):(12)	3/20 (15)	NA	NA	5.7
PTY101[h]	*pms1Δ*	8/10 (80)	(62):(38)	2/10 (20)	NA	NA	4.0
PTY104[h]	*pms1Δ mlh3Δ*	8/10 (80)	(62):(38)	2/10 (20)	NA	NA	4.0
PTY302[h]	*pms1-G128A*[i]	18/25 (72)	(94):(6)	7/25 (28)	(57):(43)		3.3[g]
PTY105	*exo1Δ*	9/20 (45)	(67):(33)	11/20 (55)	(36):(64)	NA	0.8
PTY106	*mlh1Δ exo1Δ*	13/19 (68)	(100):(0)	6/19 (32)	(33):(67)	NA	2.2
PTY207	*mlh1-E31A exo1Δ*	15/19 (79)	(87):(13)	4/19 (21)	NA	NA	3.8
PTY307	*mlh1-G98A exo1Δ*	9/20 (45)	(89):(11)	11/20 (55)	(45):(55)	NA	0.8
PTY107	*pms1Δ exo1Δ*	12/18 (67)	(92):(8)	6/18 (33)	(67):(33)	NA	2.0
PTY205	*pms1-E61A exo1Δ*[i]	15/20 (75)	(100):(0)	5/20 (25)	(40):(60)	NA	3.0
PTY305	*pms1-G128A exo1Δ*[i]	13/20 (65)	(100):(0)	7/20 (35)	(14):(86)	NA	1.9

[a] – Ratio of contractions:expansions.

[b] – Ratio of transitions:transversions.

[c] – Not applicable because frequency of BS mutations was only two to three.

[d] – Duplication events that are flanked by direct repeats.

[e] – Not applicable because frequency of complex mutations was zero.

[f] – Frameshift (FS): Base substitution (BS) ratio, where a signature MMR defective spectrum is ≥2.

[g] – This value is the FS/BS ratio with the wildtype spectrum contribution subtracted.

[h] – Spectrum taken from Tran and Liskay, 2000.

[i] – In an *mlh3Δ* background as described in the text.

ratio (FS/BS) of two or greater. The preponderance of FS over BS mutations has been shown previously for *msh2Δ* strains (Marsischky, et al., 1996). Operationally, I will consider such an excess of FS over BS mutations as reflective of a "MMR-defective" spectrum. In contrast, the *exo1Δ* strain exhibited a spectrum that was different from a MMR-defective strain, e.g. *mlh1Δ* ($P < 0.001$), but not different from the wildtype strain ($P > 0.1$) (Table 4-2). Although no single pairwise comparison was statistically significant ($P > 0.1$), deletion of *EXO1* combined with any of the *mlh1* or *pms1* single mutations as a general trend seemed to result in a shift in spectrum as represented by a change in FS/BS ratio (Table 4-2). This initial *CAN1* spectrum analysis suggested that *exo1* deficiency alone did not produce a MMR-defective spectrum and that combining *exo1Δ* with many of the *pms1* or *mlh1* mutations examined in this study appeared to cause a shift in the ratio of FS to BS mutations.

Another means to analyze mutation spectrum data is to estimate rates of specific types of mutations arising at the mutation reporter locus (Flores-Rozas and Kolodner, 1998; Harfe and Jinks-Robertson, 1999; Yang, et al., 1999). Using the *CAN1* mutation rates (from Table 4-1) and the frequency of FS and BS mutations arising at *CAN1* (from Table 4-2), I estimated the rates of FS and BS mutations at *CAN1* of my single and double mutant combinations and presented these rates relative to the wildtype rates for FS and BS mutations at *CAN1* (Table 4-3). The limited sample size of *can1* mutants analyzed for each strain and inability to perform statistical analysis on the values in Table 4-3 (see MATERIALS AND METHODS) precluded me from making arguments of synergy, additivity or epistasis of statistical significance. Despite this limitation, I observed two interesting trends. One, the *exo1Δ* mutation synergized with the *mlh1-*

Table 4-3. Relative estimated rates of frameshift and base subsitution mutations at *CAN1*[a].

STRAIN	RELEVANT GENOTYPE	CLASS OF MUTATION	
		Frameshifts Fold Mutator (Rate)[b]	Base substitutions Fold Mutator (Rate)[c]
GCY35	*Wildtype*	1	1
PTY100	*mlh1Δ*	66	11
PTY200	*mlh1-E31A*	15	6
PTY300	*mlh1-G98A*	53	6
PTY101	*pms1Δ*	64	10
PTY104	*pms1Δ mlh3Δ*	63	10
PTY202	*pms1-E61A*[e]	1[d]	1[d]
PTY302	*pms1-G128A*[e]	9	2
PTY105	*exo1Δ*	12	9
PTY106	*mlh1Δ exo1Δ*	72	22
PTY207	*mlh1-E31A exo1Δ*	122	21
PTY307	*mlh1-G98A exo1Δ*	55	42
PTY107	*pms1Δ exo1Δ*	68	21
PTY205	*pms1-E61A exo1Δ*[e]	31	6
PTY305	*pms1-G128A exo1Δ*[e]	38	13

[a] – Rates were calculated from data used to generate Table 4-1 and frequency of framshift and base subsitution mutations from Table 4-2 as described in CHAPTER 2: Materials and Methods.

[b] – Relative to the calculated wildtype rate of $1.05x10^{-7}$ for frameshifts at *CAN1*.

[c] - Relative to the calculated wildtype rate of $1.66x10^{-7}$ for base substitutions at *CAN1*.

[d] – Assuming that PTY204 genocopies the wildtype.

[e] – In an *mlh3Δ* background as described in the text.

E31A mutation and the *pms1-E61A* and *-G128A* mutations for FS mutation rates at *CAN1*, similar to the *hom3-10* reporter described above. And two, as a general trend BS mutation rates at *CAN1* suggested an additive relationship between *mlh1Δ* and *exo1Δ*; *mlh1-E31A* and *exo1Δ*; and *pms1Δ* and *exo1Δ*.

The *CAN1* mutator phenotype of *exo1Δ* is *REV3*-dependent.

The "non-MMR-like" mutational spectrum of the *exo1Δ* single mutant and the general trend of additive interaction between most MutLα mutations and *exo1Δ* for BS rates at *CAN1* suggested that *EXO1* may be involved in MMR-independent pathways for mutation avoidance. Because *rev3Δ* can suppress the mutator phenotype of strains in which certain mutation avoidance pathways are defective (Datta, et al., 2000; Harfe and Jinks-Robertson, 2000a; Scheller, et al., 2000), I examined the role of *REV3* on the *exo1Δ* mutator phenotype. Interestingly, whereas the *CAN1* mutation rate of *exo1Δ* (PTY105) was approximately 9-fold that of the wildtype (GCY35) rate, the double *rev3Δ exo1Δ* (PTY111) rate was indistinguishable from the wildtype rate (Table 4-4). These results suggested that the *exo1Δ* mutator phenotype at *CAN1* was largely *REV3*-dependent.

As described previously, I observed synergism between the *pms1-E61A* and *-G128A* mutations and *exo1Δ* for FS mutation rates (Table 4-1 and 4-3). To determine whether the FS synergy observed between *pms1-E61A* and *-G128A* mutations and *exo1Δ* was dependent on *REV3* , I analyzed the effect of *rev3Δ* mutation on the *pms1-E61A exo1Δ* and *pms1-G128A exo1Δ* double mutant strains (Table 4-4). I observed that the mutation rates of the double mutants was not affected by co-deletion of *REV3* (Table 4-

Table 4-4. Mutation rates of *rev3Δ* strains in yeast MMR mutant backgrounds.

STRAIN	RELEVANT GENOTYPE	FOLD MUTATOR RATE (95% CI)[a]			
		hom3-10[b]		*Can*^{R,c}	
GCY35[d]	*Wildtype*	1	(0-2.3)	1	(0.1-2)
PTY100[d]	*mlh1Δ*	1253	(0-3953)	29	(0-86)
PTY110	*rev3Δ*	0.3	(0.1-0.5)	0.7	(0-2)
PTY105[d]	*exo1Δ*	8	(0-24)	9	(5-14)
PTY111	*rev3Δ exo1Δ*	2	(0-4)	1	(0.6-3)
PTY112	*rev3Δ mlh1Δ*	911	(156-1668)	28	(3-53)
PTY201[d]	*pms1-E61A*	19	(6-32)	1	(0.5-2)
PTY204[d]	*pms1-E61A exo1Δ*	517	(163-872)	15	(9-20)
PTY210	*pms1-E61A exo1Δ rev3Δ*	197	(121-273)	13	(10-15)
PTY301[d]	*pms1-G128A*	78	(33-122)	4	(3-5)
PTY304[d]	*pms1-G128A exo1Δ*	611	(361-862)	24	(20-27)
PTY310	*pms1-G128A exo1Δ rev3Δ*	281	(192-370)	19	(12-25)

[a] – Experiments repeated two to four times with 5-11 cultures per experiment.

[b] – Relative to wildtype GCY35 rate of $9.90\text{x}10^{-09}$.

[c] – Relative to wildtype GCY35 rate of $3.01\text{x}10^{-07}$.

[d] – These rates are taken from Table 4-1.

4, strains PTY210 and PTY310). Consistent with this finding, I found that *mlh1Δ rev3Δ* and *msh2Δ rev3Δ* strains had similar mutation rates to *mlh1Δ* and *msh2Δ* strains, respectively, suggesting that the majority of MMR-dependent mutations are not *REV3*-dependent (compare strain PTY100 versus PTY112 in Table 4-4 and data not shown). Taken together my results suggest that *EXO1* can be involved in at least two mutation avoidance pathways, a MMR-dependent pathway and MMR-independent, *REV3*-dependent pathway.

Discussion

In this study I report results showing that Exo1p can interact physically with MutLα via the Mlh1p subunit. Using the yeast two-hybrid assay I found that a COOH-terminal fragment (400-702) of Exo1p interacts with the COOH-terminus (501-761) of Mlh1p. Epistasis analyses indicate a synergistic increase in the rate of spontaneous FS mutations when the *mlh1-E31A*, *pms1-E61A* or *pms1-G128A* mutation was combined with *exo1Δ*. In addition, the mutator effect of *exo1Δ* did not appear to be reflective of a MMR-defect based upon mutation spectrum analysis at *CAN1*. Finally, my results demonstrate that in contrast to the *mlh1Δ* and *msh2Δ* mutator phenotypes much of the *exo1Δ* mutator phenotype at *CAN1* is *REV3*-dependent.

Previous reports demonstrating physical interactions between *EXO1* and MMR involved the MutS homologue *MSH2* (Tishkoff, et al., 1998). Here I show that the domain of Mlh1p required for interaction with Pms1p (Pang, et al., 1997), Mlh2p and Mlh3p (Wang, et al., 1999) can also interact with a COOH-terminal fragment of Exo1p (Figure 4-1a). Furthermore, using a three-hybrid scheme I demonstrated that Exo1p could interact with MutLα in an Mlh1p-dependent fashion (Figure 4-1b). Whether

Mlh1p interacts with Exo1p via this COOH-terminal domain to the exclusion of the other MutL homologues or can interact simultaneously with Exo1p and the other MutL homologues will require further study. Similar to other reports for yeast and human Exo1p interacting with Msh2p (Tishkoff, et al., 1997; Rasmussen, et al., 2000) I identified a COOH-terminal fragment of Exo1p as interacting with Mlh1p, suggesting that eukaryotic Exo1p interacts with MMR proteins via a conserved COOH-terminal interaction domain. I also demonstrated by yeast two-hybrid that an Mlh1p ATP-binding mutant (LexA-mlh1-G98Ap) was still able to interact with Exo1p, suggesting that Mlh1p ATP-dependent conformational changes may not be necessary for interaction with Exo1p. Similar findings with *E. coli* MutL suggest that the MutL ATPase activity is not necessary for interaction with MutH and UvrD, but is required to activate these downstream components for incision and excision, respectively, *in vitro* (Spampinato and Modrich, 2000). By using genetic analysis as described below, I attempted to address whether the ATPase domains of MutLα are required for activation of Exo1p.

I performed epistasis analysis using MutLα ATPase and *exo1Δ* mutations because my previous studies suggested that MutLα undergoes NH_2-terminal ATP-dependent conformational changes that in turn may be important for coordinating downstream events. In view of the two-hybrid results presented here and the work of others (Tishkoff, et al., 1997; Sokolsky and Alani, 2000), *EXO1* was an obvious candidate. I detected genetic interactions for mutation avoidance between *mlh1* or *pms1* mutations and *exo1Δ*. Of most interest, the *mlh1-E31A* or "ATP-hydrolysis" mutation and both the *pms1* ATPase mutations synergized with *exo1Δ* for FS mutation rates. Similar synergistic interactions for mutation avoidance between *MLH1/PMS1* and *EXO1* were also identified by the Kolodner group during a genetic screen used to identify factors redundant to Exo1p (N. S. Amin, M.-N. Nguyen, S. Oh and R.D. Kolodner, in press). One explanation for the synergy is that the Mlh1p ATP-hydrolysis motif is necessary to coordinate a factor (e.g. another exonuclease) that is functionally redundant with Exo1p. Similarly, as synergy was also observed between *pms1* ATPase mutations and *exo1Δ*, this suggests the Pms1p ATPase motifs may also be necessary to coordinate a factor redundant to Exo1p. Specifically, I hypothesize that these MutLα ATPase motif mutations genocopy defects in factors redundant to Exo1p, such that the combination of these mutations (e.g. *pms1-E61A* and *exo1Δ*) is similar to deletion of *exo1Δ* and these "redundant" factors. This explanation is consistent with recent findings that *E. coli* MutL utilizes its ATPase activity to coordinate both incision (Ban and Yang, 1998; Spampinato and Modrich, 2000; Junop, et al., 2001) and excision *in vitro* (Spampinato and Modrich, 2000). The existence of redundant factors for Exo1p agrees with the lack of a strong mutator phenotype for the *exo1Δ* strain (Tishkoff, et al., 1997; Tran, et al., 1999) and bi-directional excision seen for eukaryotic in vitro MMR (Fang and Modrich, 1993). Alternatively, as MMR and the replication machinery may interact directly (Umar, et al., 1996; Gu, et al., 1998; Flores-Rozas, et al., 2000), these MutLα ATPase motif mutations may affect replication fidelity and result in synergistic increases in mutation rate similar to a polymerase proofreading defect combined with *exo1Δ* (Tran, et al., 1999). Another explanation for the synergism I observed for FS mutation rates is that deletion of *EXO1* in combination with specific MutLα ATPase mutations results in the "structural collapse" of a complex required for MMR. I do not favor exclusively this structural argument because studies using an exonuclease deficient allele of *EXO1* predicted to be structurally intact (Sokolsky and Alani, 2000) also results in synergistic effects when combined with *pms1* ATPase mutants (P.T. Tran and R.M. Liskay, manuscript in preparation).

Investigation of *CAN1* mutations demonstrated that *exo1Δ* exhibited a mutational spectrum different from known MMR-defective strains. In addition, estimated rates of FS and BS mutations at *CAN1* in the single and double mutants seemed to show two general trends. 1) Similar to the *hom3-10* results, the *mlh1* ATP-hydrolysis mutation and both the *pms1* ATPase mutations appeared to synergize with *exo1Δ* for rates of FS mutations at *CAN1*. 2) Using the limited number of BS events at *CAN1*, the single and double mutant calculated rates of BS mutations suggested an additive effect when *exo1Δ* was combined with several different MutLα mutations. Together these *CAN1* results suggested involvement of *EXO1* in a MMR-dependent pathway for avoidance of FS mutations and a MMR-independent pathway for avoidance of BS mutations.

What is the nature of this *EXO1* MMR-independent pathway for mutation avoidance? As *REV3* is required for the mutator phenotype observed when certain mutation avoidance pathways are defective (Broomfield, et al., 1998; Brusky, et al., 2000; Datta, et al., 2000; Harfe and Jinks-Robertson, 2000; Scheller, et al., 2000); I characterized the effect of *rev3Δ* on the *exo1Δ* mutator phenotype. Interestingly, I found that mutations at *CAN1* in the *exo1Δ rev3Δ* strain were reduced to near wildtype levels, suggesting that most of the *CAN1* mutator phenotype of *exo1Δ* is dependent on *REV3*. Presumably the *exo1Δ* mutator phenotype is caused by the action of the *REV3* gene product, whose function as a component of the error-prone polymerase ζ (Rev3p-Rev7p) is to bypass DNA lesions that stall the replicative polymerases (Lawrence and Hinkle, 1996). My data would therefore suggest that Exo1p assists in an error-free process past spontaneous DNA lesions. As Exo1p has been implicated in several DNA metabolic pathways such as repair of UV-damage, recombination and replication (Fiorentini, et al., 1997; Qiu, et al., 1998; Holbeck and Strathern, 1999; Lee and Wilson 3rd, 1999; Qiu, et al., 1999; Kirkpatrick, et al., 2000; Nicholson, et al., 2000), further studies are required to clarify the relationship between *REV3* and *EXO1*. In contrast, the synergism between *exo1Δ* and *pms1* ATPase mutations was not *REV3*-dependent, nor were the *mlh1Δ* or *msh2Δ* mutator phenotypes. These results compliment my *CAN1* data suggesting that *EXO1* can be involved in MMR-dependent and MMR-independent mutation avoidance pathways.

Until recently, mechanistic details of how the eukaryotic MutL homologues couple the mismatch binding activities of MutS homologues to downstream effectors in eukaryotes have been scarce. Studies identifying MutL homologues as members of an emerging ATPase superfamily have provided a framework with which to examine MutL homologue function during MMR-dependent mutation avoidance (Ban and Yang, 1998; Ban, et al., 1999; Dutta and Inouye, 2000; Tran and Liskay, 2000). Based upon the results presented here, I suggest that one function for MutLα ATPase domains is to coordinate Exo1p and possibly redundant activities during mutation avoidance. Because MMR proteins have also been shown to function in other pathways, such as meiotic

(Baker, et al., 1995; Baker, et al., 1996; Hunter and Borts, 1997; Wang, et al., 1999) and homeologous recombination (Selva, et al., 1995; Hunter, et al., 1996; Datta, et al., 1997; Chen and Jinks-Robertson, 1999), the use of MutLα ATPase mutations may be important reagents for a more complete understanding of the role of MMR in these other pathways.

CHAPTER 5: Concluding Discussion

I have examined the function of predicted ATPase motifs in Mlh1p and Pms1p of *S. cerevisiae* MutLα. My results support the notion that yeast MutLα is a functional member of the GHL ATPase family in that both the ATPase motifs of Mlh1p and Pms1p are absolutely required for MMR *in vivo*. Furthermore, *in vitro* and genetic findings suggest that ATP-binding induced conformational changes in MutLα are associated with heterodimerization between the NH_2-termini of Mlh1p and Pms1p. Surprisingly, my *in vivo* results suggest an intrinsic functional asymmetry with respect to the Mlh1p and Pms1p ATPase domains. In addition, I have presented evidence for both physical and genetic interactions between *EXO1* and the components of MutLα, Mlh1p and Pms1p. Furthermore, results of my genetic analysis can be interpreted to signify that one function of the MutLα ATPase domains is to facilitate Exo1p and other exonuclease action during mutation avoidance. Finally, my results also suggest that Exo1p is also involved in one or more MMR-independent mutation avoidance pathways.

In this chapter I will speculate further on specific aspects of my findings in the context of understanding how MMR operates and discuss relevant future studies.

The MutLα ATPase cycle

Work in this thesis has provided initial support for the MutLα ATPase cycle depicted in Figure 3-4. The limited proteolysis results with double ATP-hydrolysis and ATP-binding mutant forms of MutLα are in agreement with the MutLα ATPase cycle. Further *in vitro* analysis of ATPase mutant forms of MutLα will be necessary to confirm and extend the findings presented here. Future biochemical work with the single ATPase MutLα mutants will be necessary to correlate any *in vitro* asymmetry to that already observed *in vivo*. Moreover, the identification and characterization of an intrinsic MutLα ATPase activity is important, but may require additional, as yet unidentified co-factors. As all GHL ATPases possess a similar ATPase cycle (Wigley, et al., 1991; Ali, et al., 1993; Prodromou, et al., 1997a; Prodromou, et al., 1997b; Ban and Yang, 1998; Ban, et al., 1999; Chadli, et al., 2000; Prodromou, et al., 2000; Tran and Liskay, 2000; Young and Hartl, 2000); further refinements of the MutLα ATPase cycle may also hold true for other GHL ATPase cycles.

Recent collaborative work with the Alani laboratory has produced an *in vitro* assay that involves MutSα, MutLα and PCNA protein interacting on a heteroduplex substrate (Bowers, et al., 2001). This assay demonstrates that PCNA protein specifically displaces a MutSα/MutLα complex from a mismatch. One interpretation of this phenomenon is that MutSα, MutLα, and PCNA protein forms a mobile higher-order complex that is competent for recruiting further downstream MMR factors. Examination of single and double ATPase MutLα mutant combinations in this new assay will be helpful in determining if the MutLα ATPase domains are necessary for these very early steps or are restricted to subsequent steps.

In CHAPTER 4, I presented results suggesting that one function of the MutLα ATPase domains may be to direct Exo1p and potentially other redundant factors during MMR. However, another interpretation of these results is that Exo1p serves a predominantly structural role as part of a higher order complex during MMR mutation avoidance. Studies to distinguish between these possibilities will require future work with purified components. A more ambitious goal is the reconstitution of a mismatch-directed *in vitro* excision assay using MutSα, MutLα, PCNA protein, Exo1p and the appropriate substrate, all of which are now available.

EXO1 MMR-independent pathway(s)

My studies have suggested that *EXO1* is minimally involved in at least two mutation avoidance pathways, a MMR-dependent pathway and a MMR-independent pathway. Interestingly, the phenotypes of *exo1Δ*, *REV3*-dependent *CAN1* mutator and methyl methanesulfonate (MMS) sensitivity, are identical to those of *MMS2* and *UBC13* which have been placed in the post-replication repair pathway (PRR) (Broomfield, et al., 1998; Brusky, et al., 2000; Xiao, et al., 2000). PRR functions to bypass spontaneous and induced DNA damaged replication templates using both error-free and error-prone processes (Xiao, et al., 2000). Epistasis studies aimed at assigning *EXO1* to the PRR pathway are underway.

Identifying novel MMR components

As discussed in CHAPTER 3, the proposed ATP-bound NH_2-terminal dimerized form of MutLα is predicted to be an important intermediate based on studies with MutL and Hsp90 showing that these dimer intermediates facilitate novel interactions with downstream components (Ban and Yang, 1998; Grenert, et al., 1999; Chadli, et al., 2000; Prodromou, et al., 2000; Young and Hartl, 2000). I have performed two-hybrid screens with a bait intended to mimic the dimerized ATP-bound MutLα NH_2-termini. Many of the interactors from these screens have been characterized in a preliminary fashion using mutator assays (see APPENDIX C for a list of interactors). Although, none of these interactors have thus far demonstrated a "mutator" phenotype when deleted, several of these interactors deserve closer scrutiny. Recently, two reports have suggested that Hsp90 ATPase activity and ATP-dependent conformational changes may also require COOH-terminal domains (Marcu, et al., 2000; Weikl, et al., 2000). Experiments to address this possibility for MutLα should be initiated and then a corresponding full-length double-hydrolysis MutLα mutant bait should be used to screen a yeast two-hybrid library.

Alternatively, I have generated mutator strains that may be deficient for specific downstream steps of MMR, e.g. PTY204 (*pms1-E61A exo1Δ*). Conducting high-copy suppression screens with such a strain may help identify novel downstream components, i.e. helicases and/or exonucleases.

Asymmetry in MMR

During the course of my studies I obtained results suggesting an intrinsic asymmetry within MutLα with respect to Mlh1p and Pms1p ATPase domains. Specifically, I found that the Mlh1p ATPase domain appeared to be more necessary for the prevention of spontaneous mutations than did the Pms1p ATPase domain. The MutLα asymmetry could be relevant to understanding the GHL ATPase family in a more general context, as the phenomenon of dimer asymmetry, even for "structural homodimers", appears to be a recurring theme in biology (Sixma, 2001). Recent crystal structures of *E. coli* and *Thermus aquaticus* MutS homodimers complexed with mismatched DNA clearly show that similar to eukaryotic MutSα heterodimer, only one protomer of the dimer makes contacts with the mismatch (Lamers, et al., 2000; Obmolova, et al., 2000). These structural studies confirm earlier suggestions that although prokaryotic MutS homodimer is structurally symmetrical; it functions during MMR in an asymmetrical fashion (Malkov, et al., 1997). Work with MutSα has demonstrated that the Msh2p and Msh6p ATPase domains appear to contribute differentially to the total ATPase activity of the heterodimer (Iaccarino, et al., 1998; Studamire, et al., 1998). Furthermore, studies suggest that Msh6p is more important for substrate recognition (Bowers, et al., 1999; Dufner, et al., 2000) and signaling for complex formation with MutLα (Bowers, et al., 2000) (J. Bowers, P.T. Tran, R.M. Liskay and E. Alani, unpublished results). As mentioned in CHAPTER 3, a kinetic asymmetry has been detected in the homodimeric ATPases, topoisomerase II from *S. cerevisiae* and the γ complex from *E. coli* (Harkins, et al., 1998; Baird, et al., 1999; Hingorani, et al., 1999). Does this same paradigm hold true for MutL and the other GHL ATPases? Currently no studies have demonstrated that the protomers of a MutL homodimer or any of the other GHL homodimers operate in an asymmetrical manner. However, I suggest that similar to MutLα, MutL homodimer and perhaps all GHL homodimers behave in an asymmetrical manner at some stage during their action.

The phenomenon of MutLα ATPase domain asymmetry observed for mutation avoidance may imply a mechanism by which the three separate yeast MutL heterodimers (Mlh1p-Pms1p, Mlh1p-Mlh2p and Mlh1p-Mlh3p) execute their separate functions (see Figure 1-2) (Wang, et al., 1999). Specifically, each MLH ATPase domain may function separately to direct components for their respective pathways. For example, the most impressive *mlh3Δ* phenotype is reduction in the number of crossovers during meiosis

(Wang, et al., 1999). My hypothesis would predict that the Mlh3p ATPase domain is required to promote crossovers. One potential caveat is that the Mlh1p ATPase domain may be required for only some or all of the MLH functions. Collaborative studies with the Jinks-Robertson group have shown that in the presence of wildtype Mlh1p, the Pms1p ATPase domain appears dispensable for mutation avoidance, but is required for suppression of homeologous recombination. In contrast, the Mlh1p ATPase domain appears to be required for both functions (C. Welz-Voegele, J. E. Stone, P. T. Tran, H. M. Kearney, R. M. Liskay, T. D. Petes and S. Jinks-Robertson, unpublished data). It would be interesting to test this model further by examining ATPase mutants of *mlh3* and *mlh2* in conjunction with *mlh1* and *pms1* ATPase mutants using assays for the assorted MMR functions.

References

Alani, E., Cao, L. and Kleckner, N. (1987). A method for gene disruption that allows repeated use of URA3 selection in the construction of multiply disrupted yeast strains. Genetics 116, 541-5.

Alani, E., Chi, N.-W. and Kolodner, R. (1995). The Saccharomyces cerevisiae Msh2 protein specifically binds to duplex oligonucleotides containing mismatched DNA base pairs and insertions. Genes Dev. 9, 234-47.

Alani, E., Reenan, R. A. G. and Kolodner, R. (1994). Interaction between mismatch repair and genetic recombination in Saccharomyces cerevisiae. Genetics 137, 19-39.

Alani, E., Sokolsky, T., Studamire, B., Miret, J. J. and Lahue, R. S. (1997). Genetic and biochemical analysis of Msh2p-Msh6p: role of ATP hydrolysis and Msh2p-Msh6p subunit interactions in mismatch base pair recognition. Mol. Cell. Biol. 17, 2436-47.

Ali, J. A., Jackson, A. P., Howells, A. J. and Maxwell, A. (1993). The 43-kilodalton N-terminal fragment of the DNA gyrase b protein hydrolyzes ATP and binds coumarin drugs. Biochemistry 32, 2717-24.

Aronshtam, A. and Marinus, M. G. (1996). Dominant negative mutator mutations in the mutL gene of Escherichia coli. Nucleic Acids Res. 24, 2498-504.

Baird, C. L., Harkins, T. T., Morris, S. K. and Lindsley, J. E. (1999). Topoisomerase II drives DNA transport by hydrolyzing one ATP. Proc. Natl. Acad. Sci. USA 96, 13685-90.

Baker, S., Plug, A., Prolla, T., Bronner, C., Harris, A., Yao, X., Christie, D.-M., Monell, C., Arnheim, N., Bradley, A., Ashley, T. and Liskay, R. (1996). Involvement of Mlh1 in DNA mismatch repair and meiotic crossing over. Nat. Genetics 13, 336-42.

Baker, S. M., Bronner, C. E., Zhang, L., Plug, A. W., Robatzek, M., Warren, G., Elliott, E. A., Yu, J., T., A., Arnheim, N., Flavell, R. A. and Liskay, R. M. (1995). Male mice defective in the DNA mismatch repair gene PMS2 exhibit abnormal chromosome synapsis in meiosis. Cell 82, 309-19.

Ban, C., Junop, M. and Yang, W. (1999). Transformation of MutL by ATP binding and hydrolysis: a switch in DNA mismatch repair. Cell 97, 85-97.

Ban, C. and Yang, W. (1998a). Crystal Structure and ATPase activity of MutL: Implications for DNA repair and mutagenesis. Cell 95, 541-52.

Ban, C. and Yang, W. (1998b). Structural basis for MutH activation in E.coli mismatch repair and relationship of MutH to restriction endonucleases. EMBO J. 17, 1526-34.

Bergerat, A., de Massy, B., Gadelle, D., Varoutas, P. C., Nicolas, A. and Forterre, P. (1997). An atypical topoisomerase II from Archaea with implications for meiotic recombination. Nature 386, 414-7.

Borts, R. and Haber, J. (1987). Meiotic recombination in yeast: alteration by multiple heterozygosities. Science 237, 1459-65.

Borts, R. H., Leung, W. Y., Kramer, W., Kramer, B., Williamson, M., Fogel, S. and Haber, J. E. (1990). Mismatch repair-induced meiotic recombination requires the PMS1 gene product. Genetics 124, 573-84.

Bowers, J., Sokolsky, T., Quach, T. and Alani, E. (1999). A mutation in the MSH6 subunit of the Saccharomyces cerevisiae MSH2- MSH6 complex disrupts mismatch recognition. J. Biol. Chem. 274, 16115-25.

Bowers, J., Tran, P., Liskay, R. and Alani, E. (2000). Analysis of yeast MSH2-MSH6 suggests that the initiation of mismatch repair can be separated into discrete steps. J. Mol. Biol. 302, 327-38.

Bowers, J., Tran, P. T., Joshi, A., Liskay, R. M. and Alani, E. (2001). MSH-MLH complexes formed at a DNA mismatch are disrupted by the PCNA sliding clamp. J. Mol. Biol. 306, 957-68.

Broomfield, S., Chow, B. and Xiao, W. (1998). MMS2, encoding a ubiquitin-conjugating-enzyme-like protein, is a member of the yeast error-free postreplication repair pathway. Proc. Natl. Acad. Sci. U S A 95, 5678-83.

Brusky, J., Zhu, Y. and Xiao, W. (2000). UBC13, a DNA-damage-inducible gene, is a member of the error-free postreplication repair pathway in Saccharomyces cerevisiae. Curr. Genet. 37, 168-74.

Buermeyer, A. B., Deschenes, S. M., Baker, S. M. and Liskay, R. M. (1999). Mammalian DNA mismatch repair. Annu. Rev. Genetics 33, 533-64.

Chadli, A., Bouhouche, I., Sullivan, W., Stensgard, B., McMahon, N., Catelli, M. and Toft, D. (2000). Dimerization and N-terminal domain proximity underlie the function of the molecular chaperone heat shock protein 90. Proc. Natl. Acad. Sci. U S A 97, 12524-9.

Chambers, S., Hunter, N., Louis, E. and Borts, R. (1996). The mismatch repair system reduces meiotic homeologous recombination and stimulates recombination-dependent chromosome loss. Mol. Cell. Biol. 16, 6110-20.

Chen, C., Merrill, B. J., Lau, P. J., Holm, C. and Kolodner, R. D. (1999). Saccharomyces cerevisiae pol30 (proliferating cell nuclear antigen) mutations impair replication fidelity and mismatch repair. Mol. Cell. Biol. 19, 7801-15.

Chen, W. and Jinks-Robertson, S. (1998). Mismatch repair proteins regulate heteroduplex formation during mitotic recombination in yeast. Mol. Cell. Biol. 18, 6525-37.

Chen, W. and Jinks-Robertson, S. (1999). The role of the mismatch repair machinery in regulating mitotic and meiotic recombination between diverged sequences in yeast. Genetics 151, 1299-313.

Dao, V. and Modrich, P. (1998). Mismatch-, MutS-, MutL-, and helicase II-dependent unwinding from the single-strand break of an incised heteroduplex. J. Biol. Chem. 273, 9202-7.

Datta, A., Adjiri, A., New, L., Crouse, G. F. and Jinks-Robertson, S. (1996). Mitotic crossovers between diverged sequences are regulated by mismatch repair proteins in Saccaromyces cerevisiae. Mol. Cell. Biol. 16, 1085-93.

Datta, A., Hendrix, M., Lipsitch, M. and Jinks-Robertson, S. (1997). Dual roles for DNA sequence identity and the mismatch repair system in the regulation of mitotic crossing-over in yeast. Proc. Natl. Acad. Sci. U S A 94, 9757-62.

Datta, A., Schmeits, J., Amin, N., Lau, P., Myung, K. and Kolodner, R. (2000). Checkpoint-dependent activation of mutagenic repair in Saccharomyces cerevisiae pol3-01 mutants. Mol. Cell. 6, 593-603.

Drummond, J. T., Anthoney, A., Brown, R. and Modrich, P. (1996). Cisplatin and adriamycin resistance are associated with MutLalpha and mismatch repair deficiency in an ovarian tumor cell line. J. Biol. Chem. 271, 19645-8.

Dufner, P., Marra, G., Raschle, M. and Jiricny, J. (2000). Mismatch recognition and DNA-dependent stimulation of the ATPase activity of hMutSalpha is abolished by a single mutation in the hMSH6 subunit. J. Biol. Chem. 275, 36550-5.

Dutta, I. and Inouye, I. (2000). GHKL, an emergent ATPase/kinase superfamily. Trends Biochem. Sci. 25, 24-28.

Fang, W.-H. and Modrich, P. (1993). Human Strand-specific Mismatch Repair Occurs by a Bidirectional Mechanism Silimar to That of the Bacterial Reaction. J. Biol. Chem. 268, 11838-44.

Fiorentini, P., Huang, K. N., Tishkoff, D. X., Kolodner, R. D. and Symington, L. S. (1997). Exonuclease I of Saccharomyces cerevisiae functions in mitotic recombination in vivo and in vitro. Mol. Cell. Biol. 17, 2764-73.

Flores-Rozas, H., Clark, D. and Kolodner, R. D. (2000). Proliferating cell nuclear antigen and Msh2p-Msh6p interact to form an active mispair recognition complex. Nat. Genetics 26, 375-8.

Flores-Rozas, H. and Kolodner, R. D. (1998). The Saccharomyces cerevisiae MLH3 gene functions in MSH3-dependent suppression of frameshift mutations. Proc. Natl. Acad. Sci. US A 95, 12404-9.

Gietz, R. D. and Schiestl, R. H. (1991). Applications of high efficiency lithium acetate transformation of intact yeast cells using single-stranded nucleic acids as carrier. Yeast 7, 253-63.

Grenert, J. P., Johnson, B. D. and Toft, D. O. (1999). The importance of ATP binding and hydrolysis by hsp90 in formation and function of protein heterocomplexes. J. Biol. Chem. 274, 17525-33.

Grenert, J. P., Sullivan, W. P., Fadden, P., Haystead, T. A. J., Clark, J., Mimnaugh, E., Krutzsch, H., Ochel, H. J., Schulte, T. W., Sausville, E., Neckers, L. M. and Toft, D. O. (1997). The amino-terminal domain of heat shock protein 90 (hsp90) that binds geldanamycin is an ATP/ADP switch domain that regulates hsp90 conformation. J. Biol. Chem. 272, 23843-50.

Grilley, M., Holmes, J., Yashar, B. and Modrich, P. (1990). Mechanisms of DNA-mismatch correction. Mutat. Res. 236, 253-67.

Gu, L., Hong, Y., McCulloch, S., Watanabe, H. and Li, G. M. (1998). ATP-dependent interaction of human mismatch repair proteins and dual role of PCNA in mismatch repair. Nucleic Acids Res. 26, 1173-8.

Haber, L. T. and Walker, G. C. (1991). Altering the conserved nucleotide binding motif in the salmonella typhimurium MutS mismatch repair protein affects both its ATPase and mismatch binding activities. EMBO J. 10, 2707-15.

Habraken, Y., Sung, P., Prakash, L. and Prakash, S. (1997). Enhancement of MSH2-MSH3-mediated mismatch recognition by the yeast MLH1-PMS1 complex. Curr. Biol. 7, 790-3.

Hall, M. C., Jordan, J. R. and Matson, S. W. (1998). Evidence for a physical interaction between the Escherichia coli methyl- directed mismatch repair proteins MutL and UvrD. EBMO J. 17, 1535-41.

Hall, M. C. and Matson, S. W. (1999). The Escherichia coli MutL protein physically interacts with MutH and stimulates the MutH-associated endonuclease activity. J. Biol. Chem. 274, 1306-12.

Harfe, B. and Jinks-Robertson, S. (1999). Removal of frameshift intermediates by mismatch repair proteins in Saccharomyces cerevisiae. Mol. Cell. Biol. 19, 4766-73.

Harfe, B. and Jinks-Robertson, S. (2000a). DNA polymerase zeta introduces multiple mutations bypassing spontaneous DNA damage in Saccharomyces cerevisiae. Mol. Cell. 6, 1491-9.

Harfe, B. D. and Jinks-Robertson, S. (2000b). DNA mismatch repair and genetic instability. Annu. Rev. Genet. 34, 359-99.

Harfe, B. D. and Jinks-Robertson, S. (2000c). Mismatch repair proteins and mitotic genome stability. Mutat. Res. 451, 151-67.

Harkins, T. T., Lewis, T. J. and Lindsley, J. E. (1998). Pre-steady-state analysis of ATP hydrolysis by Saccharomyces cerevisiae DNA topoisomerase II. 2. Kinetic mechanism for the sequential hydrolysis of two ATP. Biochemistry 37, 7299-312.

Hingorani, M. M., Bloom, L. B., Goodman, M. F. and O'Donnell, M. (1999). Division of labor--sequential ATP hydrolysis drives assembly of a DNA polymerase sliding clamp around DNA. EMBO J. 18, 5131-44.

Holbeck, S. and Strathern, J. (1999). EXO1 of Saccharomyces cerevisiae functions in mutagenesis during double-strand break repair. Ann. N. Y. Acad. Sci. 870, 375-7.

Holliday, R. A. (1964). A mechanism for gene conversion in fungi. Genet. Res. 5, 282-304.

Hollingsworth, N. M., Ponte, L. and Halsey, C. (1995). MSH5, a novel MutS homolog, facilitates meiotic reciprocal recombination between homologs in Saccharomyces cerevisiae but not mismatch repair. Genes Dev. 9, 1728-39.

Hunter, N. and Borts, R. H. (1997). Mlh1 is unique among mismatch repair proteins in its ability to promote crossing-over during meiosis. Genes Dev. 11, 1573-82.

Hunter, N., Chambers, S. R., Louis, E. J. and Borts, R. H. (1996). The mismatch repair system contributes to meiotic sterility in an interspecific yeast hybrid. EMBO J. 15, 1726-33.

Iaccarino, I., Marra, G., Palombo, F. and Jiricny, J. (1998). hMSH2 and hMSH6 play distinct roles in mismatch binding and contribute differently to the ATPase activity of hMutSalpha. EMBO J. 17, 2677-86.

Iaccarino, I., Palombo, F., Drummond, J., Totty, N. F., Hsuan, J. J., Modrich, P. and Jiricny, J. (1996). MSH6, a Saccharomyces cerevisiae protein that binds to mismatches as a heterodimer with MSH2. Curr. Biol. 6, 484-6.

Jackson, A. P. and Maxwell, A. (1993). Identifying the catalytic residue of the ATPase reaction of DNA gyrase. Proc. Natl. Acad. Sci. U S A 90, 11232-6.

Jakob, U., Scheibel, T., Bose, S., Reinstein, J. and Buchner, J. (1996). Assessment of the ATP binding properties of Hsp90. J. Biol. Chem. 271, 10035-41.

Jiricny, J. (1998). Eukaryotic mismatch repair: an update. Mutat. Res. 409, 107-21.

Jiricny, J., Su, S.-S., Wood, S. G. and Modrich, P. (1988). Mismatch-containing oligonucleotide duplexes bound by the E.coli mutS-encoded protein. Nucleic Acids Res. 16, 7843-54.

Johnson, R. E., Kovvali, G. K., Guzder, S. N., Amin, N. S., Holm, C., Habraken, Y., Sung, P., Prakash, L. and Prakash, S. (1996a). Evidence for involvement of yeast proliferating cell nuclear antigen in DNA mismatch repair. J. Biol. Chem. 271, 27987-90.

Johnson, R. E., Kovvali, G. K., Prakash, L. and Prakash, S. (1995). Requirement of the yeast RTH1 5' to 3' exonuclease for the stability of simple repetitive DNA. Science 269, 238-40.

Johnson, R. E., Kovvali, G. K., Prakash, L. and Prakash, S. (1996b). Requirement of the yeast MSH3 and MSH6 genes for MSH2-dependent genomic stability. J. Biol. Chem. 271, 7285-8.

Junop, M. S., Obmolova, G., Rausch, K., Hsieh, P. and Yang, W. (2001). Composite Active Site of an ABC ATPase. MutS Uses ATP to Verify Mismatch Recognition and Authorize DNA Repair. Mol. Cell. 7, 1-12.

Khazanehdari, K. A. and Borts, R. H. (2000). EXO1 and MSH4 differentially affect crossing-over and segregation. Chromosoma 109, 94-102.

Kirkpatrick, D., Ferguson, J., Petes, T. and Symington, L. (2000). Decreased meiotic intergenic recombination and increased meiosis I nondisjunction in exo1 mutants of saccharomyces cerevisiae. Genetics 156, 1549-57.

Kolodner, R. D. and Marsischky, G. T. (1999). Eukaryotic DNA mismatch repair. Curr. Opin. Genet. Dev. 9, 89-96.

Lamers, M. H., Perrakis, A., Enzlin, J. H., Winterwerp, H. H., de Wind, N. and Sixma, T. K. (2000). The crystal structure of DNA mismatch repair protein MutS binding to a G x T mismatch. Nature 407, 711-7.

Lawrence, C. W. and Hinkle, D. C. (1996). DNA polymerase zeta and the control of DNA damage induced mutagenesis in eukaryotes. Cancer Surv. 28, 21-31.

Leadon, S. A. and Avrutskaya, A. V. (1998). Requirement for DNA mismatch repair proteins in the transcription- coupled repair of thymine glycols in Saccharomyces cerevisiae. Mutat. Res. 407, 177-87.

Lee, B. and Wilson 3rd, D. (1999). The RAD2 domain of human exonuclease 1 exhibits 5' to 3' exonuclease and flap structure-specific endonuclease activities. J. Biol. Chem. 274, 37763-9.

Liberfarb, R. M. and Bryson, V. (1970). Isolation, characterization and genetic analysis of mutator genes in Escherichia coli B and K12. J. Bacteriol. 104, 363-75.

Lyons, S. M. and Schendel, P. F. (1984). Kinetics of methylation in Escherichia coli K-12. J. Bacteriol. 159, 421-23.

Malkov, V. A., Biswas, I., Camerini-Otero, R. D. and Hsieh, P. (1997). Photocross-linking of the NH2-terminal region of Taq MutS protein to the major groove of a heteroduplex DNA. J. Biol. Chem. 272, 23811-7.

Maniatis, T., Fritsch, E. F. and Sambrook, J. (1982). Molecular Cloning. (Cold Spring Harbor, Cold Spring Harbor Laboratory).

Marcu, M., Chadli, A., Bouhouche, I., Catelli, M. and Neckers, L. (2000). The heat shock protein 90 antagonist novobiocin interacts with a previously unrecognized ATP-binding domain in the carboxyl terminus of the chaperone. J Biol Chem. 275, 37181-6.

Marsischky, G. T., Filosi, M., Kane, M. F. and Kolodner, R. (1996). Redundancy of Saccharomyces cerevisiae MSH3 and MSH6 in MSH2-dependent mismatch repair. Genes Dev. 10, 407-20.

Marsischky, G. T. and Kolodner, R. D. (1999). Biochemical Characterization of the Interaction between the Saccharomyces cerevisiae MSH2-MSH6 Complex and Mispaired Bases in DNA. J. Biol. Chem. 274, 26668-82.

Mechanic, L. E., Frankel, B. A. and Matson, S. W. (2000). Escherichia coli MutL loads DNA helicase II onto DNA. J. Biol. Chem. 275, 38337-46.

Mellon, I. and Champe, G. N. (1996). Products of DNA mismatch repair genes mutS and mutL are required for transcription-coupled nucleotide-excision repair of the lactose operon in Escherichia coli. Proc. Natl. Acad. Sci. USA 93, 1292-7.

Modrich, P. and Lahue, R. (1996). Mismatch repair in replication fidelity, genetic recombination, and cancer biology. Annu. Rev. Biochem. 65, 101-33.

Mushegian, A. R., Bassett, D. E., Jr., Boguski, M. S., Bork, P. and Koonin, E. V. (1997). Positionally cloned human disease genes: patterns of evolutionary conservation and functional motifs. Proc. Natl. Acad. Sci. USA 94, 5831-6.

New, L., Liu, K. and Crouse, G. F. (1993). The yeast gene MSH3 defines a new class of eukaryotic MutS homologues. Mol. Gen. Genet. 239, 97-108.

Nicholson, A., Hendrix, M., Jinks-Robertson, S. and Crouse, G. F. (2000). Regulation of Mitotic Homeologous Recombination in Yeast. Functions of mismatch repair and nucleotide excision repair genes. Genetics 154, 133-46.

Nicolaides, N. C., Littman, S. J., Modrich, P., Kinzler, K. W. and Vogelstein, B. (1998). A naturally occurring hPMS2 mutation can confer a dominant negative mutator phenotype. Mol. Cell. Biol. 18, 1635-41.

Obermann, W. M. J., Sondermann, H., Russo, A. A., Pavletich, N. P. and Hartl, F. U. (1998). In Vivo Function of Hsp90 Is Dependent on ATP Binding and ATP Hydrolysis. J. Cell Biol. 143, 901-10.

Obmolova, G., Ban, C., Hsieh, P. and Yang, W. (2000). Crystal structures of mismatch repair protein MutS and its complex with a substrate DNA. Nature 407, 703-10.

Panaretou, B., Prodromou, C., Roe, S. M., O'Brien, R., Ladbury, J. E., Piper, P. W. and Pearl, L. H. (1998). ATP binding and hydrolysis are essential to the function of the Hsp90 molecular chaperone in vivo. EMBO J. 17, 4829-36.

Pang, Q., Prolla, T. A. and Liskay, R. M. (1997). Functional domains of the Saccharomyces cerevisiae MLH1 and PMS1 DNA mismatch repair proteins and their relevance to hereditary nonpolyposis colorectal cancer-associated mutations. Mol. Cell. Biol. 17, 4465-73.

Paques, F. and Haber, J. (1999). Multiple pathways of recombination induced by double-strand breaks in Saccharomyces cerevisiae. Microbiol. Mol. Biol. Rev. 63, 349-404.

Paques, F. and Haber, J. E. (1997). Two pathways for removal of nonhomologous DNA ends during double-strand break repair in Saccharomyces cerevisiae. Mol. Cell. Biol. 17, 6765-71.

Petes, T. D., Malone, R. E. and Symington, L. S. (1991). Recombination in yeast. In The Molecular and Cellular Biology of the Yeast Saccharomyces, J. Broach, E. Jones and J. Pringle, (ed.), vol. 1, (Cold Spring Harbor, Cold Spring Harbor Laboratory), pp. 407-521.

Pochart, P., Woltering, D. and Hollingsworth, N. M. (1997). Conserved properties between functionally distinct MutS homologs in yeast. J. Biol. Chem. 272, 30345-9.

Printen, J. A. and Sprague, G. F., Jr. (1994). Protein-protein interactions in the yeast pheromone response pathway: Ste5p interacts with all members of the MAP kinase cascade. Genetics 138, 609-19.

Prodromou, C., Panaretou, B., Chohan, S., Siligardi, G., O'Brien, R., Ladbury, J., Roe, S., Piper, P. and Pearl, L. (2000). The ATPase cycle of Hsp90 drives a molecular 'clamp' via transient dimerization of the N-terminal domains. EMBO J. 19, 4383-92.

Prodromou, C., Roe, S. M., O'Brien, R., Ladbury, J. E., Piper, P. W. and Pearl, L. H. (1997a). Identification and structural characterization of the ATP/ADP-binding site in the Hsp90 molecular chaperone. Cell 90, 65-75.

Prodromou, C., Roe, S. M., Piper, P. W. and Pearl, L. H. (1997b). A molecular clamp in the crystal structure of the N-terminal domain of the yeast Hsp90 chaperone. Nat. Struct. Biol. 4, 477-82.

Prodromou, C., Siligardi, G., O'Brien, R., Woolfson, D. N., Regan, L., Panaretou, B., Ladbury, J. E., Piper, P. W. and Pearl, L. H. (1999). Regulation of Hsp90 ATPase activity by tetratricopeptide repeat (TPR)- domain co-chaperones. EMBO J. 18, 754-62.

Prolla, T., Christie, D.-M. and Liskay, R. M. (1994a). Dual requirement in yeast DNA mismatch repair for MLH1 and PMS1, two homologs of the bacterial mutL gene. Mol. Cell. Biol. 14, 407-15.

Prolla, T. A., Pang, Q., Alani, E., Kolodner, R. D. and Liskay, R. M. (1994b). Interactions between the Msh2, Mlh1 and Pms1 proteins during the initiation of DNA mismatch repair. Science 265, 1091-93.

Qiu, J., Guan, M., Bailis, A. and Shen, B. (1998). Saccharomyces cerevisiae exonuclease-1 plays a role in UV resistance that is distinct from nucleotide excision repair. Nucleic Acids Res. 26, 3077-83.

Qiu, J., Qian, Y., Chen, V., Guan, M. X. and Shen, B. (1999). Human exonuclease 1 functionally complements its yeast homologues in DNA recombination, RNA primer removal, and mutation avoidance. J. Biol. Chem. 274, 17893-900.

Rasmussen, L. J., Rasmussen, M., Lee, B., Rasmussen, A. K., Wilson, D. M., Nielsen, F. C. and Bisgaard, H. C. (2000). Identification of factors interacting with hMSH2 in the fetal liver utilizing the yeast two-hybrid system. In vivo interaction through the C-terminal domains of hEXO1 and hMSH2 and comparative expression analysis. Mutat. Res. 460, 41-52.

Rayssiguier, C., Thaler, D. S. and Radman, M. (1989). The barrier to recombination between Escherichia coli and Salmonella typhimurium is disrupted in mismatch-repair mutants. Nature 342, 396-401.

Reenan, R. A. and Kolodner, R. D. (1992). Characterization of insertion mutations in the Saccharomyces cerevisiae MSH1 and MSH2 genes: evidence for separate mitochondrial and nuclear functions. Genetics 132, 975-85.

Ross-Macdonald, P. and Roeder, G. S. (1994). Mutation of a meiosis-specific MutS homolog decreases crossing over but not mismatch correction. Cell 79, 1069-80.

Sancar, A. and Hearst, J. E. (1993). Molecular matchmakers. Science 259, 1415-20.

Schaaper, R. (1993). Base selection, proofreading, and mismatch repair during DNA replication in Escherichia coli. J. Biol. Chem. 268, 23762-5.

Scheibel, T., Neuhofen, S., Weikl, T., Mayr, C., Reinstein, J., Vogel, P. D. and Buchner, J. (1997). ATP-binding properties of human Hsp90. J. Biol. Chem. 272, 18608-13.

Scheller, J., Schurer, A., Rudolph, C., Hettwer, S. and Kramer, W. (2000). MPH1, a yeast gene encoding a DEAH protein, plays a role in protection of the genome from spontaneous and chemically induced damage. Genetics 155, 1069-81.

Selva, E. M., New, L., Crouse, G. F. and Lahue, R. S. (1995). Mismatch correction acts as a barrier to homeologous recombination in Saccharomyces cerevisiae. Genetics 139, 1175-88.

Shcherbakova, P. V. and Kunkel, T. A. (1999). Mutator phenotypes conferred by MLH1 overexpression and by heterozygosity for mlh1 mutations. Mol. Cell. Biol. 19, 3177-83.

Shelley, E. L. (1999). Mechanisms ensuring genomic integrity in yeast. in Molecular & Medical Genetics. Oregon Health Sciences University, Portland. p. 116.

Shen, P. and Huang, H. V. (1989). Effect of base pair mismatches on recombination via the RecBCD pathway. Mol. Gen. Genet. 218, 358-60.

Siegel, E. C. and Bryson, V. (1967). Mutator gene of Escherichia coli B. J. Bacteriol. 94, 38-47.

Siegel, E. C. and Ivers, J. J. (1975). mut-25, a mutation to mutator linked to purA in Escherichia coli. J. Bacteriol. 121, 524-30.

Siegel, E. C. and Kamel, F. (1974). Reversion of frameshift mutations by mutator genes in Escherichia coli. J. Bacteriol. 117, 994-1001.

Sixma, T. (2001). DNA mismatch repair: MutS structures bound to mismatches. Curr. Opin. Struct. Biol. 11, 47-52.

Sokolsky, T. and Alani, E. (2000). EXO1 and MSH6 are high-copy suppressors of conditional mutations in the MSH2 mismatch repair gene of Saccharomyces cerevisiae. Genetics 155, 589-99.

Spampinato, C. and Modrich, P. (2000). The MutL ATPase is required for mismatch repair. J. Biol. Chem. 275, 9863-9.

Stambuk, S. and Radman, M. (1998). Mechanism and control of interspecies recombination in Escherichia coli. I. Mismatch repair, methylation, recombination and replication functions. Genetics 150, 533-42.

Stancheva, I., Koller, T. and Sogo, J. M. (1999). Asymmetry of Dam remethylation on the leading and lagging arms of plasmid replicative intermediates. EMBO J. 18, 6542-51.

Studamire, B., Quach, T. and Alani, E. (1998). Saccharomyces cerevisiae msh2p and msh6p ATPase activities are both required during mismatch repair. Mol. Cell. Biol. 18, 7590-601.

Sugawara, N. and Haber, J. (1992). Characterization of double-strand break-induced recombination: homology requirements and single-stranded DNA formation. Mol. Cell. Biol. 12, 563-75.

Sugawara, N., Ira, G. and Haber, J. (2000). DNA length dependence of the single-strand annealing pathway and the role of Saccharomyces cerevisiae RAD59 in double-strand break repair. Mol. Cell. Biol. 20, 5300-9.

Sugawara, N., Paques, F., Colaiacovo, M. and Haber, J. E. (1997). Role of Saccharomyces cerevisiae Msh2 and Msh3 repair proteins in double-strand break-induced recombination. Proc. Natl. Acad. Sci. USA 94, 9214-9.

Sugino, A. and Cozzarelli, N. R. (1980). The intrinsic ATPase of DNA Gyrase. J. Biol. Chem. 255, 6299-306.

Tishkoff, D. X., Amin, N. S., Viars, C. S., Arden, K. C. and Kolodner, R. D. (1998). Identification of a human gene encoding a homologue of Saccharomyces cerevisiae EXO1, an exonuclease implicated in mismatch repair and recombination. Cancer Res. 58, 5027-31.

Tishkoff, D. X., Boerger, A. L., Bertrand, P., Filosi, N., Gaida, G. M., Kane, M. F. and Kolodner, R. D. (1997a). Identification and characterization of Saccharomyces cerevisiae EXO1, a gene encoding an exonuclease that interacts with MSH2. Proc. Natl. Acad. Sci. USA 94, 7487-92.

Tishkoff, D. X., Filosi, N., Gaida, G. M. and Kolodner, R. D. (1997b). A novel mutation avoidance mechanism dependent on S. cerevisiae RAD27 is distinct from DNA mismatch repair. Cell 88, 253-63.

Tran, H. T., Gordenin, D. A. and Resnick, M. A. (1999). The 3'-->5' exonucleases of DNA polymerases delta and epsilon and the 5'-->3' exonuclease Exo1 have major roles in postreplication mutation avoidance in Saccharomyces cerevisiae. Mol. Cell. Biol. 19, 2000-7.

Tran, P. T. and Liskay, R. M. (2000). Functional studies on the candidate ATPase domains of Saccharomyces cerevisiae MutLalpha. Mol. Cell. Biol. 20, 6390-8.

Tsubouchi, H. and Ogawa, H. (2000). Exo1 roles for repair of DNA double-strand breaks and meiotic crossing over in Saccharomyces cerevisiae. Mol. Biol. Cell. 11, 2221-33.

Umar, A., Buermeyer, A. B., Simon, J. A., Thomas, D. C., Clark, A. B., Liskay, R. M. and Kunkel, T. A. (1996). Requirement for PCNA in DNA mismatch repair at a step preceding DNA resynthesis. Cell 87, 65-73.

Viswanathan, M. and Lovett, S. T. (1998). Single-strand DNA-specific exonucleases in Escherichia coli. Roles in repair and mutation avoidance. Genetics 149, 7-16.

Vojtek, A. B., Hollenberg, S. M. and Cooper, J. A. (1993). Mammalian ras interacts directly with the serine/threonine kinase raf. Cell 74, 205-14.

Wang, T. F., Kleckner, N. and Hunter, N. (1999). Functional specificity of MutL homologs in yeast: evidence for three Mlh1-based heterocomplexes with distinct roles during meiosis in recombination and mismatch correction. Proc. Natl. Acad. Sci. USA 96, 13914-9.

Weikl, T., Muschler, P., Richter, K., Veit, T., Reinstein, J. and Buchner, J. (2000). C-terminal regions of Hsp90 are important for trapping the nucleotide during the ATPase cycle. J. Mol. Biol. 303, 583-92.

Wigley, D. B., Davies, G. J., Dodson, E. J., Maxwell, A. and Dodson, G. (1991). Crystal structure of an N-terminal fragment of the DNA gyrase B protein. Nature 351, 624-9.

Williamson, M. S., Game, J. C. and Fogel, S. (1985). Meiotic gene conversion mutants in Saccharomyces cerevisiae. I. Isolation and characterization of pms1-1 and pms1-2. Genetics 110, 609-46.

Xiao, W., Chow, B., Broomfield, S. and Hanna, M. (2000). The Saccharomyces cerevisiae RAD6 group is composed of an error-prone and two error-free postreplication repair pathways. Genetics 155, 1633-41.

Yamaguchi, M., Dao, V. and Modrich, P. (1998). MutS and MutL activate DNA helicase II in a mismatch-dependent manner. J. Biol. Chem. 273, 9197-201.

Yang, Y., Karthikeyan, R., Mack, S., Vonarx, E. and Kunz, B. (1999). Analysis of yeast pms1, msh2, and mlh1 mutators points to differences in mismatch correction efficiencies between prokaryotic and eukaryotic cells. Mol. Gen. Genet. 261, 777-87.

Young, J. and Hartl, F. (2000). Polypeptide release by Hsp90 involves ATP hydrolysis and is enhanced by the co-chaperone p23. EMBO J. 19, 5930-40.

Zahrt, T. C. and Maloy, S. (1997). Barriers to recombination between closely related bacteria: MutS and RecBCD inhibit recombination between Salmonella typhimurium and Salmonella typhi. Proc. Natl. Acad. Sci. USA 94, 9786-91.

APPENDIX A : Strains used in this work

Strain	Genotype	Source
GCY35	*MAT***a** *his3Δ200 hom3-10 ura3-52 ade2-101*$_{oc}$ *trp1 met13 met4*	New, *et. al.*, 1993
PTY100	Same as GCY35 but *mlh1::URA3*	This study
PTY101	Same as GCY35 but *pms1::hisG-URA3-hisG*	This study
PTY102	Same as GCY35 but *mlh3::hisG*	This study
PTY103	Same as GCY35 but *mlh1::URA3 mlh3::hisG*	This study
PTY104	Same as GCY35 but *pms1::hisG-URA3-hisG mlh3::hisG*	This study
PTY105	Same as GCY35 but *exo1::HIS3*	This study
PTY106	Same as GCY35 but *exo1::HIS3 mlh1::URA3*	This study
PTY107	Same as GCY35 but *pms1::hisG-URA3-hisG exo1::HIS3*	This study
PTY108	Same as GCY35 but *yer080w::KanMX4*	This study
PTY109	Same as GCY35 but *yer080w::KanMX4 exo1::HIS3*	This study
PTY110	Same as GCY35 but *rev3::hisG*	This study
PTY111	Same as GCY35 but *rev3::hisG exo1::HIS3*	This study
PTY112	Same as GCY35 but *rev3::hisG mlh1::URA3*	This study
PTY113	Same as GCY35 but *rad27::hisG-URA3-hisG*	This study
PTY113b	Same as GCY35 but *rad27::hisG*	This study
PTY200	Same as GCY35 but *mlh1-E31A*	This study
PTY201	Same as GCY35 but *pms1-E61A*	This study
PTY202	Same as GCY35 but *pms1-E61A mlh3::hisG*	This study
PTY203	Same as GCY35 but *pms1-E61A mlh3::hisG mlh2::KanMX4*	This study
PTY204	Same as GCY35 but *pms1-E61A exo1::HIS3*	This study
PTY205	Same as GCY35 but *pms1-E61A mlh3::hisG exo1::HIS3*	This study
PTY206	Same as GCY35 but *mlh1-E31A mlh3::hisG*	This study
PTY207	Same as GCY35 but *mlh1-E31A exo1::HIS3*	This study
PTY208	Same as GCY35 but *mlh1-E31A yer080w::KanMX4*	This study
PTY209	Same as GCY35 but *pms1-E61A yer080w::KanMX4*	This study

PTY210	Same as GCY35 but *pms1-E61A exo1::HIS3 rev3:: hisG-URA3-hisG*	This study
PTY211	Same as GCY35 but pms1-E61A exo1-D173A	This study
PTY212	Same as GCY35 but mlh1-E31A exo1-D173A	This study
PTY213	Same as GCY35 but pms1-E61A rad27::hisG-URA3-hisG	This study
PTY213b	Same as GCY35 but pms1-E61A rad27::hisG	This study
PTY214	Same as GCY35 but mlh1-E31A rad27::hisG-URA3-hisG	This study
PTY214b	Same as GCY35 but mlh1-E31A rad27::hisG	This study
PTY215	Same as GCY35 but pms1-E61A rad27-D179A	This study
PTY216	Same as GCY35 but pms1-E61A rad27-F346A/F347A	This study
PTY300	Same as GCY35 but mlh1-G98A	This study
PTY301	Same as GCY35 but pms1-G128A	This study
PTY302	Same as GCY35 but *pms1-G128A mlh3::hisG*	This study
PTY303	Same as GCY35 but *pms1-G128A mlh3::hisG mlh2::KanMX4*	This study
PTY304	Same as GCY35 but *pms1-G128A exo1::HIS3*	This study
PTY305	Same as GCY35 but *pms1-G128A mlh3::hisG exo1::HIS3*	This study
PTY306	Same as GCY35 but *mlh1-G98A mlh3::hisG*	This study
PTY307	Same as GCY35 but *mlh1-G98A exo1::HIS3*	This study
PTY310	Same as GCY35 but *pms1-G128A exo1::HIS3 rev3:: hisG-URA3-hisG*	This study
PTY311	Same as GCY35 but *pms1-G128A exo1-D173A*	This study
PTY312	Same as GCY35 but *mlh1-G98A exo1-D173A*	This study
PTY313	Same as GCY35 but *pms1-G128A rad27::hisG-URA3-hisG*	This study
PTY313b	Same as GCY35 but *pms1-G128A rad27::hisG*	This study
PTY400	Same as GCY35 but *mlh1-E31A pms1-E61A*	This study
PTY401	Same as GCY35 but *mlh1-E31A pms1-E61A mlh3::hisG*	This study
PTY500	Same as GCY35 but *mlh1-E31A pms1-G128A*	This study
PTY501	Same as GCY35 but *mlh1-G98A pms1-E61A*	This study
PTY600	Same as GCY35 but *mlh1-G98A pms1-G128A*	This study
PTY700	Same as GCY35 but *exo1-D173A*	This study
PTY701	Same as GCY35 but *exo1-D173A rev3:: hisG-URA3-hisG*	This study

PTY701b	Same as GCY35 but *exo1-D173A rev3:: hisG*	This study
PTY800	Same as GCY35 but *rad27-D179A*	This study
PTY900	Same as GCY35 but *rad27-F346A/F347A*	This study
BY4742	MATα *his3Δ1 leu2Δ lys2Δ ura3Δ*	Research Genetics
PTY4700	Same as BY4742 but *yer080w::KanMX4 exo1::HIS3*	This study
PTY4701	Same as BY4742 but *yfr044c::KanMX4 exo1::HIS3*	This study
PTY4702	Same as BY4742 but *ypl199c::KanMX4 exo1::HIS3*	This study
PTY4703	Same as BY4742 but *cac1::KanMX4 exo1::HIS3*	This study
PTY4704	Same as BY4742 but *ynl218w::KanMX4 exo1::HIS3*	This study
PTY4742	Same as BY4742 but *hom3-10*	This study
PTY4743	Same as PTY4742 but *exo1::KanMX4*	This study
PTY4744	Same as PTY4742 but *yer080w::KanMX4*	This study
PTY4745	Same as PTY4742 but *yer080w::KanMX4 exo1::HIS3*	This study
L40	*MAT***a** *his3Δ200 trp1-901 leu2-3, 112 ade2 LYS2::(lexAop)*$_4$ *-HIS3 URA3::(lexAop)*$_8$*-lacZ GAL4 gal80*	Vojtek, *et. al.*, 1993
AMR70	*MATα his3Δ200 trp1-901 leu2-3, 112 URA3::(lexAop)*$_8$*-lacZ GAL4 gal80*	Vojtek, *et. al.*, 1993

APPENDIX B: *CAN1* Spectrum Summary

List of *can1* mutations recovered from independent *can1* forward mutants from the designated strains with relevant genotypes in parantheses. Numbers represent clone numbers, followed by mutations denoted for the coding strand, with sequence coordinates for database entry gb|M11724|YSCCAN1, in paranthesis is the primer used to identify the mutation and lastly, the consequence of the mutation. Numbers without assocaited mutations indicate that no mutation could be found after sequencing of the *CAN1* gene. Clones with two mutations occurred at a frequency of 5/322 (or 1.6%) and may represent *Taq* polymerase generated errors. In the clones with two mutations the non-conservative changes were assumed to be the inactivating *can1* mutations.

GCY35 (wildtype)

#1: G->A @ 671 (primer E)[1] ∴ GGC->GAC (G->D)
#2: G->C @ 1514 (primer B)[1] ∴ CGT->CCT (R->P)
#3: C->T @ 770 (primer C) ∴ TCC->TTC (S->F)
#4: ΔTC @ 1269-1270 (primer A & C)
#5: 2C->C @ 1270-1271 (primer A & C)
#6: Direct duplication of sequences 1898-1935
#7: T->C @ 1051 (primer C) ∴ TGT->CGT (C->R)
#8: Direct duplication of sequences 594-620
#9: G->T @ 1291 (primer A & C)[1] ∴ GTT->TTT (V->F)
#10: 4T->3T @ 1517-1520 (primer A & B)
#11: 4A->3A @ 330-333 (primer E)
#12: G->T @ 370 (primer E) ∴ GAG->TAG (E->amber)
#13: G->T @ 848 (primer C)[1] ∴ TGG->TTG (W->L)
#14: A->T @ 870 (primer C) ∴ GAA->GAT (E->D)
#15: 6T->7T @ 938-943 (primer C)
#16: G->A @ 1213 (primer A & C) ∴ GGT->AGT (G->S)
#17: ΔC @ 409 (primer E)[1] results in a (A) run of n=4
#18: 3G->2G @ 1175-1177 (primer A & C)
#19: C->T @ 1484 (primer A & B) ∴ GCC->GTC (A->V)
#20: G->A @ 1514 (primer A & B)[1] ∴ CGT->GAT (R->D)

---

[1]-base substitution occurs adjacent to or within a repeat n>2.

[2]-confirmed with independent PCR product.

MLH1

PTY100 (*mlh1Δ*)

#1:	6T->5T	@ 938-943 (primer C)
#2:	6T->5T	@ 938-943 (primer C)
#3:	4T->3T	@ 858-861 (primer C)
#4:	4T->3T	@1292-1295 (primer C)
#5:	G->T	@ 1597 (primer B)[1] ∴ GTT->TTT (V->F)
#6:	G->A	@ 632 (primer E) ∴ GGT->GAT (G->D)
#7:	4T->3T	@ 858-861 (primer C)
#8:	4T->3T	@ 1869-1872 (primer B)
#9:	5T->4T	@ 1053-1057 (primer C)
#10:	6A->5A	@ 1282-1287 (primer C)

PTY112 (*mlh1Δ rev3Δ*)

#1:	G->A	@1036 (primer A & C)[1] ∴ GGG->AGG (G->R)
#2:	6A->5A	@ 1282 (primer A & C)
#3:	4T->3T	@ 1340 (primer A & C)
#4:	6T->5T	@ 1699 (primer A & B)
#5:	6A->5A	@ 1282 (primer A & C)
#6:	G->A	@ 670 (primer E) ∴ GGC->AGC (G->S)
#7:	G->A	@ 988 (primer C) ∴ GGT->AGT (G->S)
#8:	6T->5T	@ 1699 (primer A & B)
#9:	6T->5T	@ 938 (primer C)
#10:		
#11:		
#12:	6T->5T	@ 1699 (primer A & B)

PTY200 (*mlh1-E31A*)

#1:	6T->7T	@ 938-943 (primer C)
#2:	6T->5T	@ 938-943 (primer C)
#3:	6A->5A	@ 1282-1287 (primer A)
#4:	6T->5T	@ 1699-1704 (primer B)
#5:	5T->6T	@1053-1057 (primer C)
#6:	6T->7T	@ 1699-1704 (primer B)
#7:	C->A	@ 1255 (primer A & C)[1] ∴ CCC->ACC (P->T)
#8:	3C->2C	@ 1804-1806 (primer B)
#9:	3A->2A	@ 1795-1997 (primer B)
#10:	T->C	@ 1105 (primer C) ∴ TGG->CGG (W->R)
#11:	4T->3T	@ 782-785 (primer C)
#12:	6T->5T	@ 1699-1704 (primer B)
#13:	G->A	@ 815 (primer C) ∴ GGT->GAT (G->D)
#14:	T->C	@ 1708 (primer B)∴ TGG->CGG (W->R)

[1] -base substitution occurs adjacent to or within a repeat n>2.

[2] -confirmed with independent PCR product.

#15:	T->C	@ 1105 (primer C)∴ TGG->CGG (W->R)
#16:	4T->3T	@ 782-785 (primer C)
#17:	G->T	@ 631 (primer E) ∴ GGT->TGT (G->C)
#18:	G->A	@ 1298 (primer A & C) ∴ CGT->CAT (R->H)
#19:	4T->3T	@ 1292-1295 (primer A & C)
#20:	C->A	@ 909 (primer C)[1] ∴ TAC->TAA (Y->ochre)

PTY207 (*mlh1-E31A exo1Δ*)

#1:	6T->5T	@ 938-943 (primer C)
#2:	6T->5T	@ 1699-1704 (primer B)
#3:	G->T	@ 1514 (primer A & B) ∴ CGT->CTT (R->L)
#4:	G->A	@ 815 (primer C) ∴ GGT->GAT (G->D)
#5:		
#6:	6T->7T	@ 938-943 (primer C)
#7:	ΔC	@ 752 (primer C)
#8:	6T->5T	@ 938-943 (primer C)
#9:	G->A	@ 1176 (primer A & C) ∴ TGG->TGA (W->opal)
#10:	G->A	@ 1107 (primer A & C) ∴ TGG->TGA (W->opal)
#11:	5T->4T	@ 1053-1057 (primer A & C)
#12:	6A->5A	@ 1282-1287 (primer A & C)
#13:	5T->4T	@ 1053-1057 (primer A & C)
#14:	6T->5T	@ 1699-1704 (primer B)
#15:	4T->3T	@ 858-861 (primer C)
#16:	6T->5T	@ 938-943 (primer C)
#17:	6A->5A	@ 1282-1287 (primer A & C)
#18:	4G->3G	@ 1075-1078 (primerA & C)
#19:	4G->3G	@ 1124-1127 (primerA & C)
#20:	6T->7T	@ 938-943 (primer C)
	G->T	@ 944 (primer C) ∴ complex

PTY300 (*mlh1-G98A*)

#1:	6T->7T	@ 1699-1704 (primer B)
#2:	G->A	@ 671 (primer E)[1] ∴ GGC->GAC (G->D)
#3:	5T->4T	@ 1053-1057 (primer A & C)
#4:	6T->5T	@ 938-943 (primer C)
#5:	3T->2T	@ 645-647 (primer E)
#6:	6T->5T	@ 938-943 (primer C)
#7:	G->A	@ 617 (primer E) ∴ GGT->GAT (G->D)
#8:	4T->3T	@ 1919-1922 (primer B)
#9:	5T->4T	@ 1053-1057 (primer A & C)
#10:	5T->4T	@ 1053-1057 (primer A & C)
#11:	6A->5A	@ 1282-1287 (primer A & C)
#12:	G->A	@ 827 (primer C) ∴ GGT->GAT (G->D)

[1]-base substitution occurs adjacent to or within a repeat n>2.

[2]-confirmed with independent PCR product.

#13:	3T->4T	@1292-1295 (primer A & C)
#14:	6T->5T	@ 938-943 (primer C)
#15:	4T->3T	@ 858-861 (primer C)
#16:	4T->3T	@ 858-861 (primer C)
#17:	4T->3T	@ 858-861 (primer C)
#18:	6T->5T	@ 938-943 (primer C)
#19:	3C->2C	@ 1113-1115 (Primer C)
#20:	6T->5T	@ 1699-1704 (primer B)

PTY307 (mlh1-G98A exo1D)

#1:	G->T	@ 334 (primer E)[1] ∴ GAA->TAA (E-> ochre)
#2:	6A->5A	@ 1282-1287 (primer A)
#3:	A->T	@ 574 (primer E)[1] ∴ AGA->TGA (R->opal)
	G->T	@ 930 (primer C) ∴ TGG->TGT (W->C)
#4:	6A->5A	@ 1282-1287 (primer A & C)
#5:	G->A	@ 1106 (primer A & C) ∴ TGG->TAG (W->amber)
#6:	6T->5T	@ 938-943 (primer C)
#7:	G->A	@ 815 (primer C) ∴ GGT->GAT (G->D)
#8:	C->T	@ 1210 (primer A & C)[1] ∴ CAA->TAA (Q-> ochre)
#9:	G->T	@ 632 (primer E) ∴ GGT->GTT (G->V)
#10:	G->A	@ 840 (primer C)[1] ∴ TGG->TGA (W->opal)
#11:	G->C	@ 631 (primer E) ∴ GGT->CGT (G->R)
#12:	G->T	@ 671 (primer E)[1] ∴ GGC->GTC (G->V)
#13:	6T->5T	@ 938-943 (primer C)
#14:	5T->6T	@ 1053-1057 (primer C)
#15:	C->A	@ 1511 (primer B)[1] ∴ TCC->TAC (S->Y)
#16:	5T->4T	@ 1053-1057 (primer C)
#17:	4T->3T	@ 1292-1295 (primer A & C)
#18:	6A->5A	@ 1699-1704 (primer B)
#19:	3C->2C	@ 672-674 (primer E)
#20:	G->A	@ 1298 (primer A & C) ∴ CGT->CAT (R->H)

PTY106 (*mlh1Δ exo1Δ*)

#1:	6A->5A	@ 1282-1287 (primer A & C)
#2:	6T->5T	@ 938-943 (primer C)
#3:	4T->3T	@ 858-861 (primer C)
#4:	4T->3T	@ 1292-1295 (primer A & C)
#5:	C->A	@ 761 (primer C)[1] ∴ CCT->CAT (P->H)
#6:	6T->5T	@ 1699-1704 (primer A & B)
#7:	4G->3G	@ 1124-1127 (primer A & C)
#8:	3T->2T	@ 645-647 (primer E)
#9:	C->A	@ 845 (primer C)[1] ∴ TCT->TAT (S->Y)

[1]-base substitution occurs adjacent to or within a repeat n>2.

[2]-confirmed with independent PCR product.

#10: 6T->5T @ 938-943 (primer C)
#11: 5T->4T @ 1053-1057 (primer A & C)
#12:
#13: 6A->5A @ 1282-1287 (primer A & C)
#14: G->A @ 1337 (primer A & C) ∴ GGA->GAA (G->E)
G->T @ 1345 (primer A & C) ∴ GTT->TTT (V->F)
#15: C->A @ 1210 (primer A & C)[1] ∴ CAA->AAA (Q->K)
#16: C->A @ 966 (primer C) ∴ AAC->AAA (N->K)
#17: 5T->4T @ 1053-1057 (primer A & C)
#18: G->A @ 840 (primer C)[1] ∴ TGG->TGA (W->opal)
#19: 3C->2C @ 1113-1115 (primer A & C)
#20: 6T->5T @ 1699-1704 (primer B)

PMS1

PTY101 **(*pms1Δ*)**
#1: 6A->5A @ 1282-1287 (primer A & C)
#2: 6T->7T @ 938-943 (primer C)
#3: C->A @ 845 (primer C)[1] ∴ TCT->TAT (S->Y)
#4: C->A @ 845 (primer C)[1] ∴ TCT->TAT (S->Y)
#5: 5T->4T @ 1053-1057 (primer C)
#6: 6T->7T @ 938-943 (primer C)
#7: 5T->6T @ 1053-1057 (primer C)
#8: 6T->5T @ 938-943 (primer C)
#9: 4T->3T @ 782-785 (primer C)
#10: 6A->5A @ 1282-1287 (primer A & C)

PTY104 **(*pms1Δ mlh3Δ*)**
#1: 3T->2T @ 1178-1180 (primer A & C)
#2: 6T->7T @ 938-943 (primer C)
#3: 6T->7T @ 938-943 (primer C)
#4: 6T->7T @ 938-943 (primer C)
#5: G->T @ 631 (primer E) ∴ GGT->TGT (G->C)
#6: 3T->2T @ 800-802 (primer C)
#7: G->A @ 827 (primer C) ∴ GGT->GAT (G->D)
#8: 6T->5T @ 938-943 (primer C)
#9: 2T->1T @ 708-709 (primer E)
#10: 6T->5T @ 1699-1704 (primer B)

PTY107 **(*pms1Δ exo1Δ*)**
#1: 2G->G @ 1062-1063 (primer A)
#2: 6T->5T @ 1699-1704 (primer B)
#3: 6A->5A @ 1282-1287 (primer A)

[1]-base substitution occurs adjacent to or within a repeat n>2.

[2]-confirmed with independent PCR product.

#4: G->T @ 460 (primer E)[1] ∴ GAA->TAA (E-> ochre)
#5:
#6: 4T->3T @ 858-861 (primer C)
#7: G->A @ 632 (primer E) ∴ GGT->GAT (G-> D)
#8: 3T->4T @ 324-326 (primer E)
#9:
#10:
#11: 5T->4T @ 1053-1057 (primer C)
#12: G->A @ 989 (primer C) ∴ GGT->GAT (G-> D)
#13: G->C @ 988 (primer C) ∴ GGT->CGT (G-> R)
#14: 3T->2T @ 1786 (primer B)
#15: G->A @ 840 (primer C)[1] ∴ TGG->TGA (W-> opal)
#16: 4T->3T @ 1292-1295 (primer A & C)
#17: C->T @ 1744 (primer B) ∴ CAA->TAA (Q-> ochre)
#18: 6T->5T @ 938-943 (primer C)
#19: 6T->5T @ 938-943 (primer C)
#20: 4T->3T @ 1292-1295 (primer A & C)
#21: ΔAC @ 1369-1370 (primer A)
T->A @ 1375 (primer A) ∴ TCT->ACT (S-> T)

PTY301 (*pms1-G128A*)
#1: G->T @ 599 (primer E) ∴ GGT->GTT (G->V)
#2: C->A @ 1503 (primer A, B & C) ∴ TAC->TAA (Y->ochre)
#3: C->T @ 1210 (primer A & C)[1] ∴ CAA->TAA (Q->ochre)
#4: 5A->4A @ 1150-1154 (primer A & C)
#5: 6T->5T @ 938-943 (primer C)
#6: 2A->3A @ 335-336 (primer E)
#7: G->T @ 1243 (primer A & C) ∴ GAA->TAA (E->ochre)
#8: G->T @ 1229(primer A & C) ∴ GGT->TGT (G->C)
#9: 6A->5A @ 1282-1287 (primer A & C)
#10: T->G @ 635 (primer E)[1] ∴ CTT->CGT (L->R)
#11: 6T->5T @ 938-943 (primer C)
#12: G->A @ 944 (primer C)[1] ∴ TGG->TAG (W->amber)
#13: C->A @ 431 (primer E) ∴ TCA->TAA (S->ochre)
#14: 5T-4T @ 1053-1057 (primer C)
#15: ΔT @ 1733 (primer B) results in a (CA) run of n=3
#16: G->C @ 814 (primer C)[1] ∴ GGT->CGT (G->R)
#17: C->A @ 629 (primer E) ∴ ACA->AAA (T->K)
#18: 6T->5T @ 938-943 (primer C)
#19:
#20:

[1]-base substitution occurs adjacent to or within a repeat n>2.
[2]-confirmed with independent PCR product.

PTY301 ***(pms1-G128A mlh3Δ)***

#1:	A->G	@ 856 (primer C)[2] ∴ ACT->GCT (T->A)
#2:	ΔAT(or TA)	@ 717-719 (primer E)[2] in a dinucleotide run n=2
#3:	T->C	@ 1223 (primer A & C)[2] ∴ CTA->CCA (L->P)
#4:	ΔAT(or TA)	@ 593-595 (primer E)[2] in a dinucleotide run n=2
#5:	4T->3T	@ 782-785 (primer C)
#6:	ins AG	@ 572-579 (primer E) in a dinucleotide run n=4
#7:	6T->5T	@ 1699-1704 (primer B)
#8:	ΔAT(or TA)	@ 693-692 (primer E)[2] in a dinucleotide run n=2
#9:	5T-4T	@ 1053-1057 (primer C)
#10:	6A->5A	@ 1282-1287 (primer A & C)
#11:	6T->5T	@ 938-943 (primer C)
#12:	6A->5A	@ 1282-1287 (primer A & C)[2]
#13:		
#14:	5T-4T	@ 1053-1057 (primer A & C)[2]
#15:	C->A	@ 407 (primer E)[2] ∴ TCA->TAA (S->ochre)
#16:	G->A	@ 1106 (primer C)[2] ∴ TGG->TAG (W->amber)
#17:	4T->3T	@ 1439-1442 (primer A & B)
#18:	G->C	@ 814 (primer C)[1,2] ∴ GGT->CGT (G->R)
#19:	6A->5A	@ 1282-1287 (primer C)[2]
#20:	6T->5T	@ 938-943 (primer C)[2]
#21:	6T->5T	@ 938-943 (primer C)
#22:	G->T	@ 1214 (primer A & C) ∴ GGT->GTT (G->V)
#23:	ΔT	@ 758 (primer C)[1]
#24:	6T->5T	@ 938-943 (primer C)
#25:	C->T	@ 790 (primer C) ∴ CAA->TAA (Q-> ochre)
#26:	4T->3T	@ 1598-1601 (primer B)

PTY205 ***(pms1-E61A mlh3Δ exo1Δ)***

#1:	5T-4T	@ 1053-1057 (primer A & C)
#2:	6A->5A	@ 1282-1287 (primer A & C)
#3:	T->C	@ 1492 (primer A & B) ∴ TCA->CCA (S->P)
#4:	G->T	@ 999 (primer C) ∴ GAG->GAT (E->D)
#5:	4T-3T	@ 635-638 (primer E)
#6:	6A->5A	@ 1282-1287 (primer A & C)
#7:	5T-4T	@ 1053-1057 (primer A & C)
#8:	4T-3T	@ 782-785 (primer C)
#9:	T->G	@ 999 (primer E) ∴ CTT->CGT (L->R)
#10:	4T-3T	@ 841-844 (primer C)
#11:	T->G	@ 999 (primer E) ∴ CTT->CGT (L->R)
#12:	T->C	@ 1708 (primer B) ∴ TGG->CGG (W->R)

[1]-base substitution occurs adjacent to or within a repeat n>2.

[2]-confirmed with independent PCR product.

#13:	6A->5A	@ 1282-1287 (primer A & C)
#14:	6A->5A	@ 1282-1287 (primer A & C)
#15:	6T->5T	@ 938-943 (primer C)
#16:	2C->C	@ 1585-1586 (primer B)
#17:	4T-3T	@ 858-861 (primer C)
#18:	3G-2G	@ 1004-1006 (primer C)
#19:	ΔC	@ 1809 (primer B)
#20:	5A->4A	@ 1150-1154 (primer A & C)

PTY305 (*pms1-G128A mlh3Δ exo1Δ*)

#1:	C->A	@ 761 (primer C)[1] ∴ CCT->CAT (P->H)
#2:	T->G	@ 1340 (primer A & C)[1] ∴ CTT->CGT (L->R)
#3:	C->G	@ 1493 (primer A)[1] ∴ TCA-> TGA (S->opal)
#4:	6A->5A	@ 1282-1287 (primer A)
#5:	3T->2T	@ 1207-1209 (primer A)
#6:	6A->5A	@ 1282-1287 (primer A & C)
#7:	5T-4T	@ 1053-1057 (primer A & C)
#8:	4T-3T	@ 635-638 (primer E)
#9:	3T-2T	@ 1064-1066 (primer C)
#10:	3C->2C	@ 1804-1806 (primer B)
#11:	C->T	@ 1256 (primer A & C)[1] ∴ CCC-> CTC (P->L)
#12:	C->A	@ 1511 (primer B)[1] ∴ TCC-> TAC (S->Y)
#13:	2A->A	@ 664-665 (primer E)
	C->T	@ 666 (primer E) ∴ AAC-> AAT (N->N)
#14:	C->A	@ 966 (primer C) ∴ AAC-> AAA (N->K)
#15:	6T->5T	@ 938-943 (primer C)
#16:	4T->3T	@ 858-861 (primer C)
#17:	5T-4T	@ 1053-1057 (primer C)
#18:	T->G	@ 686 (primer E) ∴ CTT-> CGT (L->R)
#19:	6A->5A	@ 1282-1287 (primer A & C)
#20:	5T-4T	@ 1053-1057 (primer C)

---

[1]-base substitution occurs adjacent to or within a repeat n>2.

[2]-confirmed with independent PCR product.

PTY310 (*pms1-G128A exo1Δ rev3Δ*)

#1:	C->A	@ 1238 (primer A & C) ∴ GCT->GAT (A->D)
#2:	T->G	@ 581 (primer E) ∴ CTT->CGT (L->R)
#3:	6T->7T	@ 938 (primer C)
#4:	4T->5T	@ 1022 (primer C)
#5:		
#6:	4T->3T	@ 1022 (primer C)
#7:	6T->5T	@ 1699 (primer A & B)
#8:	2C->1C	@ 1129 (primer A & C)
#9:	6A->5A	@ 1282 (primer A & C)
#10:	T->C	@ 1223 (primer A & C) ∴ CTA->CCA (L->P)
#11:		
#12:	6T->5T	@ 938 (primer C)

EXO1

PTY105 (*exo1Δ*)

#1:	ΔC	@ 1793 (primer B)
#2:	3C->2C	@ 1113-1115 (primer A & C)
#3:	C->T	@ 629 (primer E) ∴ ACA->ATA (T->I)
#4:	G->T	@ 989 (primer C) ∴ GGT->GTT (G->V)
#5:	C->T	@ 1855 (primer B)[1] ∴ CAA->TAA (Q->ochre)
#6:	3A->4A	@ 1251-1253 (primer A & C)
#7:	C->A	@ 845 (primer C)[1] ∴ TCT->TAT (S->Y)
#8:	2C->C	@ 1826-1827 (primer B)
#9:	G->T	@ 976 (primer C) ∴ GTC->TTT (V->F)
#10:		
#11:	G->T	@ 520 (primer E) ∴ GAG->TAG (E->amber)
#12:	T->A	@ 847 (primer C)[1] ∴ TGG->AGG (W->R)
	C->T	@ 865 (primer C)[1] ∴ CTG->TTG (L->L)
#13:	G->A	@ 1036 (primer A & C)[1] ∴ GGG->AGG (G->R)
#14:	3A->4A	@ 1251-1253 (primer A & C)
#15:	ΔC	@ 777 (primer C)[1]
#16:	C->G	@ 580 (primer E)[1] ∴ CTT->GTT (L->V)
#17:	6A->5A	@ 1282-1287 (primer A & C)
#18:	3T->2T	@ 700-702 (primer E)
#19:	G->A	@ 1298 (primer A & C) ∴ CGT->CAT (R->H)
#20:	C->G	@ 1532 (primer A & B)[1] ∴ TCA->TGA (S->opal)
#21	6T->7T	@ 938-943 (primer C)

[1]-base substitution occurs adjacent to or within a repeat n>2.

[2]-confirmed with independent PCR product.

PTY111 (*exo1Δ rev3Δ*)

#1: G->T @ 1291 (primer A & C)[1] ∴ GTT->TTT (G->F)
#2: C->A @ 608 (primer E)[1] ∴ GCC->GAC (A->D)
#3: G->T @ 617 (primer E) ∴ GGT->GTT (G->V)
#4: C->A @ 831 (primer C) ∴ TAC->TAA (Y-> ochre)
#5: G->A @ 815 (primer C) ∴ GGT->GAT (G-> D)
#6:
#7: 6A->5A @ 1282-1287 (primer A & C)
#8: C->A @ 1493 (primer B)[1] ∴ TCA->TAA (S-> ochre)
#9: 2T->3T @ 881-882 (primer C)
#10: C->A @ 857 (primer C)[1] ∴ ACT->AAT (T-> N)
#11: C->T @ 1210 (primer A & C)[1] ∴ CAA->TAA (Q-> ochre)
#12: T->C @ 1492 (primer A & B) ∴ TCA->CCA (S-> P)
#13: C->A @ 1503 (primer A & B) ∴ TAC->TAA (Y-> ochre)
#14: C->T @ 1513 (primer A & B)[1] ∴ CGT->TGT (R-> C)
#15: C->T @ 1372 (primer A & C) ∴ CAA->TAA (Q-> ochre)

PTY700 (*exo1-D173A*)

#1: T->G @ 659 (primer E) ∴ CTG->CGG (L->R)
#2: C->G @ 580 (primer E)[1] ∴ CTT->GTT (L->V)
#3: G->T @ 999 (primer C) ∴ GAG->GAT (E->D)
#4: C->A @ 1314 (primer A & C) ∴ TAC->TAA (Y->ochre)
#5: T->G @ 833 (primer C) ∴ ATG->ACG (M->T)
#6: C->G @ 909 (primer C)[1] ∴ TAC->TAG (Y->amber)
#7: ΔC @ 1628 (primer A & B)
#8: C->T @ 409 (primer E)[1] ∴ CAA->TAA (Q-> ochre)
#9: G->A @ 902 (primer C)[1] ∴ TGG->TAG (W->amber)
#10:
#11: G->A @ 632 (primer E) ∴ GGT->GAT (G->D)
#12: ΔA @ 1775 (primer B)
#13: G->T @ 626 (primer E) ∴ GGT->GTT (G->V)
#14: G->A @ 1697 (primer B) ∴ GGC->GAC (G->D)
#15: G->A @ 930 (primer C) ∴ TGG->TGA (W->opal)
#16: ΔA @ 1628 (primer B)
#17: G->T @ 1597 (primer B)[1] ∴ GTT->TTT (V->F)
#18: G->C @ 613 (primer E)[2] ∴ GGT->CGT (G->R)
#19: G->A @ 903 (primer C) ∴ TGG->TGA (W->opal)
#20: A->T @ 964 (primer C) ∴ AAC->TAC (Q->Y)

[1] -base substitution occurs adjacent to or within a repeat n>2.

[2] -confirmed with independent PCR product.

APPENDIX C: Interactors from yeast two-hybrid screens using MutLα NH_2-terminal baits

ORF	Gene Name	Function
YMR168C[2]	CEP3	component of Cbf3 kinetochore protein complex, which binds to the CDE III element of centromeres and interacts with MIF2.
YLR029C[2]	RPL15A	ribosomal protein L15A (YL10) (rp15R) (L13A).
YMR116C[2]	ASC1	WD repeat protein (G-beta like protein) that interacts with the translational machinery
YMR173W[2]	DDR48	DNA damage inducible, implicated in the production or recovery of mutations and yeast flocculation protein.
YNL078W[2]		protein of unknown function, but interacts with NAPI (nucleosome assembly protein I).
YPR018W[1, 5]	CAC1/RLF2	p90 subunit of yeast Chromatin Assembly Factor-I (CAF-I).
YAL063C[1, 4]	FLO9	flocculation gene.
YER032W[1, 4]	FIR1/PIP1	putative participant in 3' mRNA processing
YAL035W[2]	FUN12	translation initiation factor 2 (eIF2).
YGR258C[2, 5]	RAD2	nucleotide excision repair protein (XPG homolog); endonuclease and 5'-3'exonuclease.
YFR044C[2, 5]		unknown.
YJL162C[2]		protein with similarity to DnaJ-like proteins.
YGR271W[2, 5]		protein with similarity to RNA (duplicated) helicases.
YGR100W[2]	MDR1	GTPase-activating protein for Ypt6p and Sec4p.

1 - Retrieved with bait pNBTM-pms1-61 N-401
2 - Retrieved with bait $pNCoB(lexA)_2$
3 - Retrieved with bait pBTM-pms1-K153pter
4 - Retrieved with bait pNCoB-pms1-61 N-401/mlh1-31 N-354
5 - some characterization of this candidate has been performed.

ORF	**Gene Name**	**Function**
YIR023W[2]	DAL81/UGA35	Transcriptional activator for allantoin, 4-aminobutyric acid (GABA), and urea catabolic genes; contains a Zn[2]-Cys[6] fungal-type binuclear cluster domain in the N-terminal region.
YKL203C[2]	TOR2	PI-4 kinase; involved in growth and sensitivity to the immunosuppressant rapamycin.
YOL051W[2, 5]	GAL11	component of RNA polymerase II holoenzyme.
YAL032C[2]	PRP45	required for pre-mRNA splicing, component of the spliceosome
YER080W[4, 5]		unknown.
YDL001W[3]		unknown.
YPL070W[3]		unknown.
YJL026W[3]	RNR2/CRT6	Encodes for small subunit of ribonucleotide reductase, an essential gene

1 - Retrieved with bait pNBTM-pms1-61 N-401
2 - Retrieved with bait pNCoB(lexA)$_2$
3 - Retrieved with bait pBTM-pms1-K153pter
4 - Retrieved with bait pNCoB-pms1-61 N-401/mlh1-31 N-354
5 - some characterization of this candidate has been performed.